



UNIVERSITÀ DEGLI STUDI DI MILANO

PhD in Pharmacological, Experimental and Clinical Sciences
Department of Pharmacological and Biomolecular Sciences
XXXII Cycle

BIO/14

PhD Thesis

Linking NMDA receptor-dependent plasticity and neuronal architecture: the role of RING Finger Protein 10

Candidate: Nicolò Carrano
Student Number: R11768

Tutor: Prof. Fabrizio Gardoni
Coordinator: Prof. Alberico L. Catapano

Academic Year: 2018/2019

INDEX

ABSTRACT (ENGLISH)	4
ABSTRACT (ITALIANO)	5
INTRODUCTION	7
1. Excitatory glutamatergic synapse	8
1.1. AMPA Receptors	9
1.2. NMDA receptors	10
2. SYNAPTIC PLASTICITY	13
2.1. NMDAR-dependent synaptic plasticity	15
3. DENDRITIC SPINES: THE LOCUS OF STRUCTURAL AND FUNCTIONAL PLASTICITY ..	20
3.1. Classification	20
3.2. Morphogenesis.....	23
3.3. Plasticity of dendritic spines.....	25
4. SYNAPSE-TO-NUCLEUS COMMUNICATION	26
4.1. Activity-dependent calcium signaling	27
4.2. Synapse-to-nucleus translocation of protein messengers	29
AIMS	43
MATERIALS AND METHODS	45
1. Cell cultures	46
1.1. Primary hippocampal neuronal cultures	46
1.2. COS-7 cell line	47
2. Biochemistry	48
2.1. Subcellular fractionation of Triton Insoluble Fraction (TIF) and nuclear fraction	48
2.2. Co-ImmunoPrecipitation assays (Co-IP)	49
2.3. Pull-down assay	49
2.4. Drug treatments	49
2.5. Western blotting.....	50
2.6. Luciferase assays	50
3. Molecular biology	50
3.1. Bacteria Transformation	50
3.2. Cloning, expression and purification of GST fusion protein.....	51
4. Confocal imaging	52
4.1. Immunofluorescence	52
4.2. In situ Proximity Ligation Assay (PLA)	52
4.3. Time-lapse imaging	53
4.4. Dil-labeling for spine morphology.....	53
4.5. Sholl analysis for neuronal branching and dendritic spine morphology.....	54

5. Antibodies	54
6. Animals	55
7. Quantification and Statistical analysis	55
RESULTS	56
1. PKC Activation Regulates RNF10 Translocation to the Nucleus	57
FIGURE 1	58
FIGURE 2	59
2. RNF10 Phosphorylation by PKC Modulates RNF10/NMDAR Complex Dissociation and Nuclear Localization	60
FIGURE 3	61
FIGURE 4	63
FIGURE 5	64
FIGURE 6	66
3. PKC-phosphorylation on Ser31 activates RNF10 transcriptional activity and induction of plasticity program	67
4. The Modulation of RNF10 Activity Results in the Alteration of Neuronal Morphology	69
FIGURE 8	70
5. RNF10 deficiency alters brain morphology <i>in vivo</i>	71
FIGURE 9	72
6. RNF10 deficiency induces behavioral alterations and hippocampal related cognitive impairments.....	73
FIGURE 10.....	73
FIGURE 11.....	74
FIGURE 12.....	75
FIGURE 13.....	76
FIGURE 14.....	78
7. RNF10 is necessary for the correct formation of the glutamatergic synapse <i>in vivo</i> ..	79
FIGURE 15.....	80
FIGURE 16.....	81
FIGURE 17.....	82
8. RNF10 absence alters neuronal geometry in specific hippocampal regions	83
FIGURE 18.....	84
9. RNF10 absence prevents LTP induction <i>in vivo</i>	85
FIGURE 19.....	85
DISCUSSION	86
REFERENCES	91

ABSTRACT (ENGLISH)

An active synapse-to-nucleus communication is essential for long-term changes in neurons, like the regulation of neuronal plasticity and shaping neuronal morphology. Next to the fast electrochemical signaling, neurons employ a slower mechanism that involves a recently discovered class of proteins, the synaptonuclear messengers. Different studies showed the pivotal role of synaptonuclear messengers in the modulation of synaptic transmission at excitatory synapses. On the other hand, alterations of synaptonuclear messengers' activity have been correlated to synaptic failure as observed in different synaptopathies, including both neurodevelopmental disorders and neurodegenerative diseases. Ring Finger Protein 10 (RNF10) has been recently identified as a novel synapse-to-nucleus signaling protein that specifically links the activation of synaptic GluN2A-containing NMDA receptors (NMDARs) to gene expression. RNF10 synaptonuclear trafficking is responsible for the remodeling of dendritic spines that substance the postsynaptic modifications required for long-term potentiation (LTP). However, the molecular mechanisms leading to NMDAR/RNF10 complex disruption and for initiating the importin-mediated trafficking of RNF10 to the nucleus remain unclear. In this PhD project we investigated the molecular mechanisms that underlie RNF10 activation and in this matter we discovered a protein kinase C (PKC)-dependent phosphorylation event on RNF10-Ser31, which drives RNF10 synaptonuclear trafficking. Moreover, we show that pSer31-RNF10 plays a role both in synaptonuclear signaling and in neuronal morphology. In particular, the prevention of Ser31 RNF10 phosphorylation induces a decrease in spine density, neuronal branching, and CREB signaling, while opposite effects are obtained by mimicking a stable RNF10 phosphorylation at Ser31. Based on these results, we investigated the role of RNF10 *in vivo*, in the RNF10^{-/-} mouse model. In particular we studied the putative involvement of the synaptonuclear protein in neurodevelopment, focusing our attention on the first three weeks of postnatal life, which represents the critical period for neuronal differentiation and synaptogenesis in rodents. We found that RNF10^{-/-} mice have an alteration in brain morphology, in particular in the hippocampal area, and impaired cognition. At a microscopic level, RNF10^{-/-} deficiency alters the molecular composition and the morphology of the glutamatergic synapse. In the CA1 region of the Hippocampus, dendritic arborization of RNF10^{-/-} neurons is severely reduced and LTP induction is compromised. Overall, these results add novel information about the functional and structural role of synaptonuclear protein messengers in shaping dendritic architecture and regulating synaptic plasticity in hippocampal neurons.

ABSTRACT (ITALIANO)

I neuroni necessitano di un'attiva comunicazione tra sinapsi e nucleo per portare a termine modificazioni a lungo termine, come la regolazione della plasticità sinaptica o della morfologia neuronale. Accanto al signaling rapido di natura elettrochimica, i neuroni impiegano anche un meccanismo di comunicazione più lento, che coinvolge una classe di proteine scoperte recentemente, i messaggeri sinaptonucleari. Diversi studi hanno dimostrato l'importante ruolo di queste proteine nella modulazione della neurotrasmissione della sinapsi eccitatoria. Allo stesso tempo, alterazioni dell'attività dei messaggeri sinaptonucleari è stata correlata ad alterazioni sinaptiche come quelle osservate in diverse sinaptopatie, che includono sia patologie del neurosviluppo che neurodegenerative. Recentemente è stata scoperta un nuovo messaggero proteico sinaptonucleare, Ring Finger Protein 10 (RNF10), che associa specificamente l'attivazione dei recettori NMDA sinaptici, contenenti la subunità GluN2A, all'espressione genica. Il trafficking sinaptonucleare di RNF10 è responsabile del rimodellamento delle spine dendritiche funzionale alle modificazioni post-sinaptiche necessarie per il potenziamento a lungo termine (LTP).

Tuttavia i meccanismi che portano alla dissociazione del complesso RNF10/NMDA e che inducono la traslocazione di RNF10 al nucleo in maniera importina-mediata non sono stati ancora completamente chiariti. In questo lavoro di dottorato abbiamo studiato i meccanismi molecolari sottostanti all'attivazione di RNF10; in particolare abbiamo scoperto che la fosforilazione PKC-dipendente della Ser31 di RNF10 è un evento fondamentale per l'induzione del trafficking sinaptonucleare di RNF10. Inoltre abbiamo dimostrato che la fosforilazione della Ser31 riveste un ruolo importante sia nella trasduzione del segnale di RNF10 che nella regolazione della morfologia neuronale. In particolare, interferire con la fosforilazione della Ser31 di RNF10 porta alla riduzione della densità di spine dendritiche, della ramificazione dell'albero dendritico e dell'attivazione di CREB, mentre si ottengono effetti opposti quando viene mimata una fosforilazione costitutiva della Ser31 su RNF10. Sulla base di questi risultati, abbiamo studiato il ruolo di RNF10 in vivo, nel modello murino RNF10^{-/-}. In particolare abbiamo studiato il coinvolgimento della proteina sinaptonucleare nel neurosviluppo, focalizzando la nostra attenzione sulle prime tre settimane di vita postnatale, che rappresenta il periodo critico per la differenziazione neuronale e la sinaptogenesi nei roditori. Abbiamo scoperto che i topi RNF10^{-/-} hanno un'alterazione della morfologia cerebrale, in particolare nell'area dell'ippocampo, e deficit cognitivi. A livello microscopico, il deficit di RNF10^{-/-} altera la composizione molecolare e la morfologia della sinapsi glutamatergica. Nella regione CA1 dell'ippocampo, l'arborizzazione dendritica dei neuroni RNF10^{-/-} è gravemente ridotta e l'induzione dell'LTP è

compromessa. Nel complesso, questi risultati aggiungono nuove conoscenze sul ruolo funzionale e strutturale dei messaggeri delle proteine sinaptonucleari nel modellare l'architettura dendritica e nel regolare la plasticità sinaptica nei neuroni dell'ippocampo.

INTRODUCTION

The most prominent feature of the brain, the central organ of the human nervous system, is the ability to perceive, adjust and respond to external stimuli and inner changes of the organism.

The complexity of the structure and function of the brain are most appropriately understood from the perspective of their highly specialized cells: the neurons, interconnected, highly differentiated, bioelectrically driven, cellular units (over hundred billions) of the nervous system; and their more numerous support cells, the glia.

The first scientist to postulate that nervous system was composed of discrete neurons was Ramon y Cajal in his Neuron Doctrine, against the popular theory of the contiguous network of cells espoused by luminaries such as Camillo Golgi (Ramon y Cajal, 1893) (DeFelipe, 2015). Cajal also postulated that the dendritic spines were points of contact between two neurons and that, in reaching out from the dendritic shaft, they could facilitate diverse connections with axons from many different sources (Berry & Nedivi, 2017). Moreover Cajal had the intuition that the brain's adaptability to experiences depends on the strength of and modifications in neuronal connections, and that these changes could contribute to mental and memory processes. Donald Hebb, who proposed that changes of synaptic strength efficacy could mediate learning and memory processes, extended this view. From 1970 and throughout decades, many scientists contributed to the elucidation of the mechanistics of the functional and structural changes in neurons that substantiate memory formation, processes overall known as synaptic plasticity.

For the purpose of this dissertation, I will focus on the excitatory neurotransmission-dependent synaptic plasticity, starting from the description of the glutamatergic synapse.

1. Excitatory glutamatergic synapse

The vast majority of the excitatory neurotransmission in the central nervous system (CNS) is mediated by vesicular release of glutamate, reason why scientists usually refer to CNS excitatory neurons as glutamatergic neurons. Both the pre- and postsynaptic sides have precise molecular composition and organization (Renner & Triller, 2013). The presynaptic axon terminal, or synaptic bouton, is a specialized area within the axon of the presynaptic neuron and contains neurotransmitters enclosed in small membrane-bound spheres called synaptic vesicles, which are docked at the presynaptic regions called active zones. Neurotransmitters are released in the synaptic cleft, the narrow space (about 20 nm) between pre- and postsynaptic elements after the emergence of an action potential. On the postsynaptic side, responses to the release of

neurotransmitters are generated by a set of receptors and related proteins embedded in the so-called postsynaptic density (PSD). The PSD is an electron-dense thickening of the postsynaptic membrane that is found at synaptic junction, usually located at the head of the spine and it comprise several hundred proteins with a defined spatial organization (Ramm et al., 2006), including glutamate receptors and several scaffolding proteins involved in anchoring and trafficking neurotransmitter receptors, modulating their activity, and other signaling molecules (Paoletti, Bellone, & Zhou, 2013). When examined under an electron microscope, it is possible to classify synapses into two groups. Type 1 asymmetric synapses are characterized by rounded vesicles in the presynaptic cell, and a prominent protein rich postsynaptic density and are typically excitatory. Type 2 symmetric synapses in contrast have flattened or elongated vesicles, and do not contain a prominent postsynaptic density and are typically inhibitory (Gray, 1959). The release of glutamate activates both pre and postsynaptic G-protein-coupled metabotropic glutamate receptors (mGluRs) and ionotropic glutamate receptors (iGluRs) (Hansen et al., 2018) (Traynelis et al., 2010). iGluRs are ligand-gated cation channels that are divided into three major, structurally distinct, functional classes: the α -amino-3-hydroxy-5-methyl-4-isoxasolepropionic acid receptors (AMPA), kainate receptors (KARs), and NMDA receptors (NMDARs) (Traynelis et al., 2010).

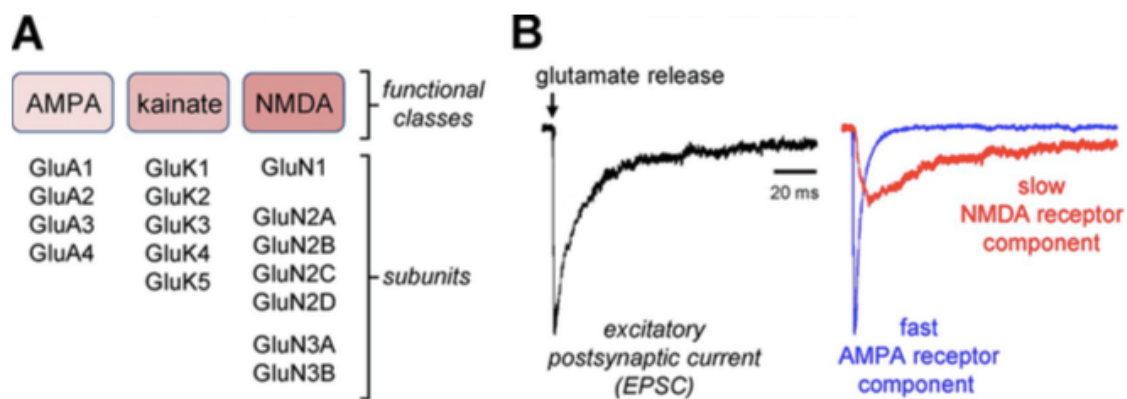


Figure 1. Functional classes of iGluRs. (A) iGluRs are divided into AMPA, kainate, and NMDA receptors with multiple subunits cloned in each of these functional classes. (B) EPSCs from central synapses can be divided into fast AMPA or slow NMDA receptor-mediated components in the absence of Mg^{2+} using the AMPA receptor antagonist CNQX or the NMDA receptor antagonist AP5. The figure is adapted from Traynelis et al. (2010)

1.1. AMPA Receptors

AMPA receptors are responsible for the rapid activation of the glutamatergic synapse, and are

activated after the binding to glutamate, becoming permeable to Na^+ . Unlike NMDARs, AMPARs can be activated by ligand binding at resting potentials to allow current flow (Traynelis et al., 2010). AMPAR activation is also one important gatekeeping element for relieving NMDAR voltage-dependent channel block by Mg^{2+} and permitting Ca^{2+} influx in the synapse, giving rise to the process that changes synaptic strength (Bliss and Collingridge, 1993; Huganir and Nicoll, 2013; Kessels and Malinow, 2009). In some cases, AMPAR may be Ca^{2+} permeable and trigger directly specific forms of postsynaptic plasticity (Cull-Candy et al., 2006; Liu and Zukin, 2007). AMPARs number, composition, partner interactions and post-translational modifications are rapidly affected by synaptic plasticity (Huganir and Nicoll, 2013; Newpher and Ehlers, 2008; Opazo and Choquet, 2011; Shepherd and Huganir, 2007). On the darker side, AMPAR activation mediates cell damage and excitotoxicity associated to various neuronal noxa (Bowie, 2008). AMPARs function as homo or heterotetramers made of four distinct subunits, GluA1-4. Each subunit contributes to the receptor properties, like channel opening time, ion permeability, trafficking properties etc., making heteromerization a considerable source of functional diversity (Seeburg and Hartner, 2003; Greger, Watson and Cull-Candy, 2017).

1.2. NMDA receptors

Several unique properties distinguish NMDARs from other ionotropic glutamate receptors, including voltage-dependent block by extracellular Mg^{2+} , high permeability to Ca^{2+} , and the requirement for binding of two co-agonists, glutamate and glycine (or D-serine), for channel activation (Traynelis et al., 2010). NMDARs allow influx of calcium ions, which act as a second messenger to elicit biochemical changes in the postsynaptic neuron and which confers on NMDARs a central role in both synaptic plasticity under physiological conditions and neuronal death under excitotoxic pathological conditions (Paoletti, 2007). NMDARs are heteromeric complexes composed by different subunits within a pool of three subtypes: GluN1, GluN2 and GluN3. There are eight different GluN1 subunits generated by alternative splicing of a gene, four different GluN2 subunits (A, B, C and D) and two GluN3 subunits (A and B), all of them encoded by separate genes (Dingledine et al., 1999). The consensus stoichiometry of NMDARs is a tetramer that most often incorporates two GluN1 and two GluN2 subunits of the same or different subtypes (Dingledine et al., 1999). In cells expressing GluN3, it is thought that this subunit co-assembles with GluN1 and GluN2 to form ternary tetrameric complexes (Sasaki et al., 2002). Each subunit has a typical modular architecture that is

made of four distinct domain: two large clamshell-like extracellular domains (the N-terminal domain (NTD) involved in assembly and channel allosteric modulation and the agonist-binding domain (ABD) that binds to glycine or D-serine in GluN1 and GluN3, and binds to glutamate in GluN2), a transmembrane domain (TMD) forming the ion channel, permeable to calcium, and a intracellular C-terminal domain (CTD) involved in receptor trafficking, anchoring and coupling with signaling. The NTD and CTD regions are the most divergent and account for much of the functional diversity of NMDARs (Paoletti et al., 2013; Traynelis et al., 2010; Hansen et al., 2018). The cytoplasmic CTDs are the least conserved region among NMDAR subunits, and thus they are the site of several subunit-specific regulations that have implication for receptor trafficking, localization and signaling (Martel et al., 2012).

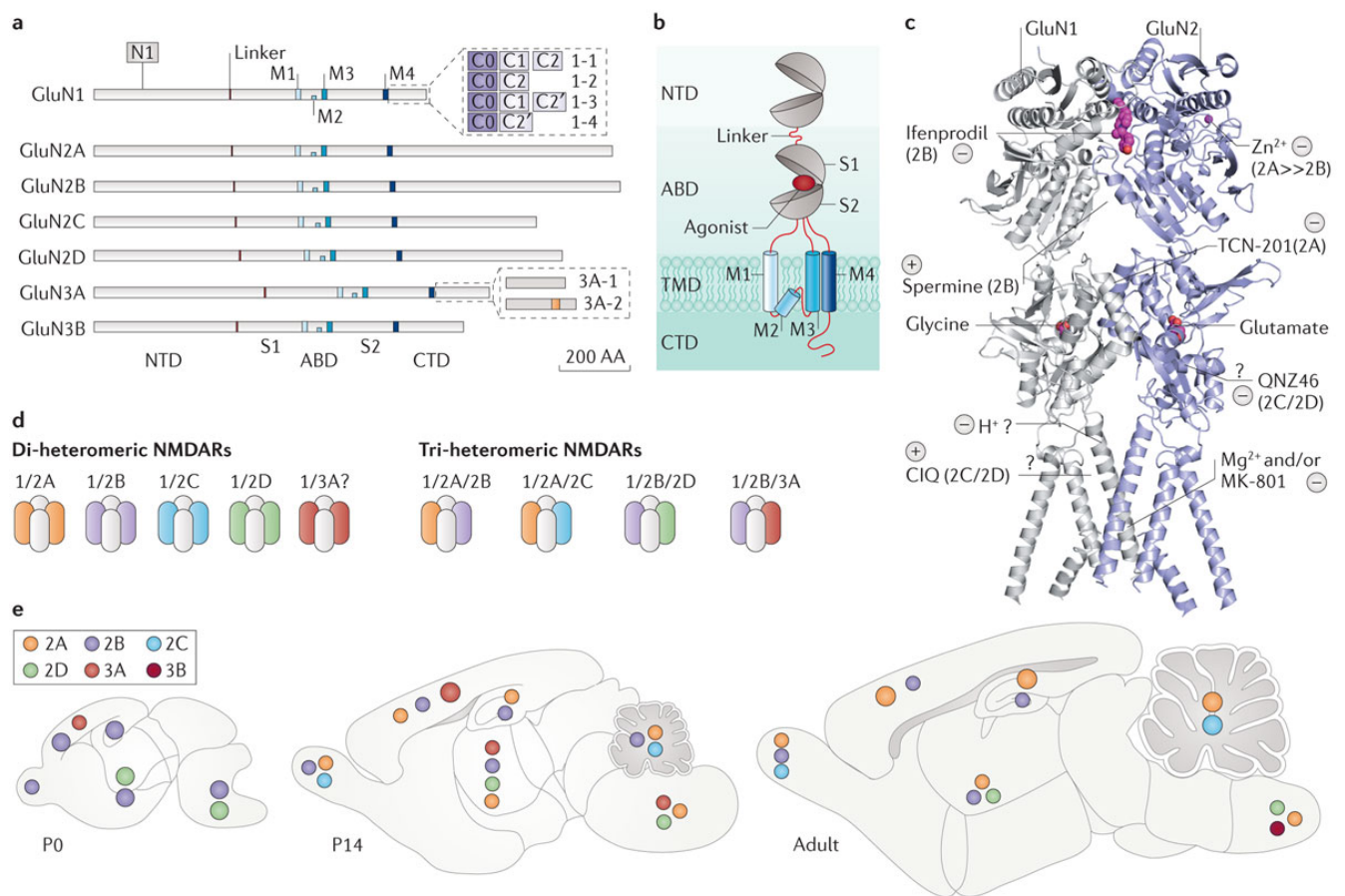


Figure 2. All GluN subunits share a modular architecture. NMDARs Extracellular harbor with multiple binding sites for small molecules acting as allosteric modulators. A sample of various populations of di-heteromeric and tri-heteromeric NMDARs. (Paoletti, Bellone and Zhou, 2013).

NMDARs are expressed throughout the CNS and play key physiological roles in synaptic function, learning, and memory and they are also implicated in the

pathophysiology of several CNS disorders (Traynelis et al., 2010) (Hansen et al., 2018) (Paoletti et al., 2013). At central excitatory synapses, glutamate released in the synaptic cleft will bind to AMPA (and/or kainate) and NMDARs, inducing the necessary conformational changes that trigger opening of the ion channel pore, a process referred to as gating (Hansen et al., 2018). As mentioned above, NMDARs show several unique characteristics, including calcium permeability and the voltage-dependent magnesium block inside the ion channel. Thus, to allow calcium influx, NMDARs requires both presynaptic glutamate release as well as postsynaptic depolarization to remove the magnesium block (Traynelis et al., 2010). This depolarization is operated by the influx of sodium, after AMPAR activation by presynaptic glutamate release. The NMDAR-mediated component of the EPSC continues to pass current for tens to hundreds of milliseconds after synaptic glutamate is removed (Lester, Clements, Westbrook, & Jahr, 1990). The remove of the block from the NMDA channel allows substantial influx of external Ca^{2+} into the dendritic spine (Hansen et al., 2018). This increase in intracellular calcium serves as a signal that leads to multiple changes in the postsynaptic neuron, including changes that ultimately produce either short-term or long-term changes in synaptic strength (Traynelis et al., 2010) (Paoletti et al., 2013). In the Hippocampal CA1 postsynaptic neuron, the most extensively studied and characterized, two different types of NMDA receptors can be found, depending on the localization on the cell membrane, activating different signaling pathways. Synaptic NMDA receptors are mainly composed by di-heteromeric GluN1/GluN2A or tri-heteromeric GluN1/GluN2A/GluN2B and play a protective role by promoting nuclear signaling to cAMP responsive element binding protein (CREB), inducing gene expression of brain-derived neurotrophic factor (BDNF), regulating extracellular signal-regulated kinases (ERK) and anti-apoptotic pathways. By contrast, extra-synaptic NMDA receptors are mainly composed of GluN1/GluN2B subunits and antagonize signaling to CREB, block BDNF expression, and cause mitochondrial membrane potential loss and cell death (Hardingham & Bading, 2010).

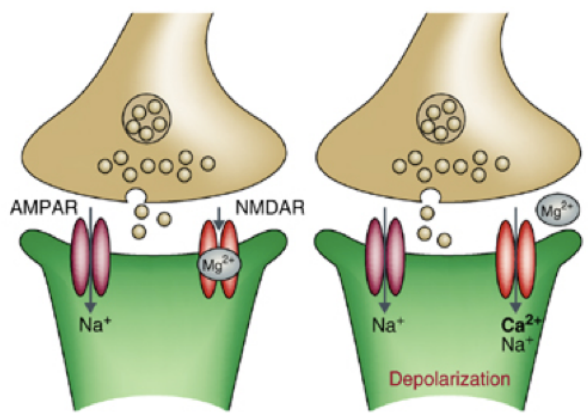


Figure 3. Model of synaptic transmission at excitatory synapses. During basal synaptic transmission (left panel), synaptically released glutamate binds both the NMDA and AMPARs. Na^+ flows through the AMPAR channel but not through the NMDAR channel because of the Mg^{2+} block of this channel. Depolarization of the postsynaptic cell (right) relieves the Mg^{2+} block of the NMDAR channel and allows both Na^+ and Ca^{2+} to flow into the dendritic spine. The resultant increase in Ca^{2+} in the dendritic spine is necessary for triggering the subsequent events that drive synaptic plasticity. (Adapted from Citri and Malenka, 2008)

NMDARs have long been thought to be less dynamic than AMPARs, especially at mature synapses in which long term plasticity is usually mediated by changes in AMPAR-mediated transmission. However, recent evidence indicates that subunit composition of NMDARs is not static but dynamically regulated in response to activity-dependent long-term plasticity, not exclusively during development, but can also occur at adult and mature synapses. Changes in subunit can be rapid and can have profound influences on the functions of synapses and networks (Paoletti et al., 2013).

2. SYNAPTIC PLASTICITY

One of the most important properties of the mammalian brain is its plasticity, the capability of the neuronal activity generated by an experience to modify neuronal circuits function. Synaptic plasticity specifically refers to the activity-dependent modification of the strength or efficacy of synaptic transmission at preexisting synapses. It is believed to play a central role in learning and memory formation (Ho, Lee, & Martin, 2011; Citri & Malenka, 2008), as experiences can modify synapses, favoring some neuronal pathways within a circuit and weakening others. Synaptic plasticity is also thought to play an important role in early development of neuronal circuits and impairment in synaptic plasticity mechanisms contribute to several neuropsychiatric disorders (Citri & Malenka, 2008). A variety of cell biological processes, including synaptic vesicle release and recycling, modification of synaptic components, neurotransmitter receptor trafficking and stimulus-induced changes in gene expression within neurons are necessary for many forms of plasticity. Several different types of synaptic plasticity have been described; both presynaptic and postsynaptic mechanisms can contribute to it, including short-term and long-term synaptic plasticity.

In this dissertation we focused on long-term synaptic plasticity mechanisms, which lead to long-lasting, activity-dependent modifications in synaptic strength. In particular, at excitatory synapses, activity-dependent modification in the number of postsynaptic glutamate receptors is one of the mechanisms responsible for NMDAR-dependent

long-term potentiation (LTP) or long-term depression (LTD), which lead to long lasting synaptic strengthening and weakening, respectively. LTP and LTD are two important forms of bidirectional long-term synaptic plasticity which, while different in molecular mechanisms, can coexist in the same synapse (Alfred Sloan, Beckman Foundations, Sheng, & Jong Kim, 2001)

2.1. NMDAR-dependent synaptic plasticity

The most extensively studied and therefore prototypic forms of long-term synaptic plasticity are the long-term potentiation (LTP) and long-term depression (LTD) observed in the CA1 region of the hippocampus, which are triggered by activation of *N*-methyl-D-aspartate (NMDA) receptors, and thus called NMDAR-dependent (Citri & Malenka, 2008). LTP and LTD are both dependent on postsynaptic increases in intracellular calcium (Alfred Sloan et al., 2001). A central puzzle in synaptic plasticity is how the activation of and calcium influx through NMDARs can give rise to opposite results (LTP or LTD). The predominant current hypothesis is that quantitative properties of the postsynaptic calcium signal within dendritic spines dictates whether LTP or LTD is triggered, with LTD requiring a modest increase in calcium, whereas LTP requires an increase beyond some critical threshold value (Alfred Sloan et al., 2001; Citri & Malenka, 2008).

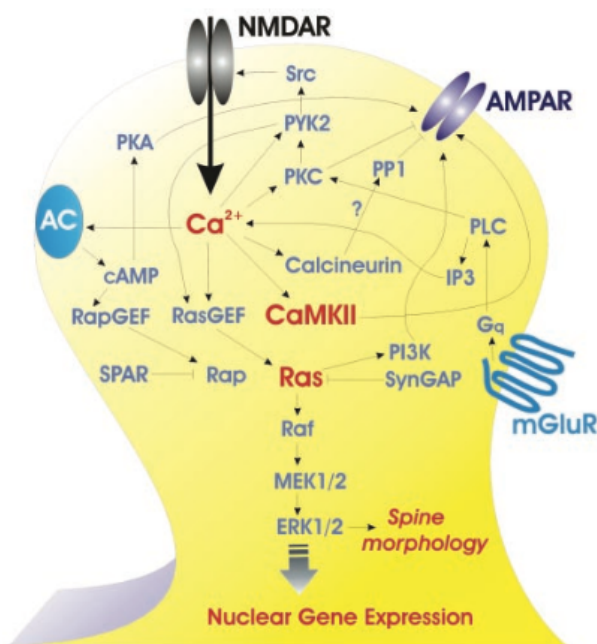


Figure 4. Postsynaptic glutamate receptor signaling pathways. Signaling pathways activated by calcium influx through NMDARs. Figure adapted from Sheng and Kim, Science 2002.

2.2.1 LTP and LTD

LTP can be generated rapidly and is strengthened and prolonged by repetition and it exhibits cooperativity, associativity, and input specificity (Citri & Malenka, 2008). Cooperativity means that LTP can be induced by the coincident activation of a critical

number of synapses. Associativity is the capacity to potentiate a weak input (a small number of synapses) when it is activated in association with a strong input (a larger number of synapses). Input specificity indicates that LTP is elicited only at activated synapses and not at adjacent, inactive synapses on the same postsynaptic cell (Citri & Malenka, 2008a). Long-term depression can be described as either homosynaptic or heterosynaptic. Homosynaptic LTD is associative as LTP; it is restricted to the individual synapse that is activated by a low frequency stimulus (Escobar and Derrick, 2007). In other words, this form of LTD is activity-dependent, because the events causing the synaptic weakening occur at the same synapse that is being activated (Nicoll et al., 2008). Heterosynaptic LTD, in contrast, occurs at synapses that are not potentiated or are inactive. The weakening of a synapse is independent of the activity of the presynaptic or postsynaptic neurons as a result of the firing of a distinct modulatory interneuron. Thus, this form of LTD impacts synapses nearby those receiving action potential.

1) Induction

Two major types of ionotropic glutamate receptors contribute to the postsynaptic response at glutamatergic synapses, AMPARs and NMDARs. These receptors are often found co-localizing on individual dendritic spines. The AMPAR has a channel that is permeable to monovalent cations (Na^+ and K^+), and activation of AMPARs provides most of the inward current that generates the excitatory synaptic response when the cell is close to its resting membrane potential. As previously mentioned, in contrast to AMPARs, the NMDAR exhibits strong voltage dependence because of the block of its channel at negative membrane potentials by extracellular magnesium. As a result, NMDARs contribute little to the postsynaptic response during basal synaptic activity. However, when the cell is depolarized, magnesium dissociates from its binding site within the NMDAR channel, allowing ions to enter the cell. Importantly, unlike AMPAR channels, the NMDAR channel allows calcium as well as sodium to enter the postsynaptic dendritic spine. Thus, the induction of LTP requires activation of NMDARs during strong postsynaptic depolarization leading to an increase in postsynaptic calcium concentration, which likely has to reach some critical threshold value to activate the biochemical processes necessary for LTP (Citri & Malenka, 2008; Malenka, 1991). Similarly to LTP, LTD also requires a calcium entry in the postsynaptic terminal, but of modest entity, as the one induced by low frequency stimulation (Xiao et al., 1995; Yi et al., 1995).

Because its contribution to postsynaptic responses requires both presynaptic release

of glutamate and postsynaptic depolarization due to the simultaneous activation of a population of synapses, the NMDAR is often referred to as a 'coincidence detector' (Malenka and Nicoll, 1993). These properties of NMDARs also explain the basic properties of LTP. Cooperativity and associativity occur because of the requirement for multiple synapses to be activated simultaneously to generate adequate postsynaptic depolarization to remove the magnesium block of the NMDAR. Input specificity is due to the compartmentalized increase in calcium, which is limited to the postsynaptic dendritic spine and does not influence adjacent spines (Nicoll, Kauer, & Malenka, 1988).

2) Signal transduction mechanisms

The increase in intracellular calcium activates multiple downstream signaling enzymes. An extensive number of signal transduction molecules have been suggested to play a role in translating the calcium signal that is required to trigger LTP or LTD into the long-lasting increase or decrease in synaptic strength (Citri & Malenka, 2008). Strong evidence indicates that calcium/calmodulin (CaM)-dependent protein kinase II (CaMKII) is a key component of the molecular machinery for LTP. CaMKII undergoes autophosphorylation after the triggering of LTP which renders the kinase autonomously active (Barria, Muller, Derkach, Griffith, & Soderling, 1997). Neuronal activity also translocates CaMKII to the PSD, where it can phosphorylate many PSD proteins, including glutamate receptors. Several other kinases have been implicated in the triggering of LTP. The extracellular signal-regulated kinase (Erk)/mitogen-activated protein kinase (MAPK) pathway has also been suggested to be important for LTP, as well as some forms of learning and memory. Protein kinase C and in particular the atypical PKC isozyme, PKM ζ , has received attention because this isozyme is rapidly expressed upon induction of LTP and recent studies have implicated PKM ζ in the maintenance of the late phase of LTP (Serrano, Yao, & Sacktor, 2005). The precise mechanism by which Ca²⁺ elicits NMDAR LTD is unclear. An hypothesis for the signal transduction pathway triggering LTD suggested that while LTP was due to preferential activation of protein kinases, LTD involves activation of calcium-dependent protein phosphatases, such as calcineurin; LTD has been found to correlate with dephosphorylation of PKC and PKA substrates, among which the dephosphorylation of Ser845 of GluR1 AMPAR subunit (Lee, Barbarosie, Kameyama, Bear, & Huganir, 2000; Citri & Malenka, 2008). Hippocalcin has also been identified as a Ca²⁺ sensor mediating induction of NMDAR-dependent LTD at CA1 synapses (Jo et al., 2010).

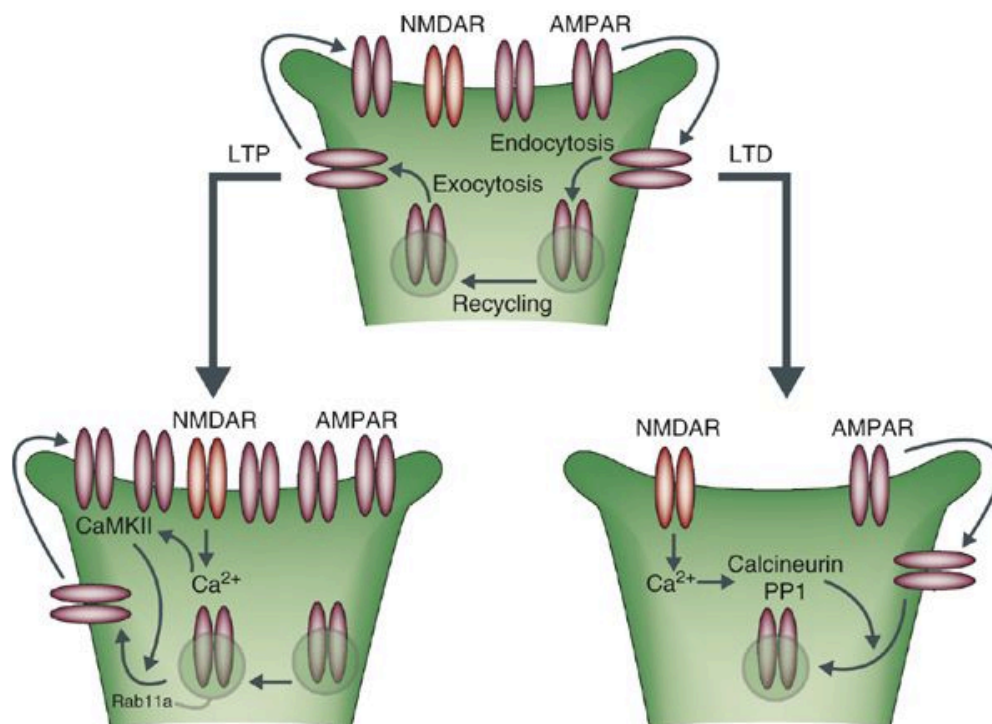


Figure 5. Model of AMPAR trafficking during LTP and LTD. In the basal state (on top), receptors cycle between the postsynaptic membrane and intracellular compartments. This is achieved through lateral mobility of the receptors out of the synapse into endocytic zones, where they are endocytosed into early endosomes in a clathrin- and dynamin-dependent manner. Normally, the receptors are transferred to recycling endosomes and returned to the plasma membrane by exocytosis, followed by lateral movement into the synapse where they are retained through interaction with MAGUKs. Following induction of LTP, there is enhanced receptor exocytosis and stabilization at the synapse through a calcium-driven process that involves CAMKII and fusion of recycling endosomes. Following the induction of LTD, enhanced endocytosis at extrasynaptic sites occurs in a process that is calcium-dependent and involves protein phosphatases. The figure is adapted from Citri & Malenka (Neuropsychopharmacology, 2008).

3) Expression mechanisms

The major mechanism of LTP expression at hippocampal synapses involves an increase in the numbers of AMPARs within the postsynaptic density, obtained through activity-dependent changes in AMPAR trafficking and the incorporation of additional AMPARs into the postsynaptic plasma membrane (Bredt & Nicoll, 2003; Derkach, Oh, Guire, & Soderling, 2007). The cytoplasmic tails of each AMPARs tetramer subunit contain multiple phosphorylation sites and changes in AMPAR function and trafficking during synaptic plasticity are mostly due to phosphorylation-induced changes in its function and abundance at the synapse (Citri & Malenka, 2008). It's believed that the delivery of new AMPARs to synapses occurs first by exocytosis at extrasynaptic sites

followed by lateral diffusion within the plasma membrane to PSDs, where the mobility of the receptors is greatly reduced thanks to the binding to scaffold proteins (Bredt & Nicoll, 2003; Citri & Malenka, 2008). Conversely, the expression mechanism of NMDAR-dependent LTD is due to activity-dependent endocytosis and removal of synaptic AMPARs (Bredt & Nicoll, 2003). Consistent with the key role for protein phosphatases in LTD induction, the endocytosis of synaptic AMPARs is regulated by calcium-dependent dephosphorylation followed by dissociation of AMPARs from their anchoring at the PSD (Beattie et al., 2000). In the end, synaptic AMPARs receptors diffuse away from the PSD and then undergo clathrin-mediated, dynamin-dependent endocytosis (Bredt & Nicoll, 2003). AMPAR trafficking occurs constitutively under basal conditions and is activity-modulated through changes in cytoskeleton dynamics, as well as interactions with scaffolding proteins and accessory subunits. In the end, complex patterns of phosphorylation and of other post-translational modifications (palmitoylation or ubiquitination) combine to regulate AMPAR localization and exo/endocytosis (Van Der Sluijs & Hoogenraad, 2011; Ho et al., 2011).

4) Maintenance

The mechanisms that allow these processes to persist for hours, days or even longer hold a great relevance in understanding learning and memory functions (Citri & Malenka, 2008). The persistence of LTP, the so called "late phase LTP", is commonly assumed to depend upon local dendritic protein synthesis, which supplies needed components to the synapse, as well as transcription in the nucleus and new gene expression (Reymann & Frey, 2007; Sutton & Schuman, 2006; Zhou et al., 2006). Several mRNA of iGluRs, CaMKII and others signaling proteins are found in dendrites and the trafficking and translation of these mRNA seems to be regulated by local activity (Citri & Malenka, 2008). The signaling to the nucleus required for long-lasting LTP has been suggested to depend on a number of protein kinases including CaMKII, CaMKIV, PKA, PKC and Erk-MAPK which activate key transcriptional factors including CREB and c-Fos (Thomas & Huganir, 2004). These transcriptional complexes very likely promote expression of effector genes that are required for the maintenance of the synaptic enhancement (Citri & Malenka, 2008). A compelling possibility for a long-term maintenance mechanism of LTP is the structural remodeling of potentiated synapses (Lüscher, Nicoll, Malenka, & Muller, 2000). Dendritic spines are dynamic structures with a variety of shapes and sizes and can undergo rapid shape shifts that are affected by neuronal activity. Morphological changes in dendritic spines reported to follow LTP include growth of new dendritic spines, enlargement of pre-existing ones along with their PSDs and the splitting of single PSDs and spines into two functional

synapses (Abraham & Williams, 2003). Although little is known about the maintenance of LTD, there is evidence that LTD is accompanied by a shrinkage in the size of dendritic spines (Nägerl, Eberhorn, Cambridge, & Bonhoeffer, 2004) and that relies on both presynaptic and postsynaptic expression mechanisms (Amtul and Rahman, 2015).

3. DENDRITIC SPINES: THE LOCUS OF STRUCTURAL AND FUNCTIONAL PLASTICITY

As mentioned above, most excitatory synapses in mammalian neurons are located on dendritic spines, the small protrusions studding many neuronal dendrites (Berry & Nedivi, 2017). Ever since their first detection by Ramon Y Cajal, dendritic spines have been demonstrated to undergo notable changes in morphology, size and density along dendrites relative to other organelles, and consequently they have been postulated to detain the anatomical locus of neuronal plasticity (Sala & Segal, 2014).

3.1. Classification

Classically, dendritic spines consist of bulbous heads attached to the dendritic shafts by narrow necks (Nimchinsky et al., 2002; Rao et al., 1998). The size, shape and number of dendritic spines display a heterogeneous variability even within a single dendritic segment of a certain neuron. The number of dendritic spines varies from 1 to 10 spines/ μm length of a dendrite depending on the type of neuron and the developmental stage (Calabrese et al., 2006). Dendritic spines in a matured brain are typically $<3 \mu\text{m}$ in length with a spherical head $0.5\text{--}1.5 \mu\text{m}$ in diameter that is connected to the parent dendrite by a thin neck ($< 0.5 \mu\text{m}$ in diameter) (Phillips et al., 2015). Classically, dendritic spines are classified into 3 types on the basis of their morphology (Harris et al., 1992; Peters and Kaiserman-Abramof, 1970) as mentioned below.

- Mushroom shaped spines, defined by their characteristically large bulbous head and narrow neck, contain the largest excitatory synapses. Mushroom-like spines are the most stable.
- Thin spines are smaller, lack the large bulbous head and thin neck, and contain smaller excitatory synapses. They are less stable and more prone to morphological changes.

- Stubby spines are shorter and squatter than thin spines, without an obvious constriction between the head and the attachment to the shaft, and are viewed as immature structures based on their prevalence during early postnatal development and relative scarcity in the mature brain (Harris et al., 1992).

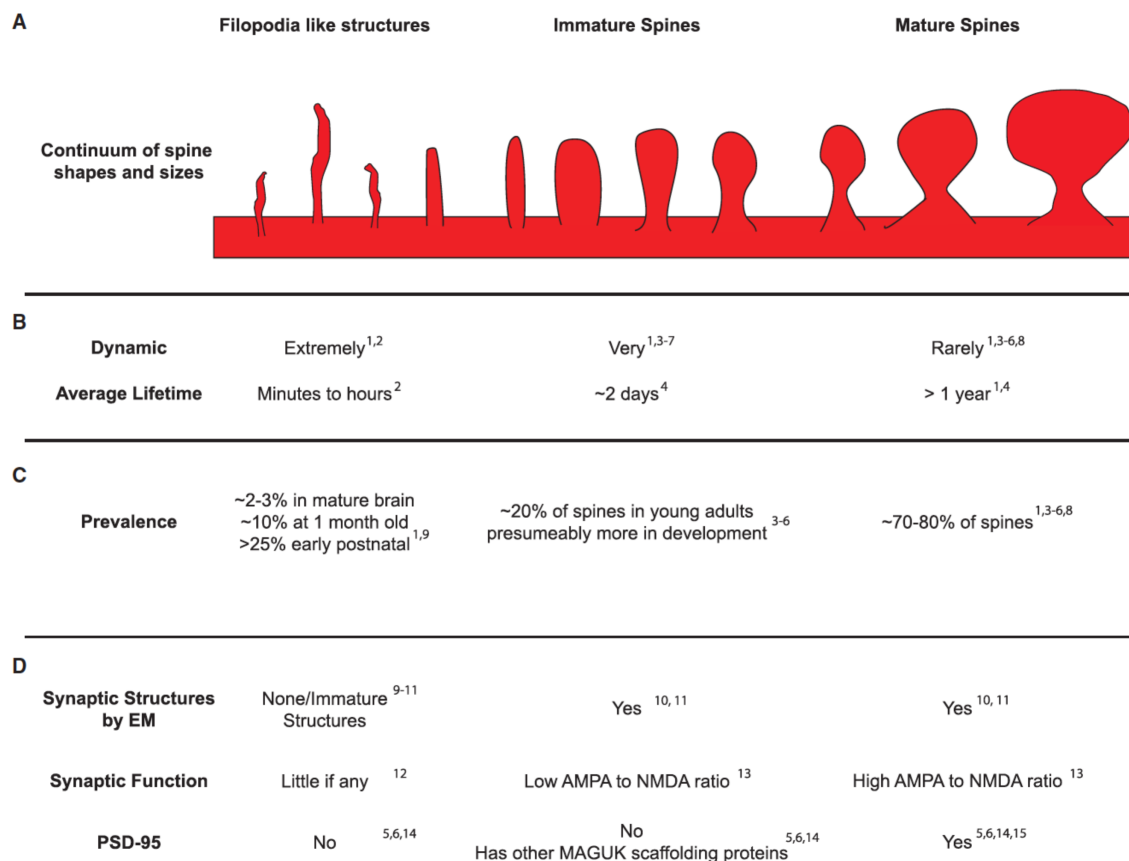


Figure 6. Spines Exist on a Continuum of Morphologies and Functions from Nonfunctional Filopodia-like Structures to Large Mature Spines. (A) Diagram showing continuum of spine shapes. These spines can be grouped into three separate categories, filopodia-like structures, immature spines, and mature spines. Distinguishing between these categories based on morphology is extremely difficult due to the limited resolution of light microscopy. (B) The history of a spine can distinguish between these types. (C) In adults, the majority of spines contain a mature synaptic contact, while 20% are either immature or filopodia like. (D) The three categories of spines are difficult to distinguish based on any one category alone. However, by comparing across several criteria the differences become clearer.

It was not until the emergence of electron microscopy that scientist had the possibility to directly visualize the synapses on dendritic spines and show that spines were the major site of excitatory synaptic plasticity (Berry & Nedivi, 2017). The dendrites of a single neuron can contain hundreds to thousands of spines and a typical mature spine has a single synapse located at its head (Sorra & Harris, 2000), even if synaptic potentiation processes may increase this number. Dendritic spines serve as compartmentalized signaling units and are not static structures, they can change their shape and size, as

well as form or disappear during synaptic plasticity (Hering & Sheng, 2001). Transmission Electron Microscopy (TEM) images show that spines characteristically contain what is classified as a type 1 asymmetric synapse, defined as a synapse with a thick (protein rich) PSD apposed by a presynaptic active zone full of round neurotransmitter vesicles (Gray, 1959; Hersch and White, 1981; LeVay, 1973; Parnavelas et al., 1977). Type 1 synapses were then associated to excitatory inputs after electrophysiology experiments in the cerebellum showed the excitatory nature of granule cell input onto Purkinje cell dendrites (Uchizono, 1965). Later, immuno-EM showed that synaptic boutons positive for glutamate only form synaptic contacts with type 1 synapses and not type 2 symmetric synapses, devoid of a visible PSD and typically inhibitory (DeFelipe et al., 1988). The PSD that defines type 1 synapses has been characterized as an articulated network of proteins forming a highly regulated scaffold complex that anchors the glutamate receptors at the postsynaptic membrane (reviewed in Sheng and Hoogenraad, 2007).

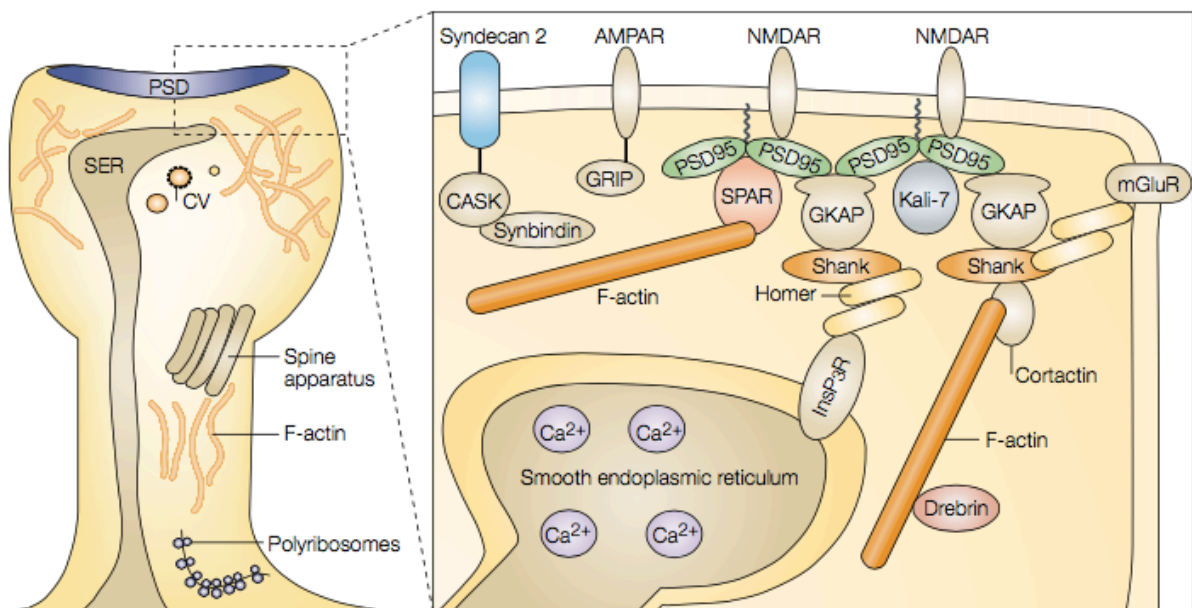


Figure 8. Structure of a mushroom dendritic spine. A dendritic spine contains various organelles, including smooth endoplasmic reticulum (SER), which extends into the spine from SER in the dendritic shaft. The SER in spines functions as an intracellular calcium store from which calcium can be released in response to synaptic stimulation. Polyribosomes have been detected in dendritic shafts, often at the base of spines, and occasionally extending into spines, indicating that protein translation might occur within the immediate postsynaptic compartment. The enlarged box illustrates specific proteins and protein-protein interactions within the PSD. The figure is adapted from Hering and Sheng (2001).

3.2. Morphogenesis

In the early postnatal stage, the dendrites lack spines and synapses. During synaptogenesis, dactylomorph actin-rich protrusions called 'filopodia' emerge from dendrites and form synaptic contacts with nearby axons (Portera and Yuste, 2001; Zhang and Benson, 2000; Ziv and Smith, 1996). On average a filopodium ranges from 3 to 40 μm in length (García-López et al., 2010) and is an extremely mobile structure that protrudes or retracts transiently to form synapses with adjacent dendritic shafts or to a new small protospine, the functional stadium that follows the transformation of a filopodium upon synaptic contact. (Dailey and Smith, 1996; Portera-Cailliau et al., 2003). In turn, the protospines undergo morphological transformations and turn either into mushroom or thin dendritic spines (Majewska et al., 2006). The fluctuation of synaptic activity and strength translates into the fluctuation of spines formation and maturation during neuronal life (Hotulainen and Hoogenraad, 2010). However, not all the filopodia progress into spines (Ziv and Smith, 1996); in fact only a small portion of filopodia (0.2%) stimulated during synaptic activity mature into functional spines (Majewska et al., 2006).

The relative abundance of filopodia versus mushroom spine types, the extreme ends of the morphological spectrum, varies during neurodevelopment and goes along with the overall rate of spine dynamics. Filopodia are prevalent during early postnatal development, when synapse formation and selection is at its peak, and, with maturation, are replaced by larger spines (Fiala et al., 1998). In mice at 2 weeks of age, more than half of all dendritic protrusions are filopodia like. This peak number drops to 10% at 1 month and to 3% in the adult (Zuo et al., 2005). This age-dependent decline in the number of filopodia along with the concomitant increase in larger spines overlaps with the age-dependent stabilization of spine dynamics overall (Holtmaat et al., 2005; Majewska et al., 2006; Zuo et al., 2005).

The maturation of small, highly dynamic spines or filopodia into larger, stable spines occurs not just at the population level, but also at the level of the individual spine. In both culture and in vivo, filopodia can form, stabilize, and grow into larger functional spines, suggesting that they represent an early stage of spine formation (Dailey and Smith, 1996; Ziv and Smith, 1996; Zuo et al., 2005). Similar to the developmental progression from small, dynamic filopodia to larger, stable spines, new spines formed in hippocampal slice cultures after activity blockade often first appear as filopodia (Kirov and Harris, 1999; Petrak et al., 2005). Like spine emergence, spine stabilization is also activity dependent (Engert and Bonhoeffer, 1999; Maletic-Savatic et al., 1999). In

addition to varying in shape and size, spines also differ in their content of organelles, postsynaptic receptors and other PSD proteins; in particular, large spine heads contain more receptors and shows a greater area of the PSD and, as the size of the spine head and the volume of the spine correlate with synaptic strength, the growth of the spine head correlates to a strengthening of synaptic transmission (Holtmaat & Svoboda, 2009).

A key step in spine maturation is the synaptic incorporation of PSD-95, protein that is a fundamental part of the PSD and provides the scaffold for clustering and stabilizing glutamate receptors at excitatory synapses (extensively reviewed in Kim and Sheng, 2004). PSD-95 possesses many protein-protein interaction domains, in particular various PDZ domains, through which is able to organize the clustering of iGluR: the MNDAR binds PSD-95 directly through a PDZ-binding domain (Kornau et al., 1995) and AMPAR via small transmembrane AMPA receptor regulatory proteins (TARPs) such as stargazin (Cheng et al., 2000; Nicoll et al., 2006; Schnell et al., 2002).

Some imaging experiments clarified that, like the developmental shift in spine morphologies, the developmental maturation of glutamatergic synapse scaffolding protein complex is displayed not just at the population level, but also at the individual spine level. In hippocampal organotypic slice cultures newly formed spines accumulate endogenous PSD-95 in 24 hours (and are consequently stabilized), but other members in the same protein family such as PSD-93, SAP102, and SAP97 show up much earlier and facilitate AMPA receptor targeting to the nascent synapse (Lambert et al., 2017). These scaffolders contribute to a temporary stability of the spine (Lambert et al., 2017), it's just upon the activity-dependent recruitment of PSD-95 that long-term stability is definitely obtained (De Roo et al., 2008; Lambert et al., 2017). In vitro studies expressing a fluorescently tagged version of PSD-95 suggest that the majority of new spines are initially deficient of PSD-95 (Chen and Featherstone, 2005; De Roo et al., 2008; Lambert et al., 2017; Waites et al., 2005). In dissociated neuronal cultures, PSD-95-GFP localization in spines takes place within a few minutes to hours after initial contact between the nascent spine and a presynaptic partner (Bresler et al., 2001; De Roo et al., 2008; Friedman et al., 2000; Okabe et al., 2001). In organotypic slice cultures, this process is much longer, and can take up to 24 hours as described before (De Roo et al., 2008; Lambert et al., 2017). In addition to it, the recruitment of PSD-95-GFP in synapses has been shown to be activity-dependent (De Roo et al., 2008; Taft and Turrigiano, 2013) and necessary for the activity-dependent stabilization of glutamatergic synapses and spines (Ehrlich et al., 2007). Its presence in spines was shown to provide an excellent prediction factor for the subsequent stabilization (De Roo et al., 2008; Ehrlich et al., 2007; Taft and Turrigiano, 2013).

3.3. Plasticity of dendritic spines

As mentioned above, many neuroscientists tried to characterize the nature of spine dynamics like; what collectively emerged is that changes in their shape and size depend upon the strength of the synaptic stimuli (Calabrese et al., 2006). Advance imaging experiment results suggest that dendritic spines are highly dynamic structures that embody the fundamental morphological changes of synaptic plasticity, like the de-novo formation of synapses, the decay of existing synapse, and turnover of dendritic spines underlie the experience-dependent plasticity processes (Bourne and Harris, 2012; Caroni et al., 2012; Hill and Zito, 2013; Holtmaat and Svoboda, 2009; Kasai et al., 2010). In the experimental setup, synaptic plasticity is demonstrated in terms of LTP and LTD induction which could be otherwise defined as long-lasting enhancement or the reduction of synaptic transmission, respectively (Bliss and Lomo, 1973; Bliss and Collingridge, 1993; Malenka and Bear, 2004; Malenka and Nicoll, 1999). In primary hippocampal neurons, the activation of NMDAR via chemically induced LTP (cLTP) (Engert and Bonhoeffer, 1999; Maletic-Savatic et al., 1999) different effects have been reported on spines:

- Rapid enlargement of spine heads (Kopec et al., 2006; Lang et al., 2004; Park et al., 2006) that precedes the increase in AMPA receptor abundance (Kopec et al., 2006).
- Rapid formation of new spines (Lin et al., 2004; Nägerl et al., 2004; Park et al., 2006).
- Stabilization of newly formed spines (Harvey and Svoboda, 2007; Matsuzaki et al., 2004; Tanaka et al., 2008).

The increased in of spine head volume is mainly due to the appearance of a complex PSD (Popov et al., 2004) followed by the accumulation of more AMPA and NMDA receptors (Kopec et al., 2006) and filamentous actin levels (Kramár et al., 2006; Lin et al., 2005) along with a significant increase in the number of recycling endosomes, coated vesicles (Harris et al., 1992) and amorphous vesicular bodies (Park et al., 2006), polyribosomes (Ostroff et al., 2002), and mitochondria (Li et al., 2004). It's not surprising that PSD-95 levels rise together with the enrichment of spines PSD induced by LTP; this increase in the protein scaffolding protein levels that accompanies spine enlargement has a similar time delay to that of PSD-95 accumulation after contact between a nascent spine and its presynaptic partner (Bosch et al., 2014; Meyer et al., 2014). Additional proofs of concept of the correlation between PSD-95 presence and

the stability of spines and synapses are given by knockdown and overexpression experiments. Indeed knockdown of PSD-95 in hippocampal slice cultures leads to an increased spine turnover rate, and a failure to add and stabilize spines after LTP induction (Ehrlich et al., 2007). In contrast, high levels of PSD-95 overexpression lead to an increased spine density as well as average spine size implying a role for PSD-95 in spine stabilization and maturation (El-Husseini et al., 2000).

On the other hand, low frequency stimulation of the synapse activates NMDA receptors to produce LTD (Lynch et al., 1977) which causes the removal of postsynaptic AMPA receptors and loss of dendritic spines (Lee et al., 2002; Lüscher et al., 1999; Man et al., 2000; Nägerl et al., 2004; Snyder et al., 2001; Xiao et al., 2001; Zhou et al., 2004). The main changes observed after LTD induction are:

- Consistent reduction in the size of dendritic spines (Nägerl et al., 2004; Okamoto et al., 2004).
- Faster shrinkage of spine head (Zhou et al., 2004).
- Spines density decreased and/or filopodia retracted (Zhou et al., 2004).

Both LTD and spine shrinkage require the activation of NMDA receptors and calcineurin (Zhou et al., 2004), and spine remodeling is mediated by the activation of cofilin (a family of actin binding proteins involved in actin filament disassembling), indicating the involvement of various downstream signaling pathways in dendritic spine shrinkage and LTD. Several studies have also shown that NMDA receptor hypofunction leads to reduction in spine numbers (Brigman et al., 2010; Ramsey et al., 2011; Roberts et al., 2009; Ultanir et al., 2007).

4. SYNAPSE-TO-NUCLEUS COMMUNICATION

Neurons are extremely polarized cells in which dendrites may extend for hundreds of microns; as a consequence synapses and nucleus are usually very distant from each other and need to be functionally connected through a signal transduction cascade (Lim, Lim, & Ch'ng, 2017; Herbst & Martin, 2017). As mentioned above, neuronal plasticity includes modifications in synaptic structure and function, and, in particular, long-term modifications require new protein synthesis and new gene transcription (Alberini, 2009). A crucial step in this process is how to relay a stimulus that comes at synaptic level to the start of gene transcription in the nucleus. Neurons employ different mechanisms to communicate extracellular signals from synapses to the nucleus: rapidly via electrochemical signaling or calcium waves or slowly through the physical

translocation of signaling proteins from synapses to the nucleus (Herbst & Martin, 2017). These two forms of synapse-to-nucleus communication generate two waves of information with different content, temporal properties and effect on gene transcriptions.

4.1. Activity-dependent calcium signaling

Calcium, as a potent activator of intracellular signaling cascade, is physiologically maintained in neurons at very low concentration within the cytoplasm. By maintaining low levels of intracellular calcium, the neuron is able to respond rapidly and effectively even to modest increases calcium concentration within the cell. There are multiple ways in which calcium may increase in the postsynaptic neuron after synaptic activation: calcium may flux in through voltage-gated calcium channels (VGCC) or iGluR (NMDAR and some types of AMPAR) or it can be released by intracellular stores (Berridge, 1998; Jonas and Burnashev, 1995).

4.1.1. Calcium influx through VGCCs

The first of the neuronal calcium channels shown to induce activity-dependent gene transcription were L-type VGCCs, a subtype of calcium channels characterized by a relatively slow inactivation rate and a high single-channel conductance for calcium. These particular properties allow them to flux into neurons the large amounts of calcium that is required to elicit a gene expression response (Gallin and Greenberg, 1995), making them particularly appropriate for conveying a calcium signal from the site of emergence at the plasma membrane to the nucleus. In addition, thanks to their mainly somatodendritic localization, L-type VGCCs are able to elevate calcium levels within the cell soma in close proximity to the nucleus, thus allowing efficient propagation of the calcium signal to the nucleus or elevating calcium levels directly within the nucleus (Catterall, 2000; Westenbroek et al., 1990). Furthermore, L-type VGCCs associate to a set of signaling proteins important for gene induction, including the protein kinase A anchoring protein (AKAP79/150), the tyrosine kinase Src, and the phosphatase calcineurin (Bence-Hanulec et al., 2000; Gray et al., 1998; Oliveria et al., 2007). As suggested by the name, AKAP79/150 recruits PKA to L-type VGCCs, leading to the phosphorylation of the channel and facilitating calcium influx. At the same time AKAP79/150 recruits the phosphatase calcineurin to L-type VGCCs. Calcineurin activation has double valence: it is required for the transcription factor NFATc4 translocation to the nucleus and activation as well as for the dephosphorylation and

activation of MEF2 family transcription factors (Chin et al., 1998; Graef et al., 1999; Mao and Wiedmann, 1999). Moreover, the calcium-sensing protein calmodulin was demonstrated to bind to the intracellular domain of the L-type channel and, upon calcium influx, to activate Ras/MAP Kinase signaling that ends up with the initiation of gene transcription within the nucleus (Dolmetsch et al., 2001). Consistent with these observations, pharmacological blockade of L-type VGCCs as well as chelation of calcium in close proximity to the plasma membrane inhibits immediate-early gene induction (Murphy et al., 1991; Deisseroth et al., 1996).

4.1.2. Calcium influx through NMDAR

Calcium influx through the NMDAR and the subsequent initiation of signaling pathways have a well-reported role in activity dependent neuronal development and plasticity. Single spine activation of NMDARs by glutamate coupled to postsynaptic membrane depolarization leads to rapid, restricted accumulation of calcium within the spine, allowing for synapse-specific induction of signaling. Over the course of cortical and hippocampal development, GluN2B-containing NMDARs are replaced by GluN2A-containing receptors that have a shortened duration of calcium influx (Carmignoto & Vicini, 1992; Bellone and Nicoll, 2007). This developmental regulation of NMDAR expression may have implications for synaptic adaptation to activity. Activity-dependent signaling to the nucleus may also be affected by the developmental regulation of the NMDAR subunit composition. In support of this idea, the ability of the NMDAR to induce the phosphorylation at serine-133 and the activation the transcription factor CREB, which detains a pivotal role in experience-dependent gene expression (Lonze & Ginty 2002), depends on the age of the hippocampal neurons. While NMDAR stimulation in immature neurons induces a durable phosphorylation of CREB serine-133, in more mature cultures it induces only a short-lived phosphorylation as the result of coincident activation of a CREB phosphatase (Sala et al. 2000). This developmental effect on CREB regulation is restricted to NMDAR-dependent signaling and, not for example, to VGCC activation.

This example introduces another important concept: although various routes of calcium entry lead to significant increases in the intracellular calcium concentration, depending on the mode of entry, different responses in terms of gene induction may be elicited (Bading et al., 1993; Ginty, 1997). For example, brain-derived neurotrophic factor (BDNF) is highly induced in excitatory neurons following calcium entry through L-type voltage-gating calcium channels (VGCCs) but much less effectively following calcium influx through NMDARs or other VGCCs (Ghosh et al., 1994; Westenbroek et al., 1992).

4.2. Synapse-to-nucleus translocation of protein messengers

The calcium-induced events described above play a key role in the fast modulation of synaptic transmission and plasticity. However, in addition to calcium-signaling, other mechanisms are required to sustain long-lasting modification of gene expression and long-term plasticity upon synaptic stimulation (Marcello, Di Luca, & Gardoni, 2018). Activity-dependent transport of signaling proteins from the postsynaptic compartment in dendrites to the nucleus is of primary importance in this regard (Lim et al., 2017). In the last decades several postsynaptic proteins that undergo long-distance translocation and subsequent regulated nuclear import, upon specific synaptic stimulation patterns, have been identified and characterized (Marcello, Di Luca, & Gardoni, 2018). Activation of NMDARs at the excitatory synapses holds primary importance in synapse-to-nucleus communication, not just for the calcium influx, but also for the nuclear translocation from dendrites or synapses of these synaptonuclear factors (Parra-Damas & Saura, 2019). In particular, at glutamatergic synapses macromolecules and several synaptonuclear protein messengers connect NMDARs activity to the nucleus enabling bidirectional transfer of information (Marcello, Di Luca, & Gardoni, 2018). Recent publications demonstrate that certain proteins, which function as transcriptional regulators, are initially localized at synapses but can translocate to the nucleus in response to synaptic activity (Ch'ng & Martin, 2011) (Dieterich et al., 2008) (Jordan, Fernholz, Khatri, & Ziff, 2007) (Dinamarca et al., 2016). Interestingly almost all of these protein messengers are part of the NMDAR signaling complex (Marcello, Di Luca and Gardoni, 2018). These synaptically localized transcriptional regulators directly transmit information regarding synaptic activity by moving to the nucleus and regulating gene transcription. Synapse-to-nucleus communication is essential for multiple processes like neural development, plasticity, and repair (Herbst & Martin, 2017b), and represent the basis of long-term functional and morphological modifications in neuronal cells (Marcello, Di Luca, & Gardoni, 2018). A critical aspect of synapse-to-nucleus signaling is the mechanism of import of signaling proteins into the nucleus; while calcium and small proteins can diffuse through the nuclear pore complex passively, proteins larger than 40-60 kDa require active transport by the family of importin proteins (Panayotis, Karpova, Kreutz, & Fainzilber, 2015). The classical active nuclear import pathway for implicates that nuclear localization signal (NLS) bearing cytoplasmatic proteins are targeted to the nucleus and transported through the nuclear pores by a large family of nuclear transport factors known as importins or karyopherins (Weis, 2002). Importin- α recognizes and binds to the NLS on the cargo protein and also binds to importin- β 1, which then docks the complex at the nuclear pore and mediates translocation from the

cytoplasm into the nucleus (Thompson et al., 2004). Glutamatergic synapses are enriched in several NLS-containing cargo proteins and different components of the nuclear import machinery, like importin- α and importin- β which can translocate to the nucleus in an activity-dependent manner (Jeffrey, Ch'ng, O'Dell, & Martin, 2009) (Dieterich et al., 2008). In vitro experiments in dendrites of rodent hippocampal neurons indicate importin- β 1 and importin- α isoforms are anchored at postsynaptic structures and respond to plasticity-inducing stimuli by translocating to the nucleus, as shown in rodent hippocampal neurons (Thompson et al., 2004). Jeffrey et al. demonstrated that importin- α binds to the NLS on the cytoplasmic tail of GluN1A subunit of the NMDAR under basal conditions, but when the NMDA receptor is activated by stimuli which establish late phase LTP in hippocampal neurons, importin- α dissociates from the NMDAR in a protein kinase C-dependent manner and is free to bind cargo proteins destined for the nucleus (Jeffrey et al., 2009). Many of the synapse-to-nucleus signaling proteins engage the classical nuclear import machinery for nuclear entry (Lim et al., 2017). Several novel synaptonuclear signaling proteins have been identified by characterizing the proteome of excitatory synapses and the interactome of NMDAR (Jordan et al., 2004) (Di Luca et al., 2016). Notably, some synaptonuclear factors converge on the transcription factor CREB, indicating that CREB signaling is a key hub mediating integration of synaptic signals into transcriptional programs required for neuronal function and plasticity (Parra-Damas & Saura, 2019), in particular synaptonuclear protein messengers located at the glutamatergic postsynaptic compartment. Moreover, increasing evidence show that alterations of the activity of synaptonuclear messengers are correlated to synaptic failure as observed in different synaptopathies, such as neurodevelopmental disorders and neurodegenerative diseases (Marcello, Di Luca, & Gardoni, 2018). It is nowadays accepted that failures in synaptic function and plasticity during brain development or in pathological conditions in the mature or aging brain represent major causes for psychiatric, neurological and neurodevelopmental disorders, including Alzheimer's disease (AD) and autism spectrum disorders (ASD) (Marcello et al., 2018). Such neurological disorders are characterized by alterations in cognition, emotion and affected memory retrieval and are often associated with synaptic frailty due to altered functional and structural dendritic spine plasticity, so that the majority of these disorders have been indicated as synaptopathies (Marcello et al., 2018). Although major efforts have been focused on identification and characterization of regulatory mechanisms of synaptonuclear factors, the relevance of synapse-to-nucleus communication in brain physiology and pathology is still unclear (Parra-Damas & Saura, 2019). However, a growing number of studies indicate that the above-mentioned long-distance synaptonuclear messengers can contribute to alterations of the activity-dependent regulation of gene expression and synapse

function observed in synaptopathies, suggesting that uncoupling synaptic activity from nuclear signaling may prompt synapse pathology, contributing to a broad spectrum of brain disorders (Parra-Damas & Saura, 2019) (Marcello et al., 2018). For instance, disturbance of intracellular transport processes is a common principle and an altered activity-dependent protein transport from synapse-to-nucleus is likely to be an important factor contributing to synaptic dysfunction in both neurodevelopmental and neurodegenerative disorders. Remarkably, dysfunction and genetic mutations of synaptonuclear factors have been recently associated with a number of neurodevelopmental, psychiatric, and neurodegenerative disorders (Parra-Damas & Saura, 2019) (Table 1), and in particular, altered function and expression of these proteins can lead to synaptic failures and a highly significant alteration of dendritic spine density (Marcello et al., 2018).

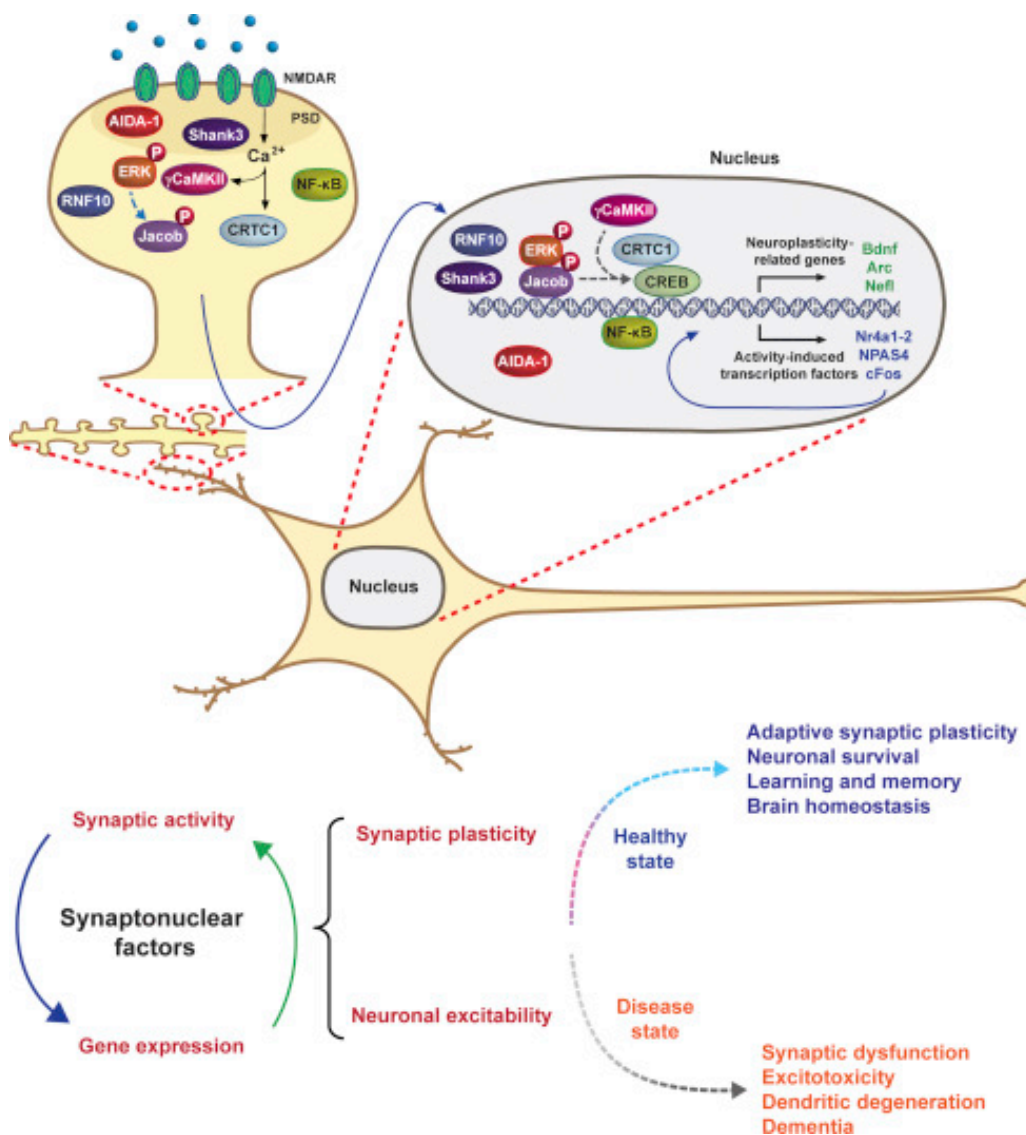


Figure 11. Synapse-to-nucleus signaling regulates neuronal excitability and synapse plasticity. Several synaptic factors (e.g., CREB- regulated transcription coactivator-1 [CRTC1], extracellular signal-regulated kinase [ERK], Jacob, nuclear factor kappa-light-chain-enhancer of activated B cells [NF- κ B], RING finger protein 10 [RNF10], SH3 and multiple ankyrin repeat domains 3 [Shank3], calcium/calmodulin-dependent protein kinase II gamma [γ CaMKII]) are activated by synaptic activity at distal dendrites, including synapses, and translocate to the nucleus to regulate cAMP-response element binding protein (CREB)-mediated transcription. Adapted from Parra-Damas and Saura 2019.

For this dissertation I will give a brief description of some synaptonuclear messengers, with particular relevance to a new GluN2A protein interactor discovered in my lab, RNF10 (Dinamarca et al., 2016)

Table 1. Synaptonuclear messengers, physiological functions and related pathological conditions

<u>Synaptonuclear protein</u>	<u>Activation mechanism</u>	<u>Downstream Targets</u>	<u>Physiological Functions</u>	<u>Related conditions</u>
AIDA-1/ANKS1B	NMDAR, CaMKII	Protein synthesis	Synaptic plasticity, regulation of nucleolar number	Schizophrenia, ASD, AD
CRTC1	Calcineurin/PP2B	CREB target genes (BDNF, FOS, NR4A1/2)	Synaptic plasticity, learning and memory, neuronal survival	AD, neurodegeneration, mood and affective disorders
CREB2/ATF4	Importin- α , NMDA/LTD	CREB target genes	Synaptic plasticity	AD, PD
Jacob	ERK	CREB target genes	Synaptic plasticity, dendritic morphology, learning and memory	Kallmann syndrome, AD
Shank3	NMDAR	CREB target genes	Synapse morphology, excitatory/inhibitory balance	ASD, intellectual disability, schizophrenia, Phelan-McDermid syndrome
RNF10	NMDAR, LTP	MMP-9, ARHGEF6, ARHGAP4, OPHN1	Synapse morphology	Fragile X Syndrome

4.2.1. Jacob

Jacob was first identified as a binding protein of the postsynaptic calcium sensor caldendrin. As synaptonuclear messenger, it translocates to the nucleus by a mechanism involving both synaptic and extrasynaptic GluN2B-containing NMDARs (Dieterich et al., 2008). At the synapse, Jacob associates with Caldendrin, which competes with importin- α for access to the NLS in Jacob (Dieterich et al., 2008). Upon NMDAR activation, the calcium influx at the postsynaptic compartment induces Caldendrin dissociation from Jacob, allowing importin- α to bind to the exposed NLS (Dieterich et al., 2008). Jacob activity depends on which pool of GluN2B-containing NMDAR is stimulated, if synaptic or extra-synaptic. Upon synaptic NMDARs activation, in particular NMDAR-dependent long-term potentiation, but not long-term depression, Jacob is phosphorylated by the MAP Kinase ERK1/2 at Ser180 and is translocated to the nucleus (Karpova et al., 2013). Once in the nucleus, phosphorylated Jacob promotes CREB signaling and transcription of neuroplasticity genes resulting in enhanced

synaptic strength, whereas its inactivation impairs CREB signaling (Dieterich et al., 2008) (Karpova et al., 2013). Conversely, if Jacob enters the nucleus with Ser180 dephosphorylated, CREB will be shut-off and a cell death pathway activated. The long-distance nuclear translocation of phosphorylated Jacob is dynein-mediated and to prevent dephosphorylation during the nuclear transit, Jacob interacts with α -internexin, an intermediate filament present at dendrites (Karpova et al., 2013) Alternatively, extrasynaptic NMDARs induce Jacob nuclear import independently of Ser180 phosphorylation, reduce CREB phosphorylation and synapse and dendritic complexity, and elicit neuron death (Dieterich et al., 2008). These results demonstrate that the phosphorylation state of a synaptonuclear factor may determine its function (Parra-Damas & Saura, 2019). Consistent with the role of this synaptonuclear signal in neuronal development, long-lasting plasticity, and memory, Jacob KO mice display hippocampal dysplasia, defects in hippocampal long-term potentiation (LTP) and impaired hippocampal-dependent learning (Spilker et al., 2016).

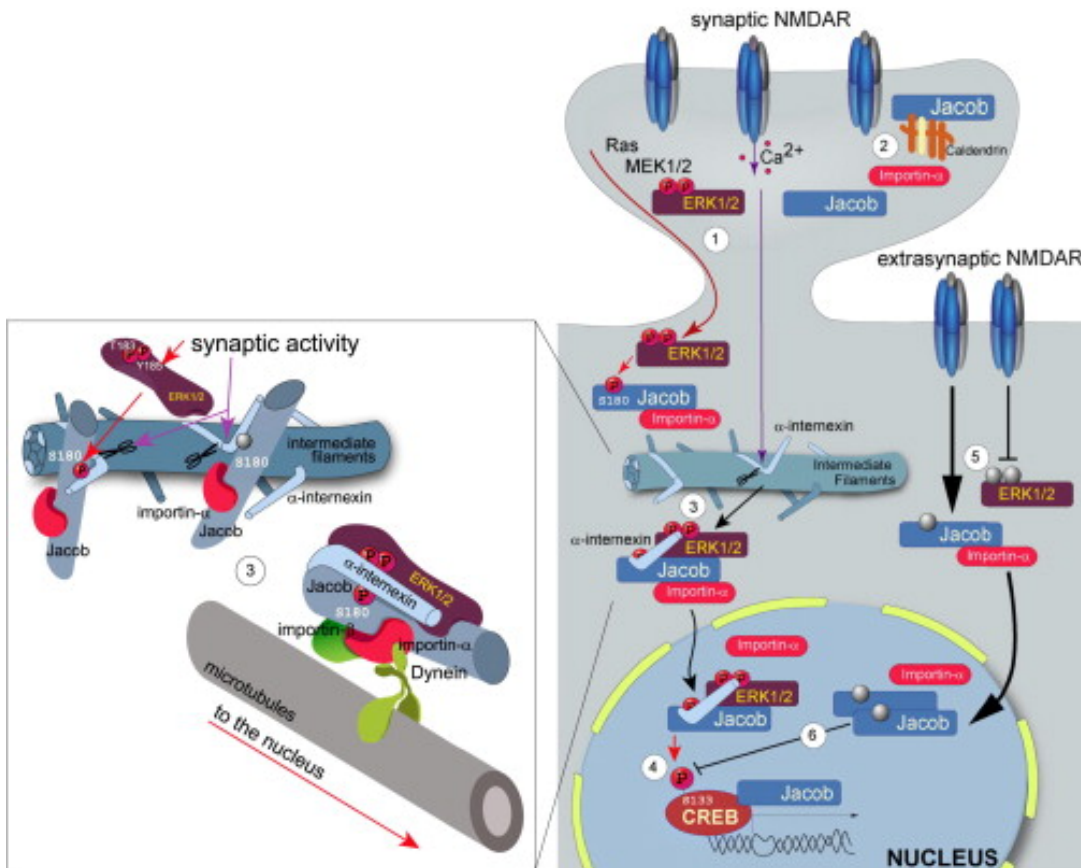


Figure 13. The Jacob Pathway Encodes the Synaptic or Extrasynaptic Localization of Activated NMDAR. (1) Synaptic NMDAR activity leads to activation of ERK1/2 and subsequent binding and phosphorylation of Jacobs Ser180 at synaptic sites that in turn is a prerequisite for Jacob to leave the synapse. (2) A fraction of pJacob might be kept at the synapse via an interaction with Caldendrin (3) Synaptic activity and subsequent increase in intracellular Ca^{2+} concentrations activate calpain, which in turn cleaves α -internexin and Jacob. Soluble α -internexin interacts with the pJacob/pERK complex and protects pJacob and pERK against dephosphorilation during long-distance transport. The interaction of Jacob with α -internexin is stronger in case of Ser180 phosphorylation and α -internexin binding does neither compete with Jacob/ERK-binding nor does it prevent phosphorylation of Jacob by ERK. The pERK-internexin-pJacob complex can be linked via importin- α to a dynein motor, which might mediate active transport of the complex along microtubuli. (4) The presence of pJacob in the nucleus correlates with enhanced CREB phosphorylation, increased expression of plasticity-related genes. (5) The nuclear translocation of Jacob after extrasynaptic NMDAR activation does not require ERK activity and Jacob is not phosphorylated prior to nuclear import. (6) The nuclear accumulation of non-phosphorylated Jacob results in CREB shut-off and is followed by a series of deteriorative events in terms of synaptic and dendritic integrity and causes subsequent cell death. (Adapted from Karpova et al, 2013).

4.2.2. CRTC1

CREB Regulated Transcriptional Coactivator 1 (CRTC1) it's an activity-dependent synapse-to-nucleus signaling molecule that acts to activate CREB-mediated transcription in neurons, throughout various forms of neuronal plasticity (Lim et al.,

2017). At basal conditions, CRTC1 is extensively phosphorylated and is bound to 14-3-3 proteins, which localizes CRTC1 at the synapse (Herbst & Martin, 2017a) (Lim et al., 2017). Upon iGluRs (both AMPARs and NMDARs) activation, CRTC1 is dephosphorylated at specific residues by calcineurin, released from 14-3-3 proteins, and then actively translocated to the nucleus in an energy-dependent mediated by the motor protein dynein on microtubules (Ch'ng et al., 2015). In addition, CRTC1 undergoes active transport into the nucleus in a non-canonical import pathway, importin α/β 1-independent (Ch'ng et al., 2015). Once in the nucleus, CRTC1 binds to CREB and enhances the transcription of specific neuroplasticity-related CREB target genes, including *Bdnf*, *Arc*, and *Fos* (Ch'ng et al., 2012a). In vivo evidence indicates that CRTC1/CREB-dependent transcription impacts memory, mood and reward circuits, moreover CRTC1 signaling alterations have been reported in several neurodegenerative and psychiatric diseases, such as AD, Parkinson's disease (PD) and Huntington's disease but merits further investigation (Parra-Damas & Saura, 2019). In particular, recent studies indicate that aberrant activity-dependent nucleocytoplasmic shuttling of CRTC1 and subsequent dysregulation of gene transcription are implicated in the pathophysiology of Alzheimer's disease (Parra-Damas et al., 2014).

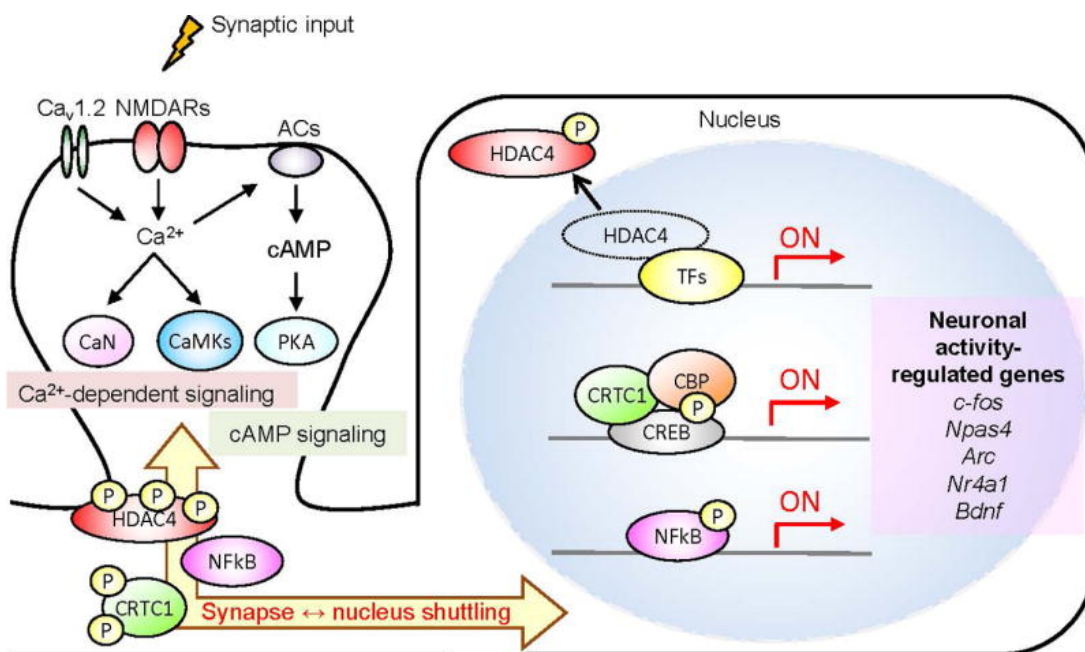


Figure 14. CRTC1 Synapse-to-nucleus shuttling. Activation of glutamatergic synapses triggers calcium influx and induces calcium-dependent signaling molecules, such as calcineurin and CaMKs. These signaling molecules modulate the synapse-to-nucleus translocation of transcription modulators like CRTC1 via phosphorylation and dephosphorylation. In the nucleus, CRTC1 contribute to the control of activity-dependent gene transcription which is required for synaptic plasticity and memory formation. Adapted from Uchida and Shumyatsky 2017.

4.2.3. CREB2 or ATF4

CREB2, also known as activating transcription factor 4 (ATF4) is a member of the CREB family of transcription factors. It acts as a CREB transcriptional repressor in regard of the modulation of synaptic plasticity and memory (Chen et al., 2003) (Pasini, Corona, Liu, Greene, & Shelanski, 2015). CREB2 trafficking and importin- α -dependent nuclear translocation is specifically activated during NMDA-dependent long-term depression, but not during long-term potentiation, suggesting CREB2/ATF4 involvement may be critical for synaptic plasticity and memory (Lai, Zhao, Ch'ng, & Martin, 2008). Apart from retrograde movement from the postsynaptic compartment to the nucleus, recent reports indicate that CREB2 also undergoes local synthesis in axons and growth cones, and transported to the nucleus when exposed to the toxic A β 1-42 oligomers (Baleriola et al., 2014). In an experimental model of Alzheimer's Disease, exposure of axons to A β causes pathogenic changes that spread retrogradely by unknown mechanisms, affecting the entire neuron (Baleriola et al., 2014). Among these effects, A β 1-42 initiates axonal synthesis of a defined set of proteins including the transcription factor CREB2 and culminates in neurodegeneration. Inhibition of CREB2/ ATF4 axonal retrograde transport reduces A β -induced neurodegeneration (Baleriola et al., 2014). Notably, ATF4 Biochemical analysis of post-mortem brains of patients with Alzheimer's Disease reveals an upregulation in ATF4 protein levels. Once in the nucleus, CREB2 mediates transcription of CHOP which triggers the cell death pathway (Baleriola et al., 2014). CREB2 is the first transcription factor that as been characterized to undergo regulated nuclear import from both presynaptic and postsynaptic compartment (Lai et al., 2008) (Baleriola et al., 2014).

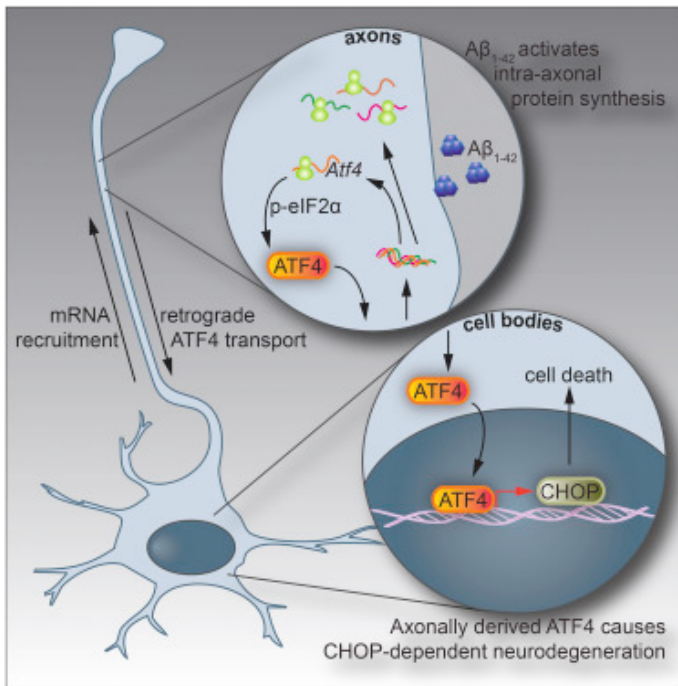


Figure 15. CREB 2/ATF4 undergoes nuclear translocation after LTD induction. The CREB transcriptional repressor CREB2 undergoes nuclear accumulation after LTD induction and undergoes local synthesis in axons and nuclear translocation after exposure to Aβ₁₋₄₂ oligomers. Adapted from Baleriola et al. 2014.

4.2.4. AIDA-1 or ANKS1B

Amyloid precursor protein intracellular domain associated-1 (AIDA-1), also known as Ankyrin repeat and sterile alpha motif domain containing 1B (ANKS1B), is a family of postsynaptic density proteins identified as protein interactors of the intracellular domain of APP (Ghersi, Vito, Lopez, Abdallah, & D'Adamio, 2004). AIDA-1 binds also to PSD95 and NMDAR and is required for NMDAR-mediated synaptic transmission and plasticity (Tindi et al., 2015). AIDA-1 affects APP processing by inhibiting the activity of the γ-secretase, consequently diminishing the amyloidogenic Aβ secretion (Ghersi et al., 2004). Moreover, AIDA-1 regulates NMDAR subunit composition at synapses and, thereby, its function by facilitating transport of GluN2B from the endoplasmic reticulum to synapses, which is critical for NMDAR plasticity (Tindi et al., 2015). As far as concern its role as synapse-to-nucleus messenger, AIDA-1 has a canonical NLS and undergoes activity-dependent proteolytic cleavage after synaptic NMDAR activation that triggers its dendrite-to-nucleus trafficking. Upon AIDA-1 translocation increases in nucleoli number and protein synthesis are observed (Jordan et al., 2007). Unlike most synaptonuclear factors that regulate gene expression by modulating CREB-dependent transcription, ANKS1B/AIDA-1 synapse-to-nucleus signaling seems to enable protein synthesis triggered by synaptic activity independently of CREB (Parra-Damas & Saura, 2019).

4.2.5. SHANK3 or ProSAP2

ProSAP/Shank proteins are a family of scaffolding molecules found at excitatory glutamatergic synapses and at the PSD these proteins are capable of interacting with structural elements as well as ligand gated ion channels and cell adhesion molecules. Shank3, also known as proline-rich synapse-associated protein 2 (ProSAP2), is an abundant synaptic protein that regulates synapse formation, morphology, and acts by interacting with postsynaptic density proteins, such as homer, cortactin, dynamin and Abelson interacting protein 1 (Jiang & Ehlers, 2013). Two putative NLS sequences have been identified within ProSAP2/Shank3 and it undergoes activity-dependent nuclear transport in hippocampal neurons (Grabrucker et al., 2014). In humans, genetic missense, deletion, and duplication mutations in the SHANK3 gene are linked to neurodevelopmental conditions like autism spectrum disorders (ASD) and schizophrenia (Durand et al., 2006). These mutations generally lead to loss of Shank3 function resulting in altered synapse morphology and presynaptic and postsynaptic signaling and autistic-like behaviors in animal models, whereas Shank 3 overexpression leads to manic behavior caused by excitatory/inhibitory imbalance (Arons et al., 2012). In particular, a schizophrenia-linked mutation that alters the synaptic localization of Shank3 resulting in constitutive nuclear localization independent of synaptic activity and deregulates transcription of multiple schizophrenia-related synaptic genes, including synaptotagmin and LRRTM1, affects synapse number and function (Grabrucker et al., 2014). Moreover, Shank3 gene mutations have been found in individuals with ASD and intellectual disability and usually, in animal models, these mutations lead to alterations of dendritic spines and synaptic function (Durand et al., 2006). Remarkably, Shank3 regulates ERK and CREB by affecting calcium and metabotropic glutamate receptor 5, suggesting that synaptonuclear signaling mediated by Shank3 is also integrated into CREB-regulated transcription (Verpelli et al., 2011). Together, these results indicate that uncoupling Shank3/ProSAP2 synapse-to-nucleus signaling may contribute to synaptic dysfunction in intellectual disability in mental disorders (Parra-Damas & Saura, 2019).

4.2.6. Abi1

Abelson-interacting protein 1 (Abi1) is found in axons and growth cones during neuronal development and at enriched concentrations in the PSD of mature neurons (Proepper et al., 2007). Abi1 knockdown in neurons affects both dendrite formation and synaptogenesis, suggesting that Abi1 localization in growth cones regulates actin dynamics, a key regulator of cytoskeletal formation (Proepper et al., 2007). In mature neurons, Abi1 interacts with ProSAP2/Shank3 at the postsynaptic compartment and

undergoes nuclear translocation during NMDAR-mediated stimulation. Once localized in the nucleus, Abi1 interacts with the Myc/Max proteins and enhances E-box-regulated gene expression, thus indicating Abi1 as a specific synaptonuclear messenger and is essentially involved in dendrite and synapse formation (Proepper et al., 2007).

4.2.7. RNF10: a novel synaptonuclear messenger encoding activation of NMDARs

The laboratory of Prof. Di Luca and Prof. Gardoni, in which I developed my PhD project, recently discovered a new synaptonuclear messenger, RNF10. RING (Really Interesting New Gene) Finger protein 10 (RNF10) is 804 amino acids long (89.9 kDa) in humans and it is a member of the Ring Finger Protein family, which have been shown to regulate protein turnover by functioning as ubiquitin ligases (Lin et al., 2005) and have been generally implicated in development, transcriptional regulation, signal transduction, DNA repair and oncogenesis (Saurin, Borden, Boddy, & Freemont, 1996). RNF10 has an ubiquitrary expression and only recently has been studied in the nervous system, both in glial cells and neurons (Dinamarca et al., 2016) (Hoshikawa, Ogata, Fujiwara, Nakamura, & Tanaka, 2008). In Schwann cells, RNF10 has a function in the transcriptional regulation of myelin formation (Hoshikawa, Ogata, Fujiwara, Nakamura, & Tanaka, 2008) binding to the promoter of MAG1 gene, a master regulator of myelination. In hippocampal neurons, RNF10 displayed a nuclear and somatodendritic distribution (Dinamarca et al., 2016). RNF10 protein sequence contains a binding domain for the transcription factor Mesenchyme Homeo-box 2 (Meox2) (Meox2 Binding Domain (MBD)) (Lin et al., 2005), a Ring Finger Domain (RFD), which is known to be involved in protein-protein interactions, and two putative nuclear localization sequences (NLS1, aa 591-599 and NLS2, aa 784-791) (Dinamarca et al., 2016). These protein characteristics, together with its synaptic and nuclear localization, suggested its role in synapse-to-nucleus communication. Recent works of my lab showed that RNF10 undergoes activity-dependent translocation to the nucleus during synaptic NMDARs activation and, once in the nucleus, it modulates expression of a series of target genes, involved in cell differentiation and structural plasticity (Seki, Hattori, Sugano, Muramatsu, & Saito, 2000) (Dinamarca et al., 2016). At dendritic spines level RNF10 is localized at the PSD and specifically binds to the cytoplasmatic tail of GluN2A-, but not GluN2B-, containing NMDARs. In particular, the C-terminal domain (aa 991-1049) of GluN2A and the N-terminal region (aa1-221) of RNF10 are involved in the binding between GluN2A and RNF10 (Dinamarca et al., 2016). Interestingly, GluN2A (aa 991-1029) domain was previously shown to be responsible for a calcium-dependent binding of the NMDAR subunit with Calmodulin (CaM) (Bajaj et al., 2014), suggesting a competition mechanisms between RNF10 and CaM for the binding to the same C-terminal domain

in GluN2A. Since CaM activation depends on intracellular calcium levels, it was evaluated whether calcium could modulate GluN2A/RNF10 interaction and the capability of Calcium/CaM to disrupt RNF10/GluN2A complex following synaptic activity-dependent calcium influx (Dinamarca et al., 2016). These data showed that, in basal conditions, RNF10/GluN2A complex formation is preferred; RNF10 binding to GluN2A plays a key role for RNF10 anchoring at the excitatory synapse but also interferes with the formation of CaM/NMDAR complex (Dinamarca et al., 2016). Activation of GluN2A-containing NMDARs triggers translocation of RNF10 to the nucleus. The calcium influx following synaptic NMDARs activation results in a rapid dissociation of RNF10 from the C-tail of GluN2A at postsynaptic sites and a tighter association with neuronal importin- α 1 and importin-dependent nuclear translocation (Dinamarca et al., 2016). The NLS2 within RNF10 is responsible for the binding to importin- α 1 and, similar to other synaptonuclear protein messengers, this binding represent a key step for RNF10 trafficking to the nucleus (Di Luca et al., 2016) (Ch'ng & Martin, 2011). Furthermore, both chemical and electrical LTP, but not LTD, induction detaches RNF10 from GluN2A subunit and triggers RNF10 translocation to the nucleus (Di Luca et al., 2016). Once in the nucleus, RNF10 associates with Meox2 and modulates expression of Meox2/RNF10 target genes, such as p21 and Ophn1, associated with synaptic transmission or dendritic spine morphology (Di Luca et al., 2016). In accordance, RNF10 silencing induces molecular and morphological modifications of the glutamatergic synapses (Di Luca et al., 2016), specifically, a significant decrease in dendritic spine density and in the protein levels of the main component of the excitatory synapse, such as GluN2A, PSD-95 and the GluA1 subunit of the AMPA receptor in the total cell homogenate (Di Luca et al., 2016). Interestingly, RNF10 knock-down in hippocampal neurons not only produces a significant reduction in dendritic spine density, but also prevents the expression of chemical LTP, interfering with the LTP-dependent modulation of dendritic spine size (Di Luca et al., 2016). In this view, the modulation of RNF10 expression in hippocampal neurons, in particular its synaptonuclear signalling mechanism, demonstrated its relevant role in regulating dendritic spine morphology under resting conditions as well as following activity-dependent plasticity (Di Luca et al., 2016). A deeper investigation on the effect of RNF10 knock-down on gene expression showed that RNF10 silencing modulates the expression of several genes involved in the regulation of the excitatory synaptic function and dendritic spine morphology such as MMP9, Ophn1, ArhGap4 and ArhGef6 (Vogt, Gray, Young, Orellana, & Malouf, 2007) (Michaluk et al., 2011) (van Galen et al., 2011) (Bagni, Tassone, Neri, & Hagerman, 2012). In particular, RNF10 silencing induced a dramatic up-regulation of the matrix metalloproteinase-9 (MMP9) expression, which appears to cause transformation of mature mushroom-shaped spines into long

filopodia-like structures in cultures of dissociated neuronal cells in a NMDARs dependent manner (Bilousova et al., 2009). By contrast, RNF10 silencing lead to a reduction of Arhgef6, ArhGap4 and Ophn1 expression levels, which are all involved in Rho GTPase signaling and are essential for cognitive function and synaptic plasticity (van Galen et al., 2011) (Di Luca et al., 2016). Interestingly, all these genes are mutated or dysregulated in intellectual disability (ID) syndromes in humans and/or in the corresponding mouse models (Vogt et al., 2007) (Michaluk et al., 2011) (van Galen et al., 2011) characterized by synaptic and dendritic spines alterations, thus making RNF10 potential new target to investigate in neuropsychiatric conditions characterized by synaptic alterations. Interestingly, a recent study identified a strong downregulation of RNF10 expression in blood samples of male carriers of the *FMR1*premutation and in brain samples of a FXTAS mouse model (Mateu-Huertas et al., 2014).

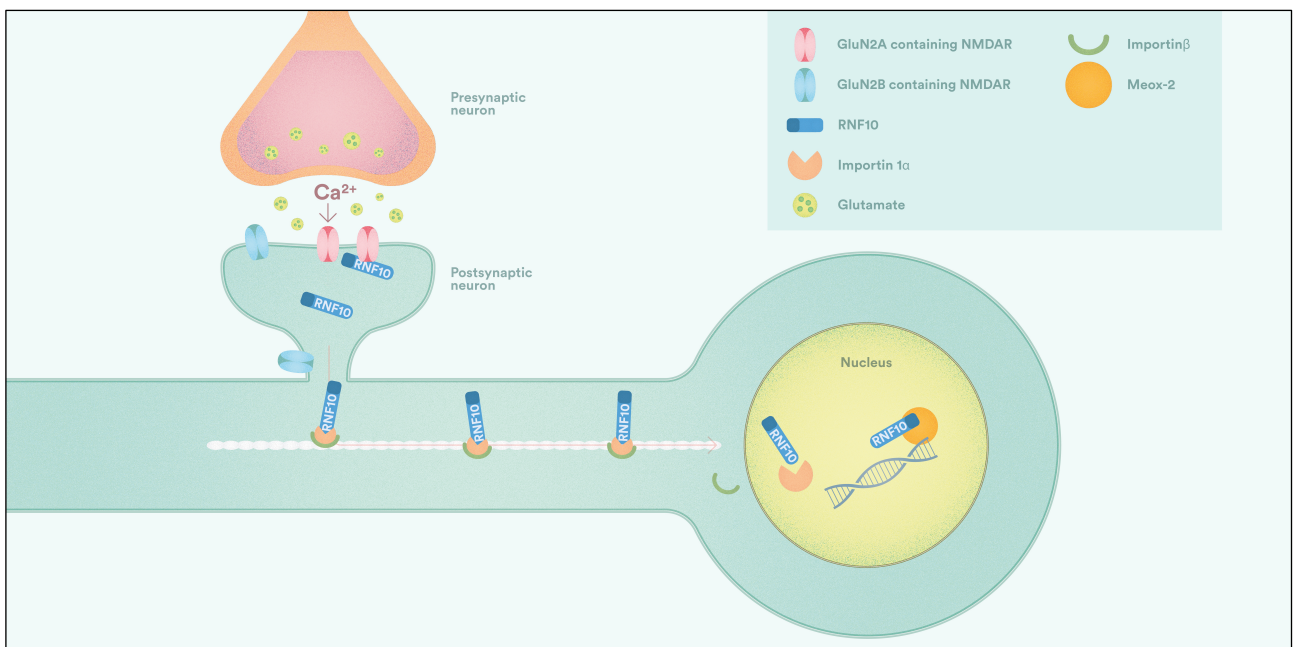


Figure 15. RNF10 synapse to nucleus translocation. RNF10 dissociates from GluN2A subunit of NMDAR after synaptic stimulation on LTP, in a calcium-dependent manner. RNF10 interacts with importin- α 1 and translocate into the nucleus, where it binds to Meox-2 and regulates structural plasticity-related gene expression.

AIMS

Synaptonuclear protein messengers (i.e., Jakob, Abi-1, and CRTC1) represent fundamental players for the regulation of neuronal morphology both in health and diseases (Marcello, Di Luca & Gardoni, 2018). Accordingly, Jakob KO mice show hippocampal dysplasia with a reduced number of synapses and dendritic branching (Spilker et al., 2016), Abi-1 silencing leads to aberrant dendrite branching and decreased spine density, whereas Abi-1 overexpression shows opposite effects (Proepper et al., 2017). Finally, CRTC1 plays a key role BDNF-induced dendritic development (Finsterwald, 2010; Li et al., 2008). Elaborated branched structures are indeed a key requirement to maintain a correct synaptic capacity; on the other hand, the transcriptional regulation of gene expression has been proven as an asset in dictating neuronal architecture in an activity-dependent manner.

Ring Finger Protein 10 (RNF10) has been recently identified as a novel synaptonuclear signaling protein that specifically links activation of synaptic GluN2A-containing NMDARs to nuclear gene expression. Moreover, RNF10 silencing has been associated to an alteration of synaptic development and synaptic plasticity (Dinamarca et al., 2016), which could prelude to an involvement in neurodevelopment regulation. However, the molecular mechanisms of NMDAR/RNF10 complex disruption and the subsequent importin mediated RNF10 translocation to the nucleus as well as the broader role of RNF10 in regulating neuronal morphology remain unclear. Therefore, the main aims of this PhD work are:

1. To identify the molecular events that regulate RNF10 trafficking from synapse to the nucleus after activation of synaptic NMDARs;
2. To investigate the involvement of RNF10 synaptonuclear communication in the regulation of neuronal architecture and neurodevelopment

MATERIALS AND METHODS

1. Cell cultures

1.1. Primary hippocampal neuronal cultures

Hippocampal neuronal cultures were prepared from embryonic day 18-19 (E18-E19) Sprague-Dawley rat hippocampi (Charles River, Milan, Italy). We prepared dissection media (Hanks' balanced salt solution HBSS), plating media and Neurobasal medium supplemented with B27. The day before the dissection we coated nitric acid-washed coverslips with poli-L-lysine (PLL, Sigma) solution to cover the bottom of the plates and incubated them overnight at 37°C in a humidified incubator. The day of the dissection we collected the PLL from the MW or the petri dishes and we washed them with sterile water four or more times and we added plating medium, composed by DMEM (Invitrogen) addioned with 1% Glutamax (Invitrogen), 10% Horse Serum (Eruclone) and 1% Pen/Strep (Invitrogen). For culture preparation, we anesthetized and sacrificed the pregnant rat and we removed the E18-19 embryos by cesarean section. Next we put the embryos in a 100 mm glass Petri dish filled with ice-cold HBSS. We sacrificed the embryos by decapitation with scissors and removed the brains. We separated the brain hemispheres and removed the cerebellum with forceps and carefully removed the meninges under a dissecting microscope. Then we dissected and isolated the hippocampi and transferred the tissue to a 15 ml plastic tube filled with ice-cold HBSS. Under a biological hood, we removed the HBSS from the Falcon tube using a glass Pasteur pipette and washed the hippocampi four times with cold HBSS. Then, we added 4.5 mL of HBSS and 500 µL of 10X trypsin solution to dissociate the tissue and incubated the tube at 37°C for 13 minutes in a water-bath. In this step the hippocampi are sticked to form a clump, we removed the tube from the water-bath and allowed the tissue to precipitate at the bottom of the tube. We carefully removed the supernatant containing the trypsin solution and washed the hippocampi with 10 mL of Plating media for five times to neutralize the remaining enzyme. After the washes, we used a micropipette to reduce the clump and dissociate the tissue pipetting up and down the hippocampi suspension. After dissociation of the cells, the suspension becomes cloudy. Finally we counted cells and we plated them at the appropriated density. Cells were plated in plating medium and 12-16 hours after plating, the medium was changed to Neurobasal addioned with 2% B27 supplement (Gibco), 1% Glutamax (Invitrogen) and 1% Pen/Strep (Invitrogen).

1.1.1 Neuronal transfection

Neurons were transfected between DIV7 and DIV10 using calcium-phosphate co-precipitation method with 1-4 μg plasmid DNA. The insoluble calcium-phosphate precipitate with the attached DNA adheres to the cell surface and is brought into the cells by endocytosis. We prepared 2,5 M CaCl_2 solution in water, we filter sterilized and kept at room temperature; we also prepared HBS 2X solution. One hour before transfection, we collected the medium from the MW plates and replaced it with fresh DMEM media. 30 minutes before transfection, we prepared the DNA- CaCl_2 precipitates using the following protocol and incubated them at the dark for 25 minutes. For each condition we prepare mixtures in two separate tubes (solution A and solution B):

1. prepare solution A with 80 μl of HBS 2X.
2. prepare solution B with 4 μg of plasmid DNA, 10 μl of 2,5M CaCl_2 solution and ddH₂O up to 80 μl .
3. add solution B slowly to solution A while mixing gently solution A. this is the most important step for forming calcium-phosphate/DNA co-precipitate.
4. after mixing the two solutions, incubate at room temperature for 25 min at the dark.
5. gently tap the mixture and add to each well 80 μl of the mixture by dripping slowly and incubate it for 20 minutes at 37°C in the incubator.

After that we checked under the microscope the presence of visible calcium-phosphate/DNA precipitates. In order to clean the wells from the excessive DNA- CaCl_2 precipitates, we washed the plates with pre-warmed DMEM media every 30 minutes for three times and then we replaced it with the conditioned Neurobasal media. Finally, we let the cells grow in culture for 7-8 days 37°C in the incubator. Neurons were then treated accordingly to their purposes.

1.2. COS-7 cell line

Splitting and Plating: we pre-warmed the reagents in the water-bath at 37°C. We eliminated the supernatant culture media from the cell culture plates and washed them twice with PBS (1X) to eliminate any serum media left. Then, we added 2 mL of Trypsin-EDTA (1X) and put again the plates in the incubator for 5 minutes. After that, we used a

P1000 pipette to dissociate the cells mechanically from the plates and stopped the trypsin action by adding serum media. So, we counted the number of cells using a Neubauer cell counter and plated 75000 cells on each well of the 12 well MW plates. We left cell cultures in DMEM + Glutamax medium supplemented with 10% Fetal Bovine Serum (FBS, Euroclone) and Pen/Strep in the incubator for 24h at 37°C.

Transfection: COS-7 cells were transfected using the lipofectamine method as following described. The day prior to transfection, the cells were plated in 6 wells multiwell plates (for biochemistry) or on coverslips in 12 wells multiwell plates (for immunostaining). We prepared a DNA mix by adding 1.5 µg/3 µg of DNA in Optimem media containing 1.5/3 µL of Plus Reagent (Invitrogen) for 12 well/6 well plate and incubated at room temperature for 10 minute. Then, we added 4/10 µL of Lipofectamine LTX Reagent (Invitrogen) to the DNA mix and incubated for other 25 minutes. So, we changed the media of the COS-7 cells with DMEM without serum and added DNA mix drop-wise, incubating over night at 37°C in the incubator. The next day we changed the media with DMEM containing 10% FBS and incubated 24h before fixing the cells with PFA or collecting them for protein quantification.

2. Biochemistry

2.1. Subcellular fractionation of Triton Insoluble Fraction (TIF) and nuclear fraction

Neurons were washed with PBS $\text{Ca}^{2+}/\text{Mg}^{2+}$, scraped out and lysed in an ice-cold lysis buffer containing 0.32 M Sucrose, 1 mM Hepes, 1 mM NaF, 0.1 mM PMSF, 1 mM MgCl, using a glass-glass homogenizer. To purify post-synaptic triton insoluble fractions (TIF) (Gardoni et al., 2001), a fraction highly enriched in PSD proteins but absent of presynaptic markers, lysates were centrifuged at 1,000 g for 5 min at 4°C, to remove the nuclear contamination. The supernatant was collected and centrifuged at 13,000 g for 15 min at 4°C. The pellet was dissolved in a buffer containing 0.5% Triton and 150 mM KCl, incubated on ice for 15 min and centrifuged at 100,000 g for 1h at 4°C. The resulting pellet (TIF) was homogenized by passing through a 1ml hypodermic syringe in 20mM HEPES buffer. To prepare a crude nuclear fraction, the lysates were centrifuged at 1,000 g for 10 min and the pellet was dissolved in 20mM HEPES buffer. All steps were done in presence of protease inhibitors (Complete™, GE Healthcare, Mannheim, Germany) and phosphatase inhibitors (PhosSTOP™, Roche Diagnostics GmbH, Mannheim, Germany). Protein content of the samples has been quantified by using the

Bio-Rad protein assay reagent (Hercules, CA, USA) and equivalent amounts of proteins loaded in individual lanes for western blot analysis.

2.2. Co-ImmunoPrecipitation assays (Co-IP)

Homogenate/TIF aliquots containing 150 µg/50 µg of proteins were incubated overnight at 4°C with primary antibody in RIPA buffer containing 50 mM Tris HCl (pH 7.2), 150 mM NaCl, 1% NP-40, 0.5% deoxycholic acid, 0.2% sodium dodecyl sulphate (SDS). As control, one sample was incubated in the same experimental conditions without the antibody or without any homogenate/TIF added. Protein A/G-sepharose beads (Sigma-Aldrich) were added and incubated for additional 2 h, at room temperature, on a rotator. Beads were precipitated by mild centrifugation (1200 rpm), washed three times with RIPA buffer containing 0.1% SDS and boiled for 10 min in SDS-PAGE sample buffer. Beads were precipitated using centrifugation, the supernatant loaded onto 7%-12% SDS-PAGE gels and revealed using the antibody for the interacting protein of. For the input lane, 10% of the Homogenate/TIF aliquot used for the Co-IP experiment was loaded onto the SDS-PAGE.

2.3. Pull-down assay

Neuronal homogenates containing 250 µg of proteins were incubated at room temperature with GST-beads to a final volume of 1 ml with Tris Buffered Saline (TBS) solution for 1h on an eppendorf rotator. The GST-beads were precipitated by centrifugation and the supernatant re-incubated at room temperature with GST fusion proteins or GST alone, for an additional 2h on a rotator. Beads were precipitated and washed three times with TBS containing 0.1% Triton X-100. Beads were boiled in SDS-PAGE sample buffer, loaded onto SDS-PAGE gels and analyzed by western blotting.

2.4. Drug treatments

Stimulation of synaptic NMDARs (SynStim) was obtained by treating hippocampal neurons at DIV14 with bicuculline (50 µM; Tocris) and 2,5 mM 4-aminopyridine (4-AP; Tocris) in Neurobasal medium supplemented with B27 for 30 min as previously reported (Di Luca et al., 2016). Bisindolylmaleimide I (BIM, 10 µM; Tocris) or Autocamtide II-related inhibitory peptide (10 nM, Calbiochem) were incubated for 10 min followed by the SynStim protocol for 30 min (post-translational effect) or 2h (transcriptional effect). Phorbol 12-myristate 13-acetate (PMA, 10 µM; Tocris) was

incubated in Neurobasal medium supplemented with B27 for 15 minutes at 37°C.

2.5. Western blotting

After lysate preparation from cell culture or tissue, we determined protein concentration for each lysate. We determined how much protein to load, and we separated proteins by electrophoresis using a polyacrylamide gel in denaturing conditions (SDS-PAGE). We then transferred the separated proteins onto a nitrocellulose membrane. We performed the transfer at 250 mA for 2h in 1x blotting buffer (25mM Tris, 192mM glycine) in presence of 20% methanol. After the transfer we fast detected the protein bands on nitrocellulose membrane using Ponceau staining. Then, we blocked membranes in iBlock-TBS or 5% milk in TBS for 1 hour and incubated the membranes with primary antibody over night at 4°C. The day after, membranes were washed in TBST 3 times for 10 minutes each wash, at room temperature. Membranes were then incubated with secondary antibody coupled with horseradish peroxidase for 1 hour at room temperature and washed again 3 times in TBST for 10 minutes at room temperature. For detection we used Biorad ECL substrates. For chemiluminescence western blot detection we used the ChemiDoc MP system (Bio-Rad Laboratories).

2.6. Luciferase assays

The 5HRp21_Luc2_T2A_TdTomato luciferase reporter plasmid was co-transfected in primary hippocampal neurons with a plasmid containing an expression cassette for *Renilla* luciferase for normalization with or without either RNF10WT, RNF10S31D or RNF31S31A. Neurons were harvested 4 days post-transfection. Luciferase activities were measured with the Dual-Glo Luciferase assay kit (Promega) following manufacturer's instructions.

3. Molecular biology

3.1. Bacteria Transformation

We used *E.Coli* DH5 α /BI21 strain for our transformation protocol. We added 1 μ g of DNA into 50 μ L aliquot of the competent cells and incubated on ice for 20 minutes. Then, we shocked the cells with increasing the temperature until 42°C for 50/90 seconds and putting them again in ice for 2 minutes. We added 250 μ L of S.O.C. Media to the cells and incubated them for 1h at 37°C with vigorous shaking. Finally, we plated

the cells on LB-agar plates with the antibiotic of choice and incubated at 37°C overnight for colonies to grow.

3.2. Cloning, expression and purification of GST fusion protein

Point mutations were generated in the RNF10 sequence either in the pGEX-KG, tdEOS, GFP-tag or Myc-tag vectors, using primers designed to create a missense mutation in a PCR reaction using Pfu polymerase (Stratagene). Glutathione-S-transferase (GST)-RNF10 fusion proteins containing wild-type or mutated RNF10 were expressed in *Escherichia coli* and purified on glutathione agarose beads (Sigma Aldrich, St. Louis, MO) as previously described (Gardoni et al., 1999). Briefly, overnight cultures from single colonies of *E. coli* transformed with the plasmid were grown in 50 ml of Luria-Bertani medium (Sigma, St. Louis, MO, USA) containing 100 µg/ml ampicillin (Sigma, St. Louis, MO, USA) at 37°C, diluted 1:10 with Luria-Bertani medium containing 100 µg/ml ampicillin and incubated under the same conditions for 2 h. Synthesis of recombinant proteins was induced by 0.1 mM isopropyl-β-D-thiogalactopyranoside (Sigma, St. Louis, MO, USA), the bacteria were grown for another 4 h and harvested by centrifugation. Bacterial pellets were resuspended with ice-cold PBS (8.4 mM Na₂HPO₄, 1.9 mM NaH₂PO₄, 150 mM NaCl, pH 7.4) containing 5 mM dithiothreitol (DTT), 100 µg/ml lysozyme, 0.1 mM PMSF and incubated on ice for 15 min. Lysis was achieved by the addition of 1.5% *N*-laurylsarcosine (sarkosyl) from a 10% stock in PBS. Bacteria were sonicated on ice for 1 min and the lysate was clarified by centrifuging at 10 000×g (5 min, 4°C) in a SS-34 rotor (Sorvall). Supernatants were adjusted to 2% Triton X-100 and incubated with glutathione-agarose beads (50% v/v in PBS) for 2 h at room temperature. The beads were then extensively washed with ice-cold PBS.

The p21prom-Luc2-T2A-tdTomato reporter system was created by cloning 4.5 Kb promoter region of the mouse p21waf1/cip1 gene upstream a bicistronic reporter system containing the luc2 (Paguio et al., 2005) and td-Tomato (Shaner et al., 2004) genes joined by the T2A self-cleaving peptide sequence. The 4.5 Kb promoter region was amplified with Platinum™ Pfx DNA Polymerase (Thermo Fisher Scientific) from genomic DNA using the following primers:

m_p21_3b_for 5'-GGATTCGCATATGGCAGATCCACAGCGATATCC-3'

m_p21_4530a_rev 5'-CTGGTCAGTCGACCATGGTGCCTGTGGCTGAAA-3'

4. Confocal imaging

4.1. Immunofluorescence

Primary hippocampal neurons were treated at DIV14 and fixed for 5 minutes with 4% paraformaldehyde (PFA)-4% sucrose in PBS solution at 4°C. Neurons were then washed with PBS at least three times. After that, cells were permeabilized with 0.2% Triton-X100 in PBS for 15 minutes and blocked with 5% BSA in PBS for 1 h at room temperature. Neurons were then labeled with primary antibodies in 3 % BSA in PBS in a humidified chamber at 4°C overnight, followed by extensive washing with PBS at room temperature. Secondary antibodies were applied in 3% BSA in PBS for 1 hour at room temperature, washed with PBS and coverslips were mounted on glass slides using Fluoroshield mounting medium (Sigma). We stored the slides at 4°C until confocal imaging studies. Fluorescence images were acquired by using Zeiss Confocal LSM510 system or Nikon A1 Ti2 system with a sequential acquisition setting at 1024x1024 pixels resolution; cells were selected from different coverslips at random for quantification. For all images the signals for each image were kept within the linear range and settings were consistent between different experimental conditions for an unbiased comparison.

4.2. In situ Proximity Ligation Assay (PLA)

PLA was performed in primary hippocampal neurons as previously described (Söderberg et al., 2006). Cells were fixed with 4% PFA - 4% Sucrose in PBS solution for 5 min at 4°C. Cells were then rinsed in PBS, permeabilized with 0.1% Triton X-100 in PBS for 15 min at room temperature and blocked with 5% BSA in PBS for 30 min at room temperature. Neurons were then incubated with mouse monoclonal anti-Myc antibody (1:2000; Millipore) and rabbit polyclonal anti- GluN2A antibody (1:200; Lifetechnologies) or anti-RNF10 antibody (1:200; Proteintech) and anti-GluN2A antibody (1:200; Neuromab) overnight at 4°C in a humidified chamber. After washes with PBS, cells were incubated for 1h with the PLA secondary probes anti-mouse Plus and anti-rabbit Minus (Olink Bioscience) at 37°C. Cells were washed thrice with Duolink II Wash Buffer A (Olink Bioscience) and incubated with the ligation in ligase buffer (Olink Bioscience) for 30 min at 37°C. After two additional rinsing with Wash Buffer A, cells were incubated with DNA polymerase (1:80; Olink Bioscience) in the amplification buffer (Olink Bioscience) for 100 min at 37°C in dark. Cells were next washed with Duolink II Wash Buffer B (Olink Bioscience) and then, if necessary, incubated with chicken polyclonal anti-GFP (1:400; Milipore) overnight at 4°C. After washing with PBS,

cells were incubated with secondary goat anti-chicken-AlexaFluor 488 for 1h at room temperature. The cells were washed in PBS and mounted on glass slides with Fluoroshield mounting medium (Sigma). Fluorescence images were acquired by using Zeiss Confocal LSM510 system or Nikon A1 Ti2 system with a sequential acquisition setting at 1024x1024 pixels resolution. All images were acquired standing the signals within the linear range in order to perform a reliable quantification and to compare appropriately all experimental conditions.

4.3. Time-lapse imaging

Zeiss Confocal LSM510 system was used for time-lapse imaging of RNF10 fused to tdEOS. For the photoconversion of tdEOS, ROIs were selected along distal dendrites and then 405 nm stimulation at 50% laser power was applied. Along the z-axis at list 10 optical sections with focus depth of 300-400 nm were taken in order to cover the complete volume of imaged neurons. Neurons were imaged for 42 minutes under controlled temperature and CO₂ levels.

4.4. Dil-labeling for spine morphology

For confocal microscopic imaging of dendritic spines we labeled neurons with Dil dye (Invitrogen), a fluorescent lipophilic carbocyanine dye, as it diffuses along the neuronal membrane labeling finely dendritic arborization and spine structures in hippocampal slices prefixed with 1.5% PFA (Kim, Dai, McAtee, Vicini, & Bregman, 2007). We performed the Dil labeling procedure as previously described (Kim et al., 2007). In short, Dil solid crystals were applied using a thin needle by lightly touching or gently poking the region of interest on both sides of 3 mm hippocampal piece, prepared after cardiac perfusion with 1.5% PFA in PB 0.1 M. Dil dye was left to diffuse for 1 day in the dark at room temperature, then slices were post-fixed with 4% PFA in PB 0.1 M for 45min at 4°C. The first slice containing the Dil crystals were discarded and 100 µm hippocampal slices were then obtain using a vibratome and collected in PBS. Slices were then mounted on Superfrost glass slides (Thermo Fisher) with Fluoroshield (Sigma) for confocal imaging. Fluorescence images were acquired by using Zeiss Confocal LSM510 system or Nikon A1 Ti2 system with a sequential acquisition setting at 1024x1024 pixels resolution at 555 nm channel. For each image between 40 and 100 sections of 0.5 µm were acquired and an appropriate z-projection was obtained.

4.5. Sholl analysis for neuronal branching and dendritic spine morphology

For analysis of neuronal branching and dendritic spine morphology, primary hippocampal neurons were transfected with GFP-containing constructs at DIV7. Cells were fixed and immunolabeled for GFP at DIV14. For three-dimensional morphological Sholl analysis, total dendritic length and dendrite morphology were calculated by using Fiji freeware software with the Simple Neurite Tracer plug-in. Briefly, a z-stack acquisition was imported, calibrated in Fiji, and semi-automatically traced. Total dendritic length was then computed. The shell interval was set at 5 μm . All analyses were performed blind. In all the experiments, for each condition, a minimum of 5 neurons from 3 independent preparations was analyzed. For spine morphology analysis, FIJI freeware software was used. Stacks were projected along the z ax to obtain a bidimensional image with all the spines in focus. For each spine the length of spine, the head width and the neck width were measured with straight-line function. When all the spines of the image have been measured, the total length of the dendrites was measured using the segmented line function of FIJI and spines were counted. Spine density were then analyzed.

5. Antibodies

The following antibodies were used: monoclonal antibody (mAb) anti- α -calcium/calmodulin-dependent kinase II (αCaMKII), polyclonal antibody (pAb) anti-GluN2A, pAb anti-CREB, pAb anti-p-CREB (Ser-133) and mAb anti-Myc were purchased from Millipore (Billerica, MA, USA); mAb anti-Meox2 was purchased from Abcam (Cambridge, MA, USA); pAb anti-p44/42 MAPK, pAb anti-p-p44/42 MAPK (Thr202/Tyr204) were purchased from Cell Signalling (Danvers, MA, USA); mAb anti-GFP, mAb anti-GST and anti-PSD-95 were purchased from NeuroMab (Davis, CA, USA); mAb anti-alpha-Tubulin and mAb anti-Flag were purchased from Sigma-Aldrich (St. Louis, MO, USA); mAb anti-p21 were purchased from BD Biosciences (NJ); pAb anti-histone H3 and pAb anti-RNF10 were purchased from Proteintech (Chicago, MI, USA, USA); mAb anti-JL8 was purchased from Clontech (Mountain View, CA, USA); pAb anti-HA was purchased from Santa Cruz Biotechnology (Dallas, TX, USA) p-RNF10(S31) was custom generated from Primm (Cambridge, MA, USA). Peroxidase-conjugated secondary anti-mouse Ab and peroxidase-conjugated secondary anti-rabbit Ab was purchased from Bio-Rad (Hercules, CA, USA). AlexaFluor secondary Abs were purchased from Invitrogen (Carlsbad, CA, USA).

6. Animals

The animals used in this project were male C57BL6 mice lacking the RNF10 gene (RNF10^{-/-}) or wildtype (WT) littermates. Mice were placed with a maximum of five per cage under standard environmental conditions (ambient temperature of 21 ± 1 °C and a relative humidity of 50-60%; 12h light/dark cycle (lights on at 8:00 A.M.; dark at 8:00 P.M.) with ad libitum access to food and water. The Institutional Animal Care and Use Committee of the University of Milan and the Italian Ministry of Health (#191/2016) approved the experiments involving RNF10 KO mice. Animal handling and surgical procedures were carried out with care taken to minimize discomfort and pain, in accordance with the ethical guidelines and regulations of the European Parliament and of the Council on protection of animals used for scientific purposes (Directive of 22 September 2010, 2010/63/EU).

7. Quantification and Statistical analysis

Quantification of Western Blot analysis was performed using the software ImageLab (BioRad Laboratories). The levels of the proteins were expressed as relative optical density (OD) normalized on actin or tubulin levels as housekeeping proteins. Statistical analysis was performed with GraphPad Prism6 software and data were presented as mean \pm SEM (standard error of the mean). The tests used to assess data significance are indicated in the figure legends, we used 2-tailed Student *t* test (a *p* value less of 0.05 was considered significant) or one-way ANOVA followed by Tukey or Bonferroni's as a post-hoc test. Images acquired with confocal microscope were analyzed with the use of Fiji / Image J software. Colocalization analysis were performed using Zeiss AIM 4.2 software. For WB, IP and GST-pulldown assay, at least 3 independent experiments were performed. For confocal studies, at least 10 neurons coming from 3 different experiments were analyzed.

RESULTS

1. PKC Activation Regulates RNF10 Translocation to the Nucleus

RNF10 association with the NMDAR complex is strictly dependent on the interaction between RNF10 N-terminal domain (aa 1-74) and the C-tail of the GluN2A subunit. Of note, calcium significantly reduces the formation of GluN2A/RNF10 complex by promoting the association of calmodulin (CaM) at the same GluN2A binding site (Dinamarca et al., 2016). Bioinformatic tools (NetPhos 3.1, KinasePhos 2.0, and phosphosite.org) indicated the presence of several putative PKC-dependent phosphosites within the RNF10 sequence aa 1-74 (Fig. 1a). Thus, we sought to investigate the possible role of PKC in the disruption of RNF10/NMDAR complex and RNF10 trafficking to the nucleus.

Our lab has previously demonstrated that stimulation of synaptic NMDARs induces RNF10 synaptonuclear trafficking leading to its nuclear accumulation (Dinamarca et al., 2016). To characterize the role of PKC in the modulation of RNF10 trafficking induced by activation of the excitatory synapse, NMDAR synaptic stimulation was applied in primary hippocampal cultures in presence or absence of a highly selective, cell-permeable, and reversible PKC inhibitor (Bisindolylmaleimid; BIM) (Toullec et al, 1991). Proximity ligation assay (PLA) experiments revealed that synaptic stimulation of NMDAR induces a significant reduction of the interaction between RNF10 and GluN2A, as a lower number of PLA clusters was detected compared to the control (Fig. 1b). BIM co-incubation fully prevented the synaptic stimulation-induced loss of interaction between RNF10 and GluN2A (Fig. 1b). Moreover, confocal imaging (Fig. 1c) and western blotting analyses performed in crude nuclear extracts (Fig. 1d) indicate that BIM completely prevented the expected RNF10 nuclear accumulation induced by activation of synaptic NMDARs. Further, PKC inhibitor also blocked the synaptic stimulation-mediated up-regulation of p21WAF1/Cip1 protein levels (Fig. 1e), a well-validated target gene of the RNF10 pathway (Dinamarca et al., 2016; Lin et al., 2005; Malik et al., 2013). Since the main factors implied in RNF10 trafficking induction are NMDA activation and rise in calcium levels (Dinamarca et al., 2016), we thought to investigate the possible role of another NMDAR associated kinase, that plays a fundamental role in LTP (Malinow, Schulman and Tsien, 1998, Barria and Malinow, 2005), CaMKII. Inhibition of CaMKII using a specific pharmacological inhibitor (Autocamtide II)(Gardoni et al., 2001) did not block RNF10 nuclear accumulation induced by synaptic stimulation of NMDAR (Fig. 1f), revealing no involvement of the protein kinase in RNF10 induction.

FIGURE 1

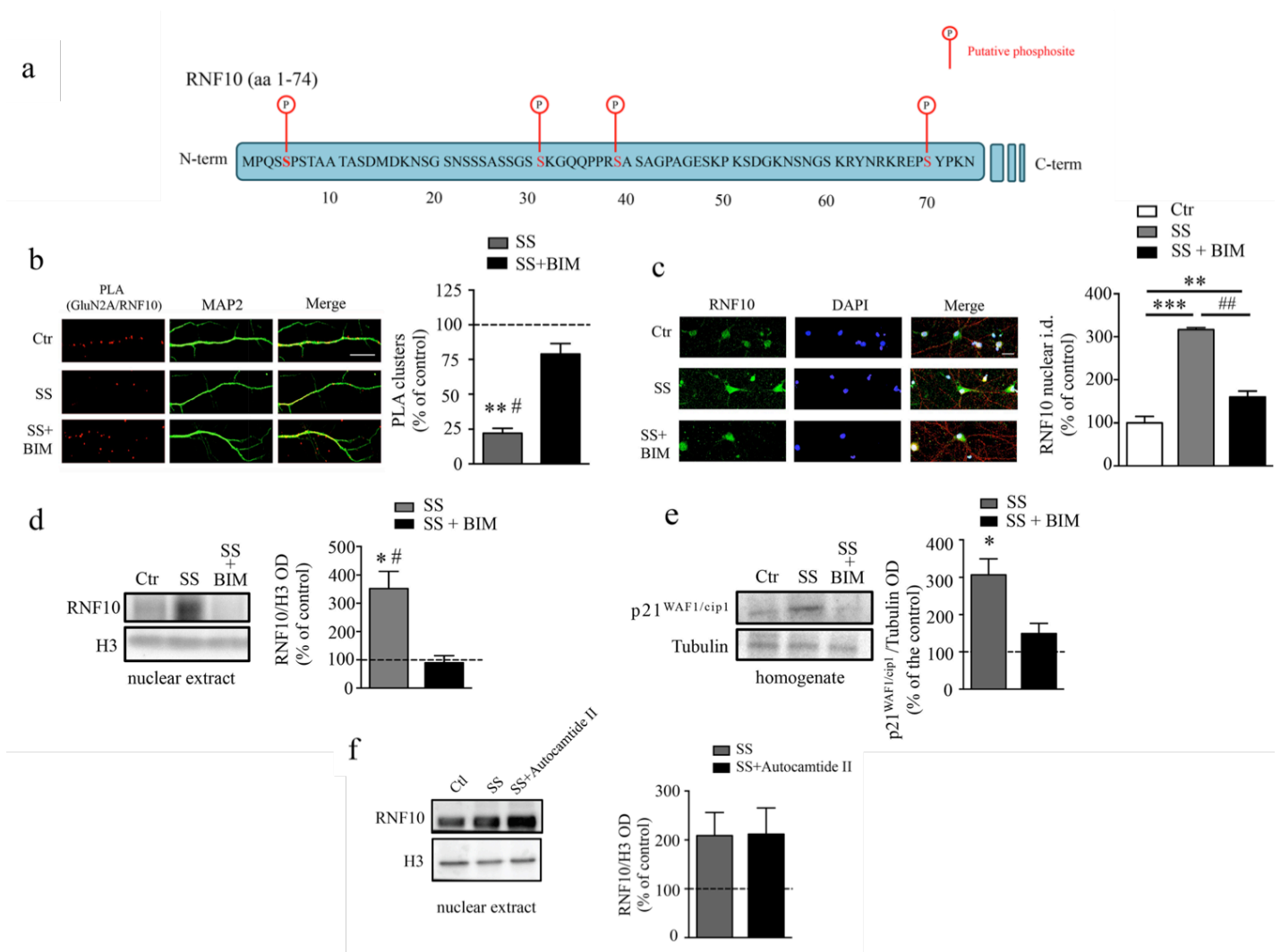


Fig. 1 Synaptic NMDAR stimulation induces RNF10 trafficking and it's prevented by PKC inactivation.

a Representative scheme of RNF10 1-74 aa. Putative PKC-dependent phosphosites are evidenced. **b** In situ detection of proximity ligation assay (PLA) between RNF10 and GluN2A (red; left panels) along MAP2-positive dendrites (green; middle panels) in DIV14 hippocampal neurons treated with vehicle (Ctr), SS (2,5 mM 4-AP and 50 μM bicuculline for 30 min), or SS+BIM (preincubation with 10 μM BIM for 10 min, then SS). The histogram shows the quantification of the number of PLA clusters along MAP2-positive dendrites expressed as % of control. Scale bar: 10 μm. **c** Representative confocal images and quantification of RNF10 (green) nuclear localization in hippocampal neurons treated at DIV14 with vehicle, SS, or SS+BIM. DAPI (blue) and PSD-95 (red, see merge panels) were used to stain nuclei and mature dendritic spines, respectively. The histogram shows the quantification of RNF10 integrated density (i.d.) in the nucleus expressed as % of control. Scale bar: 20 μm. **d** Representative immunoblots and quantification of WB for RNF10 in nuclear extract from DIV14 hippocampal neurons treated with vehicle, SS, or SS+BIM. H3 was used as loading control. The histogram shows the quantification of RNF10 optical density (OD) normalized on histone-H3 and expressed as % of control. **e** Representative immunoblots and quantification of WB for p21WAF1/cip1 in nuclear extract from primary hippocampal neurons at DIV14 treated with vehicle, SS, or SS+BIM. Tubulin was used as loading control. The histogram shows the quantification of p21WAF1/cip1 optical density (OD) normalized on tubulin and expressed as % of control. **f** Representative immunoblots and quantification of WB for RNF10 in nuclear extract from DIV14 hippocampal neurons treated with vehicle, SS or SS+Autocamtide II. H3 was used as loading control. Statistical analysis: one-way ANOVA; *p < 0.05, **p < 0.01, ***p < 0.001 (vs Ctr); #p < 0.05, ##p < 0.01 (vs SS+BIM)

In addition, treatment of primary hippocampal neurons with the PKC activator phorbol 12-myristate 13-acetate (PMA; 10 μ M) (Robinson, 1992) led to an increase of RNF10 nuclear levels measured by confocal imaging (Fig. 2b) and western blotting analyses of crude nuclear fractions (Fig. 2c). Taken together, these results indicate that PKC activation is essential for the induction of RNF10 translocation to the nucleus and modulation of the expression of RNF10 target genes.

FIGURE 2

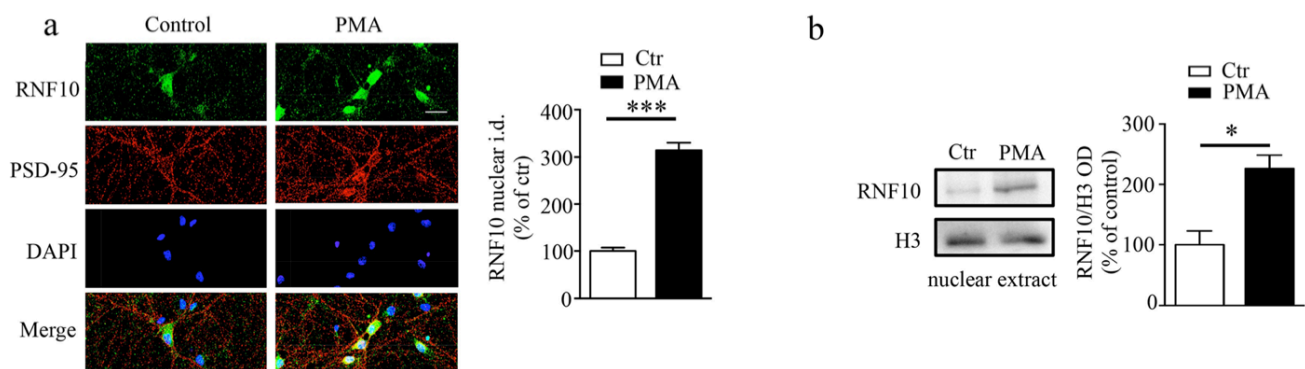


Fig. 2 PKC activation induces RNF10 nuclear accumulation

a Representative confocal images and quantification of RNF10 (green) nuclear localization in hippocampal neurons treated at DIV14 with vehicle or 10 μ M PMA for 15 min. DAPI (blue) and PSD-95 (red) were used to stain nuclei and dendritic spines, respectively. The histogram shows the quantification of RNF10 integrated density (i.d.) in the nucleus expressed as % of control (ctr). Scale bar: 20 μ m. **b** Representative immunoblots and quantification of WB for RNF10 in nuclear extract from DIV14 hippocampal neurons treated with vehicle or PMA. The histogram shows the quantification of RNF10 optical density (OD) normalized on histone-H3 and expressed as % of control. Statistical analysis: one-way ANOVA; * $p < 0.05$, *** $p < 0.001$ (vs Ctr);

2. RNF10 Phosphorylation by PKC Modulates RNF10/NMDAR Complex Dissociation and Nuclear Localization

In order to confirm that PKC-dependent modulation of RNF10 trafficking is directly correlated to a kinase-substrate event, we analyzed RNF10 phosphorylation in primary hippocampal neurons following synaptic stimulation in presence or absence of the PKC inhibitor BIM. Neuronal homogenates were immunoprecipitated using an anti-phosphoserine antibody. Western blotting analysis of RNF10 revealed an increase of RNF10 phosphorylation on serine residues following stimulation of synaptic NMDARs in the immunocomplex (Fig. 3a). The PKC inhibitor fully prevented RNF10 serine phosphorylation, suggesting that PKC is the main kinase involved in the process (Fig. 2a). As already mentioned, the analysis of RNF10(1-74) domain (see Fig. 1a) revealed the presence of at least four serine residues (Ser5, Ser31, Ser39, Ser70) that might represent a putative phosphate acceptor site for PKC and possibly involved in the regulation of RNF10 binding to GluN2A. A point mutation strategy was used to determine the effects of PKC site-specific phosphorylation of RNF10. GST fusion proteins of RNF10(1-74) wild-type (wt) and with single Ser/Asp mutation, mimicking the phosphorylation, were generated and used in an *in vitro* pull-down assay from rat hippocampal homogenates. As shown in Fig. 3b, Ser31Asp (S31D) mutation completely abolished the capability of GST-RNF10 fusion protein to bind the GluN2A subunit. No significant difference in RNF10's ability to form the GluN2A/RNF10 complex was observed by using S5D, S39D, and S70D constructs compared to the wild type counterpart (Fig. 3b), suggesting that phosphorylation of Ser31 is the main responsible for the modulation of the interaction with GluN2A. To confirm the *in-vitro* assay we then transfected COS-7 cells with GFP-GluN2A and Myc-RNF10wt, Myc-RNF10S31D (mimicking phosphorylation), or Myc-RNF10S31A (not permissive of phosphorylation as control). A co-immunoprecipitation assay was performed in cell lysates to confirm the role of RNF10 Ser31 phosphorylation in the modulation of RNF10 interaction with the NMDAR subunit. No effect was observed by the S31A mutation (Fig. 3c). Conversely, S31D mutation induced a significant reduction of RNF10 binding to GluN2A (Fig. 3c). These results confirm that also in a heterologous system the phosphorylation of Ser31 residue interferes with the formation of GluN2A/RNF10 complex (Fig. 3c). In addition, no effect of S31D and S31A mutations on RNF10 interaction with importin- α 1 was observed (Fig. 3d), thus suggesting that Ser31 phosphorylation does not affect importin-mediated trafficking of RNF10 to the nucleus (Dinamarca et al., 2016).

FIGURE 3

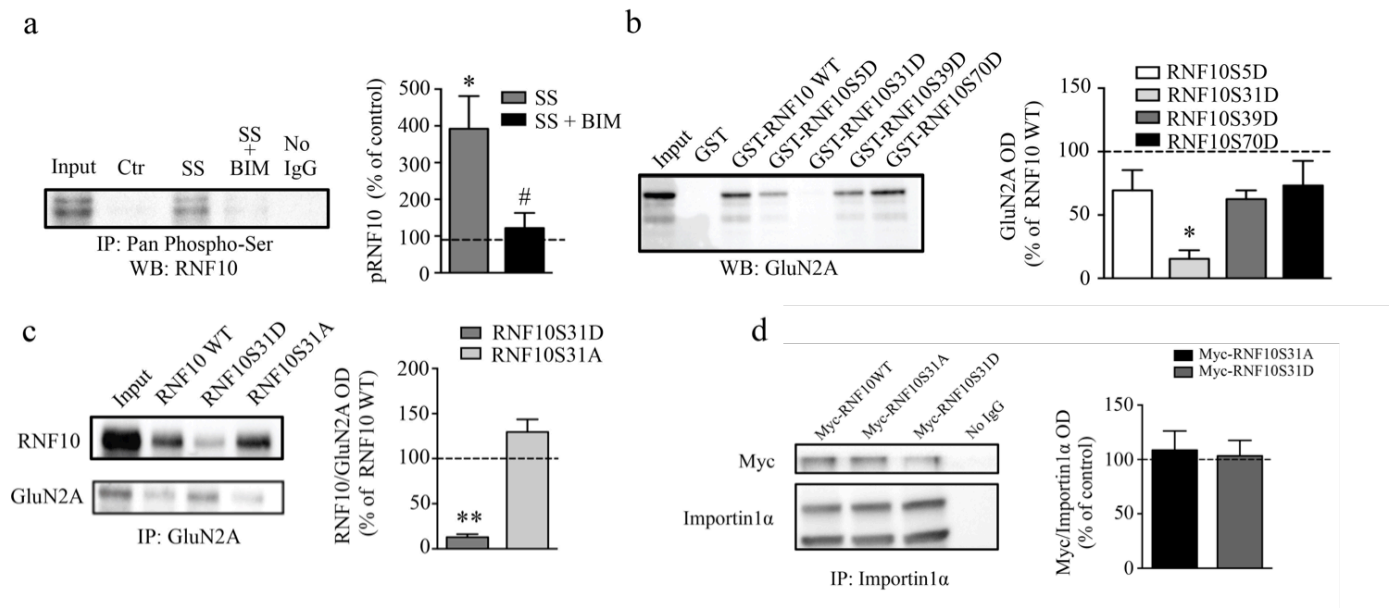


Fig. 3 Ser31 phosphorylation regulates RNF10 interaction with NMDA receptor but not importin- α 1.

a Representative immunoblots and quantification of an immunoprecipitation (IP) experiment on homogenates of DIV14 hippocampal neurons treated with vehicle, SS, or SS+BIM. Phospho-Ser proteins were immunoprecipitated and RNF10 revealed by western blotting in the immunoprecipitated material. The histogram shows the quantification of the phosphorylated RNF10 (pRNF10) optical density (OD) expressed as % of control. **b** GST and GST-RNF10WT, GST-RNF10S5D, GST-RNF10S31D, GST-RNF10S39D, GST-RNF10S70D fusion proteins were incubated in a pull-down assay with rat hippocampal extracts. GluN2A was revealed by western blotting analysis. The histogram shows the quantification of GluN2A optical density (OD) expressed as % of pull-down assay performed with RNF10WT. **c** Representative immunoblots and quantification of Co-IP experiment on homogenates of COS-7 cells transfected with Myc-RNF10WT, Myc-RNF10S31D, or Myc-RNF10S31A. GluN2A was immunoprecipitated and RNF10 revealed. GluN2A was used as loading control. The histogram shows the quantification of RNF10 interaction with GluN2A (RNF10/GluN2A optical density, OD) expressed as % of the sample transfected with RNF10WT. **d** Representative immunoblots and quantification of IP experiment on homogenates of DIV14 hippocampal neurons transfected with Myc-RNF10WT, Myc-RNF10S31A or Myc-RNF10S31D. Importin1 α was immunoprecipitated and Myc revealed. Statistical analysis: one-way ANOVA; * $p < 0.05$, ** $p < 0.01$ (vs Ctr); # $p < 0.05$ (vs SS+BIM).

To unravel the functional significance of PKC-dependent phosphorylation of RNF10 in hippocampal neurons, a phosphospecific antibody–RNF10S31P–was produced, affinity purified, and characterized. RNF10S31P antibody recognized with higher affinity the purified GSTRNF10S31D mutated fusion protein, mimicking the phosphorylation, compared to GST-RNF10WT (Fig. 4a). Moreover, the RNF10S31P antibody detected myc-RNF10S31D but not myc-RNF10S31A in lysates derived from transfected COS-7 cells (Fig. 4b). Finally, we infected primary hippocampal neurons with either the LKO-shRNF10 lentivirus targeting RNF10 expression or scrambled sequence as a control. RNF10 silencing via shRNF10 lentivirus significantly reduced the RNF10 protein level compared to scramble construct as previously demonstrated (Dinamarca et al., 2016). No signal was detected in the shRNF10 sample both using the commercial RNF10 antibody (ProteinTech) and the custom made RNF10S31P (Fig. 4c). Western blotting analysis for RNF10S31P in primary hippocampal neurons revealed an increase of RNF10 Ser31 phosphorylation in post-synaptic membrane fractions (triton insoluble fractions, TIF) following synaptic stimulation of NMDAR (Fig. 4d), in agreement with the results observed using the pan-phosphoserine antibody (Fig. 3a). The PKC inhibitor BIM completely prevented Ser31 phosphorylation (Fig. 4d). Similarly, a highly validated protocol to induce cLTP (Dinamarca et al., 2016) was sufficient to increase RNF10 Ser31 phosphorylation as measured 15 min after cLTP induction (Fig. 4e).

FIGURE 4

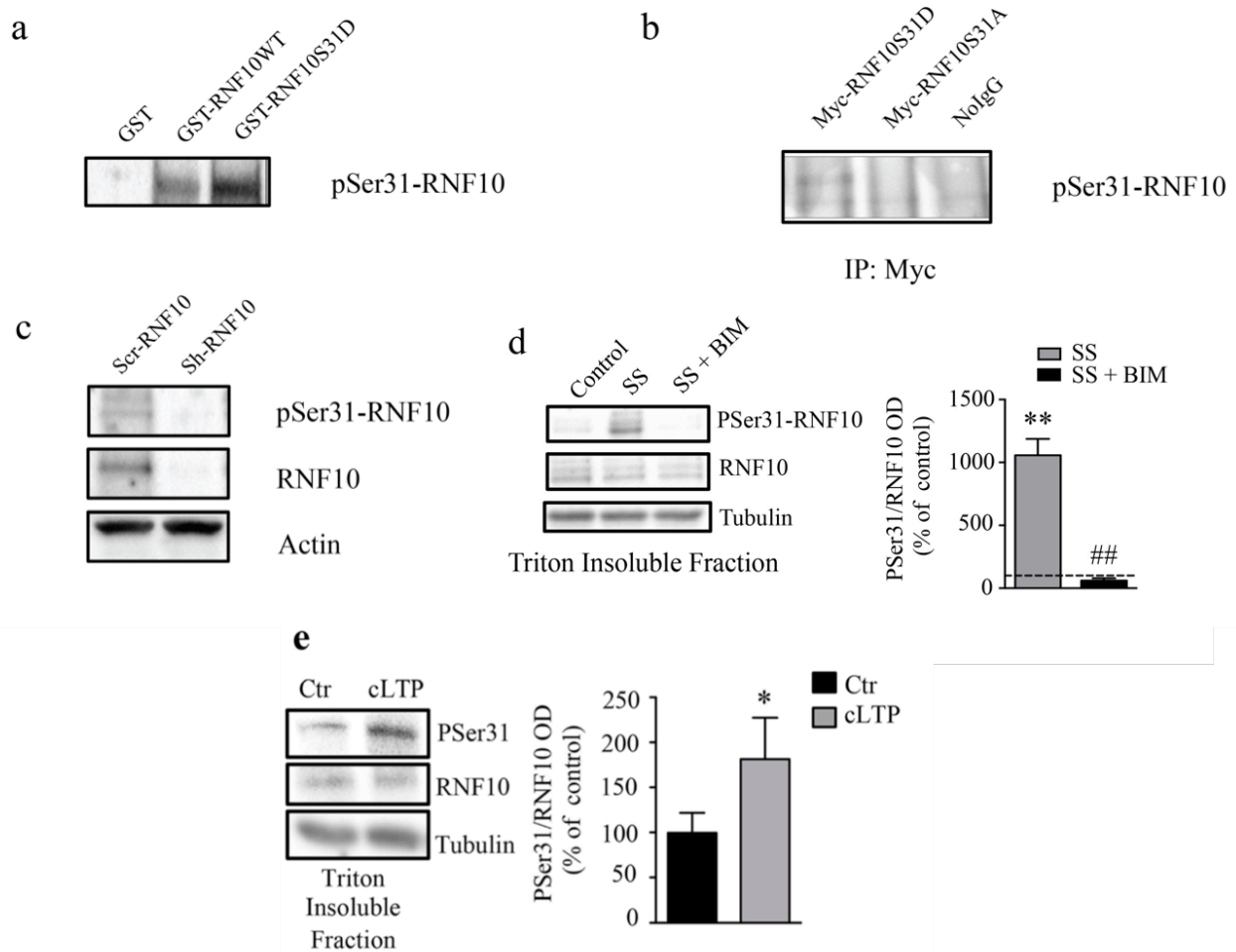


Fig. 4 Synaptic NMDAR stimulation and LTP both induce RNF10 phosphorylation in Ser31.

a Representative immunoblot of GST, GST-RNF10WT, GST-RNF10S31D fusion proteins. Custom made pSer31-RNF10 antibody was used for the WB. **b** Representative immunoblot of IP experiment on homogenates of COS-7 cells transfected with MycRNF10S31A or Myc-RNF10S31D. Myc was immunoprecipitated and pSer31-RNF10 revealed in WB. **c** Representative immunoblot of pSer31-RNF10 and RNF10 in homogenates from DIV14 hippocampal neurons infected with scrRNF10 or shRNF10 lentivirus. Actin was used as loading control. **d** Representative immunoblots and quantification of western blotting for Pser31-RNF10, RNF10, and tubulin in Triton Insoluble Fractions of primary hippocampal neurons treated at DIV14 with vehicle, SS, or SS+BIM. Tubulin was used as loading control. The histogram shows the quantification of Pser31- RNF10/RNF10 ratio optical density (OD) after normalization on tubulin and expressed as % of control. **e** Representative immunoblots and quantification of western blotting for Pser31-RNF10, RNF10, and tubulin in Triton insoluble fractions of primary hippocampal neurons treated at DIV14 with vehicle or cLTP. Tubulin was used as loading control. The histogram shows the quantification of Pser31-RNF10/RNF10 ratio optical density (OD) after normalization on tubulin and expressed as % of control.

Statistical analysis: (a-d) one-way ANOVA; **p < 0.01 (vs Ctr); (e) Student t test; *p < 0.05 (vs Ctr).

These results show that all the stimuli that are able to trigger RNF10 detachment from NMDAR and translocation to the nucleus are able to induce a PKC-dependent phosphorylation of RNF10 in Ser31. We then used two different experimental approaches to monitor if RNF10 accumulated in the nucleus after synaptic stimulation remains phosphorylated on Ser31. Western blotting analysis for RNF10S31P revealed an increase of RNF10 Ser31 phosphorylation in the crude nuclear fraction following synaptic stimulation of NMDAR (Fig. 5a, left graph). However, considering the above-described accumulation of RNF10 in the nucleus after synaptic stimulation (see Fig. 1d, 1e), we did not observe any increase in the nucleus of the PSer31-RNF10/total RNF10 ratio (Fig. 5d, right graph). To better address this issue, we performed PLA experiments using the RNF10S31P antibody and total RNF10 antibody for the assay. As shown in Fig. 4g, we found a significant increase of nuclear PLA clusters indicating Ser31 phosphorylation following stimulation of synaptic NMDARs.

FIGURE 5

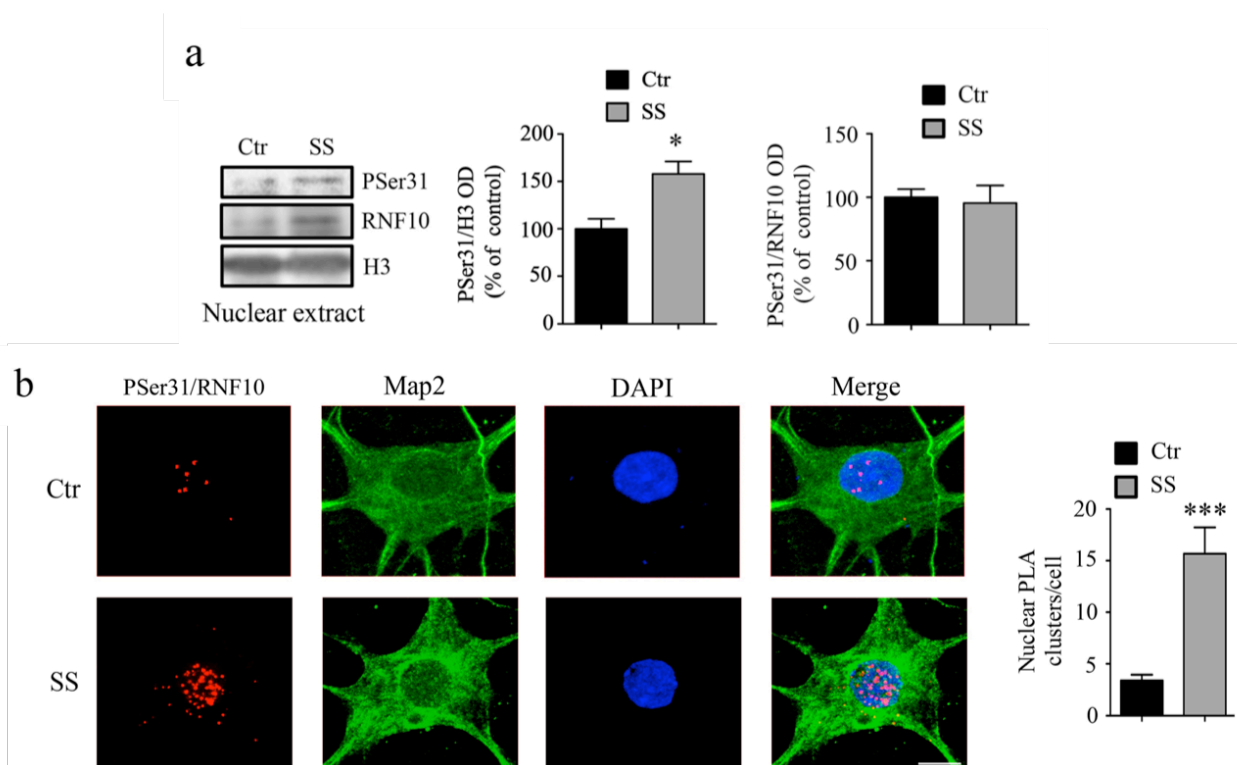


Fig. 5 P-Ser31-RNF10 is located in the nucleus.

a Representative immunoblots and quantification of western blotting for P-Ser31-RNF10, RNF10, and H3 in crude nuclear fractions of primary hippocampal neurons treated at DIV14 with vehicle (Ctrl) or SS protocol. H3 was used as loading control. The histograms show the quantification of P-Ser31-RNF10 optical density (OD) after normalization on H3 (left graph) or on total RNF10 (right graph) and expressed as % of control. **b** In situ detection of PLA assay with RNF10S31P and total RNF10 antibodies (red; left panels) in the nucleus (DAPI, blue) in DIV14 hippocampal neurons treated with vehicle (Ctrl) or SS protocol. Map2 staining is shown in green. The histogram shows the quantification of the number of nuclear PLA clusters. Scale bar: 10 μ m. Statistical analysis: Student t test; * $p < 0.05$, *** $p < 0.001$ (vs Ctrl).

These results suggested that Ser31 phosphorylation could control the synaptic stimulation-induced RNF10 translocation from the synapse to the nucleus. To further validate these data and to analyse the dynamic of these events, we used a live imaging approach based on TdEOS plasmid. TdEOS is a bright and photostable photoconvertible fluorescent tag that after stimulation changes its emission wavelength from green to red allowing the tracking of the movement of the labeled protein into biological systems (Karpova et al., 2013; Dinamarca et al., 2016). We monitored the nuclear translocation of RNF10 WT-TdEOS and the RNF10 S31A-TdEOS mutant by confocal imaging following synaptic stimulation. As expected (Dinamarca et al., 2016), after photoconversion in distal dendrites, RNF10 WT moved from the synapse to the nucleus in NMDA synaptic stimulation conditions (Fig. 3a). Photoconverted RNF10S31A mutant wasn't able to accumulate into the nucleus (Fig. 3a), confirming that RNF10 Ser31 phosphorylation is crucial for the dissociation from GluN2A and the subsequent nuclear trafficking. We confirmed the specific role of Ser31 phosphorylation in the modulation of RNF10 clustering with GluN2A by PLA in primary hippocampal neurons transfected with GFP-GluN2A and either Myc-RNF10WT or Myc-RNF10S31D. A significant lower number of PLA signals were detected for the S31D construct indicating a decreased number of RNF10 molecules in close proximity (< 40 nm) to the receptor subunit (Fig. 3b). In addition, immunofluorescence on primary hippocampal neurons transfected with Myc-RNF10WT or Myc-RNF10S31D revealed that Myc-RNF10S31D spontaneously accumulated in the nucleus in absence of any stimulation (Fig. 3c), compared to Myc-RNF10WT that localized more in the cytosolic compartment, as previously reported (Dinamarca et al., 2016).

FIGURE 6

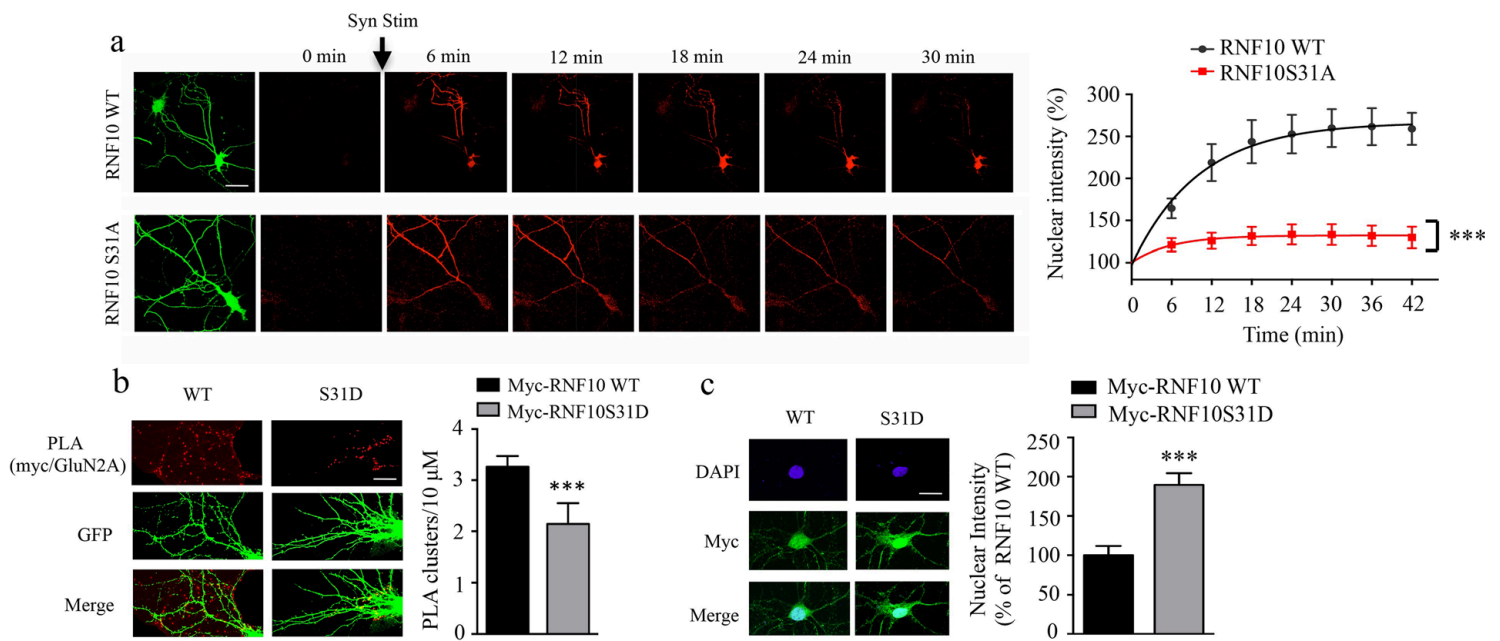


Fig. 6 PKC-dependent phosphorylation on Ser31 modulates RNF10 trafficking.

a Synaptic stimulation treatment induces RNF10WT-tEOS but not RNF10S31A-tEOS translocation from distal dendrites to the nucleus in hippocampal neurons. Left panels: baseline confocal image of RNF10WT-tEOS and RNF10S31A-tEOS expressing hippocampal neuron illuminated sequentially with 488 nm (green panels) and 555 nm laser excitation wavelengths showing no emitted signal in the red spectra (0 min panels). Distal dendrite selected for photoconversion was illuminated with violet laser (405 nm wavelengths) repetitively through the image z-stack. Right panels: depicted are confocal max intensity projection images at respective time points (6, 12, 18, 24, and 30 min) after synaptic stimulation protocol. The histogram shows a significant increase in RNF10WT-tEOS but not RNF10S31A-tEOS photoconverted fluorescent intensities (red) in the nucleus following synaptic stimulation protocol. Scale bar: 30 μm. **b** Representative confocal images and quantification of PLA (GluN2A/Myc-RNF10 interaction; red, upper panels) in DIV14 primary hippocampal neurons transfected with Myc-RNF10WT or Myc-RNF10S31D. The histogram shows the quantification of PLA clusters along GFP-positive dendrites expressed as number of clusters in 10 μm of dendrite. PLA clusters outside GFP-positive dendrites were not considered for the quantification. Scale bar: 20 μm. **c** Representative confocal images and quantification of Myc-RNF10 (green) nuclear localization in primary hippocampal neurons at DIV14 transfected with Myc-RNF10WT or Myc-RNF10S31D. DAPI (blue) was used to stain nuclei. The histogram shows the quantification of Myc-RNF10 integrated density in the nucleus expressed as % of Myc-RNF10WT. Scale bar: 15 μm. Statistical analysis: (a, b, c) Student t test; ***p < 0.001.

3. PKC-phosphorylation on Ser31 activates RNF10 transcriptional activity and induction of plasticity program

To assess whether the Ser31 phosphorylation-triggered RNF10 translocation to the nucleus affects gene expression, we performed a luciferase assay on primary hippocampal neurons transfected with a reporter construct expressing the firefly luciferase under the promoter of the validated RNF10 target p21WAF1/cip1 (5HRp21_Luc2_T2A_TdTomato, see methods) (Dinamarca et al., 2016; Lin et al., 2005; Malik et al. 2013). Neurons were transfected with RNF10WT, RNF10S31A, or RNF10S31D together with the luciferase reporter and normalizer (Renilla luciferase) constructs. As expected, RNF10S31D expression was associated to a higher firefly luciferase activity (Fig. 3d), indicative of a higher transcriptional activity induced by the mutant. RNF10S31A did not show difference in comparison to control (Fig. 3d). We previously reported the role of RNF10 in implementing LTP-mediated cellular effects and LTP maintenance (Dinamarca et al., 2016). Since Ser31-mediated nuclear accumulation affects the functionality of RNF10, we investigated whether manipulations of Ser31 phosphorylation could affect the capacity of RNF10 to convey LTP signaling pathways. We used CREB phosphorylation in Ser133 as a marker for the synaptic activation of NMDAR and plasticity, since CREB has been shown to be a hub in which many synaptic plasticity pathways converge (Dash, Hochner and Kandel, 1990; Hardingham, Fukunada and Bading, 2002; Sheng, McFadden and Greenberg, 1990; Robertson et al., 1999; Kanterewics et al., 2000; English and Sweatt, 1997). RNF10S31A transfected neurons had a decreased amount of pCREB levels compared to control, while RNF10S31D was able to induce pCREB expression (Fig. 7b). Taken together, our results suggest that the phosphorylation state of Ser31 on RNF10 is key for its nuclear accumulation and for signaling events downstream of NMDAR activation that are associated to synaptic plasticity.

FIGURE 7

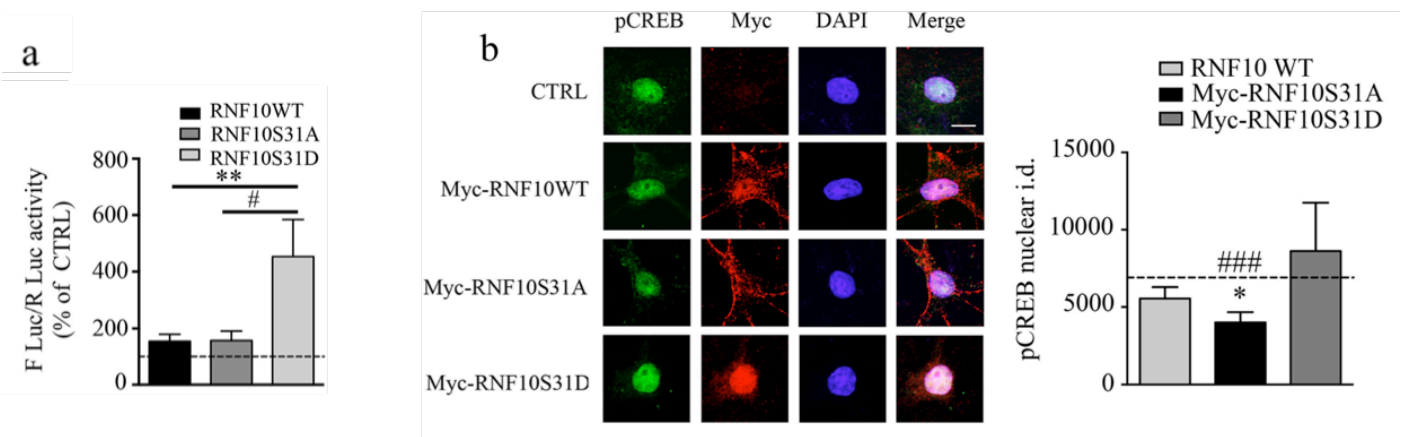


Fig. 7 Modulation of RNF10 phosphorylation in Ser31 affect its downstream signaling

a Histogram showing the quantification of Luciferase assay performed on lysates of neurons in which the p21prom-Luc2-T2A-tdTomato reporter plasmid was co-transfected in primary hippocampal neurons with a plasmid containing an expression cassette for Renilla luciferase for normalization with or without either RNF10WT, RNF10S31D, or RNF31S31A. Representative confocal images and quantification of pCREB (green) levels in DIV14 hippocampal neurons transfected with Myc-RNF10WT, Myc-RNF10S31A, or Myc-RNF31S31D. DAPI (blue) was used to stain nuclei. Transfected neurons were recognized with anti-Myc antibody (red). The histogram shows the quantification of pCREB integrated density (i.d.) in the nucleus expressed as % of control. Scale bar: 10 μ m. one-way ANOVA; * $p < 0.05$, ** $p < 0.01$ (vs RNF10WT); # $p < 0.05$, ### $p < 0.01$ (vs RNF10S31D).

4. The Modulation of RNF10 Activity Results in the Alteration of Neuronal Morphology

We previously found that RNF10 downregulation was associated to a decreased number of dendritic spines in hippocampal neurons (Dinamarca et al., 2016). Synaptic and dendritic developments are known to be strictly interconnected and to sustain each other reciprocally (Cline, 2001). Besides previous works reported the importance of the synaptonuclear signaling in the correct neuronal arborization (Marcello, Di Luca and Gardoni, 2018). For these reasons we decided to investigate the role of RNF10 in the regulation of dendritic morphology. Interestingly interfering with the expression of RNF10 via shRNA-mediated silencing (shRNF10) induced a significant simplification of dendrite arborization in primary hippocampal neuronal cultures in comparison to controls suggesting that RNF10 might have a global effect on dendritic architecture (Fig. 8c). We then analyzed if RNF10 Ser31 phosphorylation state, since important for RNF10 trafficking and signaling, could also regulate its functional outputs, in particular spine density and dendritic geometry. Morphometric analyses of primary hippocampal neurons transfected with RNF10WT, RNF10S31A, and RNF10S31D showed that RNF10S31A mutant had a similar behavior to RNF10 knockdown (Dinamarca et al., 2016) and induced a severe reduction of spine number (Fig. 8b) thus acting as a dominant negative protein. RNF10S31D had the opposite effect (Fig. 8b). No effect on spine density was observed following overexpression of RNF10WT, suggesting that a strong activation of a PKC-RNF10Ser31-dependent pathway, as for RNF10S31D, is needed for an increase of spine density (Fig. 8b). Notably, RNF10S31A expression reduced also dendritic arbor complexity compared to control (Fig. 8c). RNF10WT and RNF10S31D, on the contrary, did not alter neuronal geometry. Taken together, these results show that RNF10 functioning, encoded by its Ser31 phosphorylation, is necessary for the regulation of dendritic spines number and dendritic arborization.

FIGURE 8

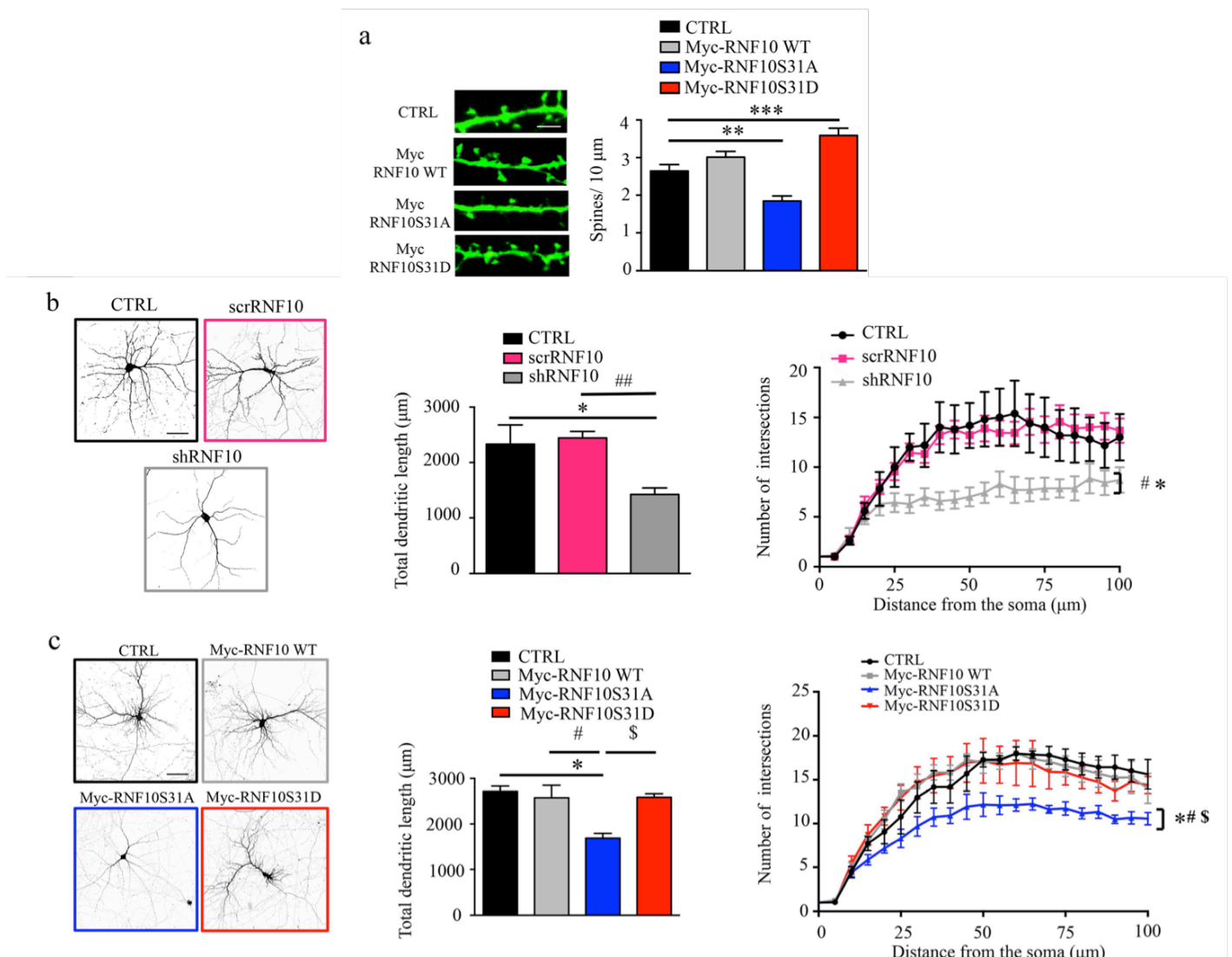


Fig. 8 Modulation of RNF10 levels or activity affects neuronal morphology.

a Representative confocal images and quantification of dendritic spine density in DIV14 hippocampal neurons transfected with GFP alone (upper panel) or co-transfected with GFP and Myc-RNF10WT, Myc-RNF10S31A, or Myc-RNF10S31D. The histogram shows the quantification of dendritic spine density expressed as number of spines in 10 μm of dendrite. Scale bar: 5 μm . **b** Representative confocal images (left panels) and Sholl analysis (right graph) of DIV14 hippocampal neurons transfected with scr-RNF10, sh-RNF10, or controls. The histogram in the middle shows the quantification of total dendritic length. Scale bar: 40 μm . **c** Representative confocal images (left panels) and Sholl analysis (right graph) of DIV14 hippocampal neurons transfected with Myc-RNF10WT, Myc-RNF10S31A, or Myc-RNF10S31D. The histogram in the middle shows the quantification of total dendritic length. Scale bar: 40 μm . Statistical analysis: one-way ANOVA; * $p < 0.05$, ** $p < 0.01$, *** $p < 0.001$ (vs Ctrl); # $p < 0.05$ (vs Myc-RNF10WT), ## $p < 0.01$ (vs scr-RNF10), ### $p < 0.001$ (vs Myc-RNF10S31D); \$ $p < 0.05$ (vs Myc-RNF10S31D).

5. RNF10 deficiency alters brain morphology *in vivo*

The *in vitro* results described above envisage a critical role for RNF10 as a regulator of neuronal morphology. As already mentioned, synaptonuclear messengers with a strong connection to synaptic plasticity resulted critical for a correct neuronal development *in vivo*, for instance Jacob depletion in mice induces hippocampal dysplasia with a reduced number of synapses and dendritic branching (Spilker et al., 2016). For this reason, we decided to evaluate if RNF10 synaptonuclear communication could be a necessary signal that links NDMAR activation to the correct neuronal morphological shaping. To achieve this aim, we took advantage of the RNF10^{-/-} mouse model, purchased from Knockout Mouse Project (KOMP) Repository (UC Davis). No published studies are reported about this animal model, so we decided to perform an intensive characterization of RNF10^{-/-} mice. As a first indication of the impact of RNF10 absence at brain level, in collaboration with the group of Binnaz Yalcin (IGBMC, Université de Strasbourg), we performed a gross neuroanatomical study of RNF10^{-/-} mice. Several brain parameters were measured in coronal section of RNF10^{-/-} and WT male adult mice (16 weeks old). From the analysis, different parameters resulted altered (Fig. 9a), among which total brain area (TBA), corpus callosum (cc) height and width; hippocampus (HP) area and total length of the pyramidal cell layer (TILpy) (Fig. 9b) resulted to be the most affected.

These results suggest that RNF10 absence induces *in vivo* a general alteration of brain development, with a particular impact on cerebral structures that are involved in inter-hemisphere connectivity or in learning and memory.

FIGURE 9

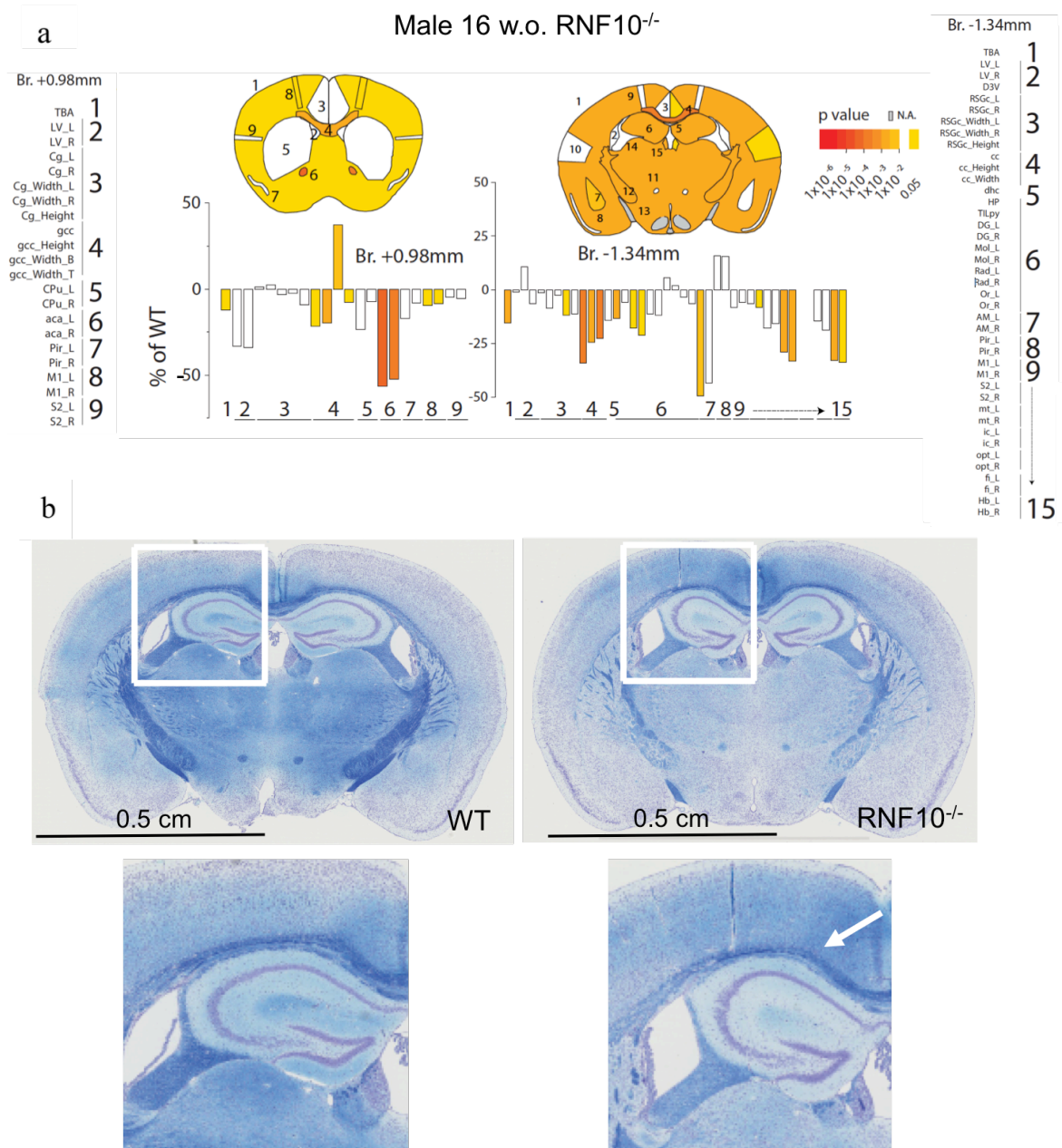


Fig. 9 RNF10 knockout results in altered brain morphology

a Representative scheme of RNF10^{-/-} coronal brain section analyzed, rostral (left) and caudal (right). The different parameters analyzed are indicated and their quantification represented in the histograms as percentage of control (WT brain). The parameters analyzed are total brain area (TBA), Lateral ventricle (LV) left (_L) and right (_R), cingulate cortex (Cg) left and right, width and height; genu of the corpus callosum (gcc), width and height, Caudate putamen (CPu) left and right, anterior commissure anterior part (aca), piriform cortex (Pir) left and right, primary motor cortex (M1) left and right, secondary somatosensory cortex (S2), dorsal 3rd ventricle (D3V), retrosplenial granular cortex area c (RGCc) left and right, width and height; corpus callosum (cc) width and height, dorsal hippocampal commissure (dhc), hippocampus (HP), total length of the pyramidal cell layer (TILpy), dentate gyrus (DG) left and right, inner molecular layer of hippocampus (Mol), radiatum layer of the hippocampus (Rad) left and right, oriens layer of the hippocampus (Or) left and right, Anteromedial thalamic nucleus (AM) left and right, mammillothalamic tract (mt) left and right, internal capsule (ic) left and right, optical tract (opt) left and right, fimbria of the hippocampus (fi) left and right, habenula (hb) left and right. **b** Coronal whole brain sections of WT (left) and RNF10^{-/-} mouse with double staining Luxol-Nissl and relative magnification of the hippocampal area. The arrow indicates the morphological anomaly. Statistical analysis: Student T-test, p-values represented as a heat map.

6. RNF10 deficiency induces behavioral alterations and hippocampal related cognitive impairments

The neuroanatomical findings on RNF10^{-/-} mice evidenced macroscopic morphological anomalies that could prelude to behavioral alterations.

We thence decided to perform a series of behavioral test in collaboration with the laboratory of Prof. Maria Elvina Sala (CNR, Milano) in order to characterize the phenotype of the animal. For all behavioral tests we used young-adult male animals (8 weeks old). We first performed an open field test to assess general activity. RNF10^{-/-} animals showed a lower spontaneous motor activity compared to controls when free to explore an empty arena, with less horizontal and vertical movements made (Fig.10a and b).

FIGURE 10

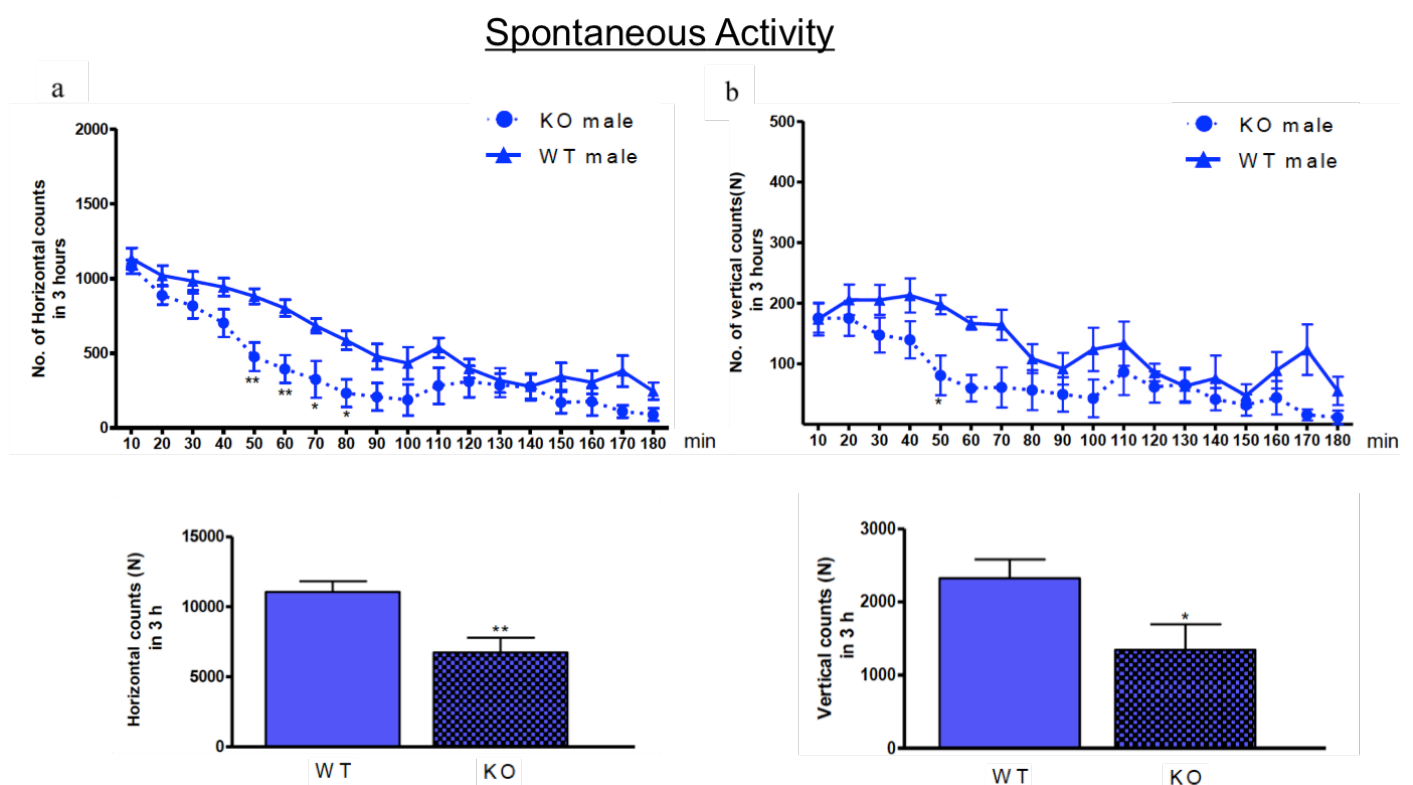


Fig. 10 RNF10^{-/-} mice have a reduced spontaneous motor activity.

a Time course quantification of the horizontal and vertical counts evaluated in an automated activity relative to RNF10^{-/-} and WT animals (n=10). **b** Cumulative mean of horizontal and vertical counts evaluated for 3 h in an automated activity cage relative to RNF10^{-/-} and WT animals (n=10). Statistical analysis: (a) one-way ANOVA; *p < 0.05, **p < 0.01; (b) Student T-test; *p < 0.05, **p < 0.01.

To analyse if the reduced activity in the cage was correlated to higher anxiety levels, we performed different tests for anxiety assessment. Surprisingly RNF10^{-/-} mice resulted to have a significantly reduced anxiety level, as showed by Elevated Plus maze (Fig. 11a), Marble Burying (Fig. 11b) and Hole board tests (Fig. 11c).

FIGURE 11

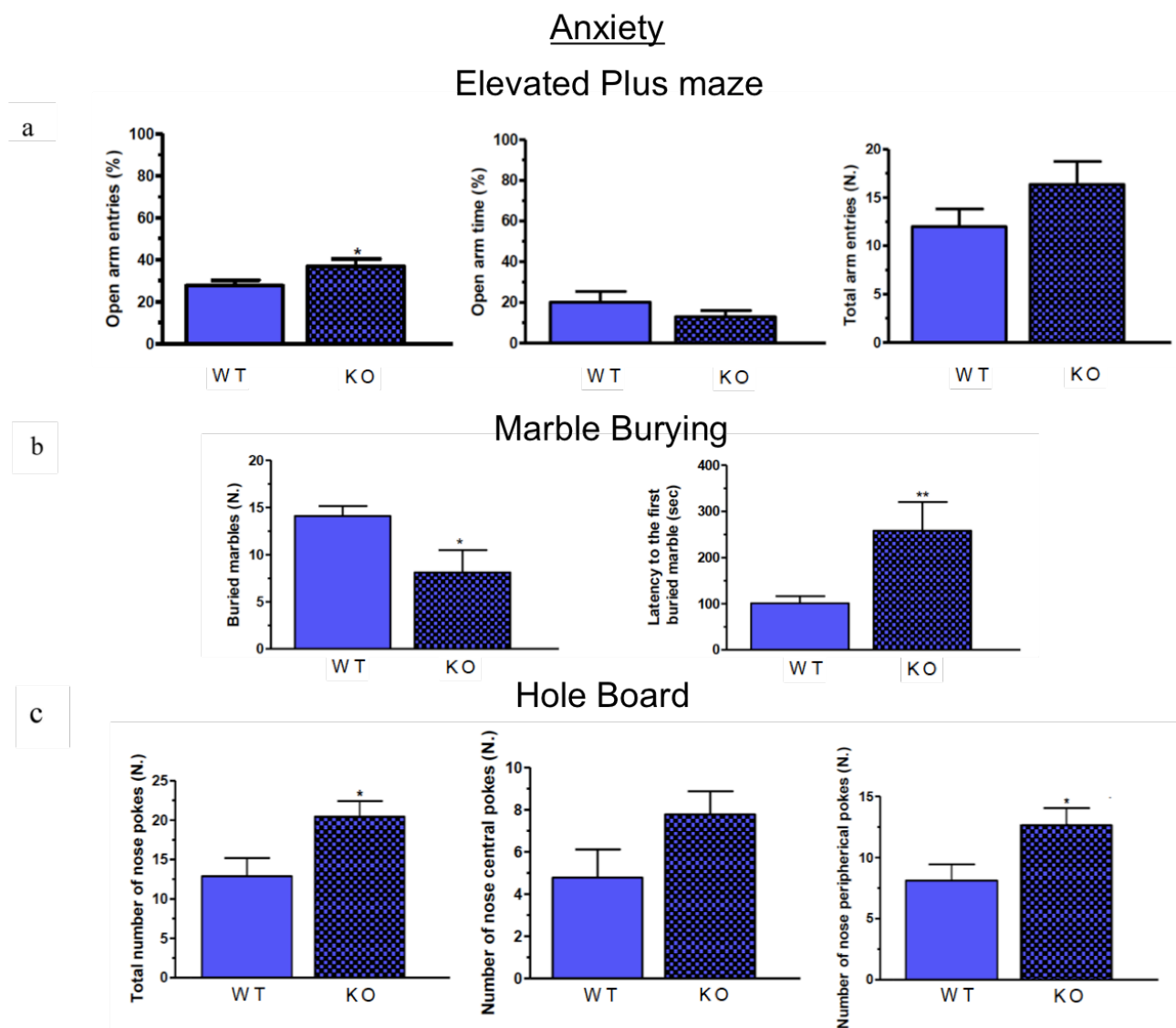


Fig. 11 RNF10^{-/-} mice have a reduced anxiety.

a Quantifications of the percentage open arms entries (left panel), the total time spent in the open arm (central panel) and the number of the entries in the open arm (right panel) performed in the Elevated Plus Maze by RNF10^{-/-} and WT animals (n=10). **b** Quantification of the number of the buried marbles (left panel) and of the latency to the first buried marble (right panel) performed in the Marble Burying Test by RNF10^{-/-} and WT animals (n=10). **c** Quantification of the total number of nose pokes (left panel), central nose pokes (central panel) and peripheral nose pokes (right panel) performed in the Hole Board Test by RNF10^{-/-} and WT animals (n=10). Statistical analysis: Student T-test; *p < 0.05, **p < 0.01.

RNF10^{-/-} mice showed also an increased tendency to perform stereotypies, repetitive movements or actions that characterize some neuropsychiatric disorders, like Schizophrenia or Autistic Spectrum Disorders (ASD). In particular, in absence of a stress stimulus, RNF10^{-/-} mice had more episodes of self-grooming behavior and for longer time compared to WT animals (Fig. 12a).

FIGURE 12

Stereotypical behavior Self-grooming

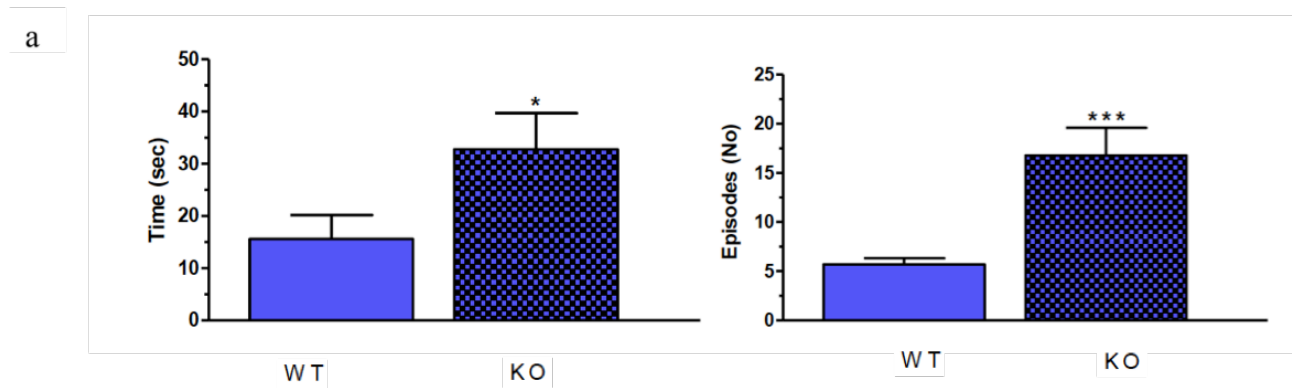


Fig. 12 RNF10^{-/-} mice display a higher tendency to do stereotypies.

a Quantifications of the time (left panel) and the number of events (central panel) of self-grooming performed by RNF10^{-/-} and WT animals (n=10). Statistical analysis: Student T-test; *p < 0.05, ***p < 0.001.

RNF10^{-/-} didn't show alterations in sociability, as they preferred to interact with a stranger animal rather than an inanimate object (Fig. 13a) in the three-chambers test. Social memory resulted also intact, as RNF10^{-/-} favored the interaction with a novel conspecific stranger over an already known stranger (Fig. 13b). Despite normal social interactions, RNF10^{-/-} mice resulted to be socially dominant on WT mice, as indicated by t tube test (Fig. 13c).

FIGURE 13

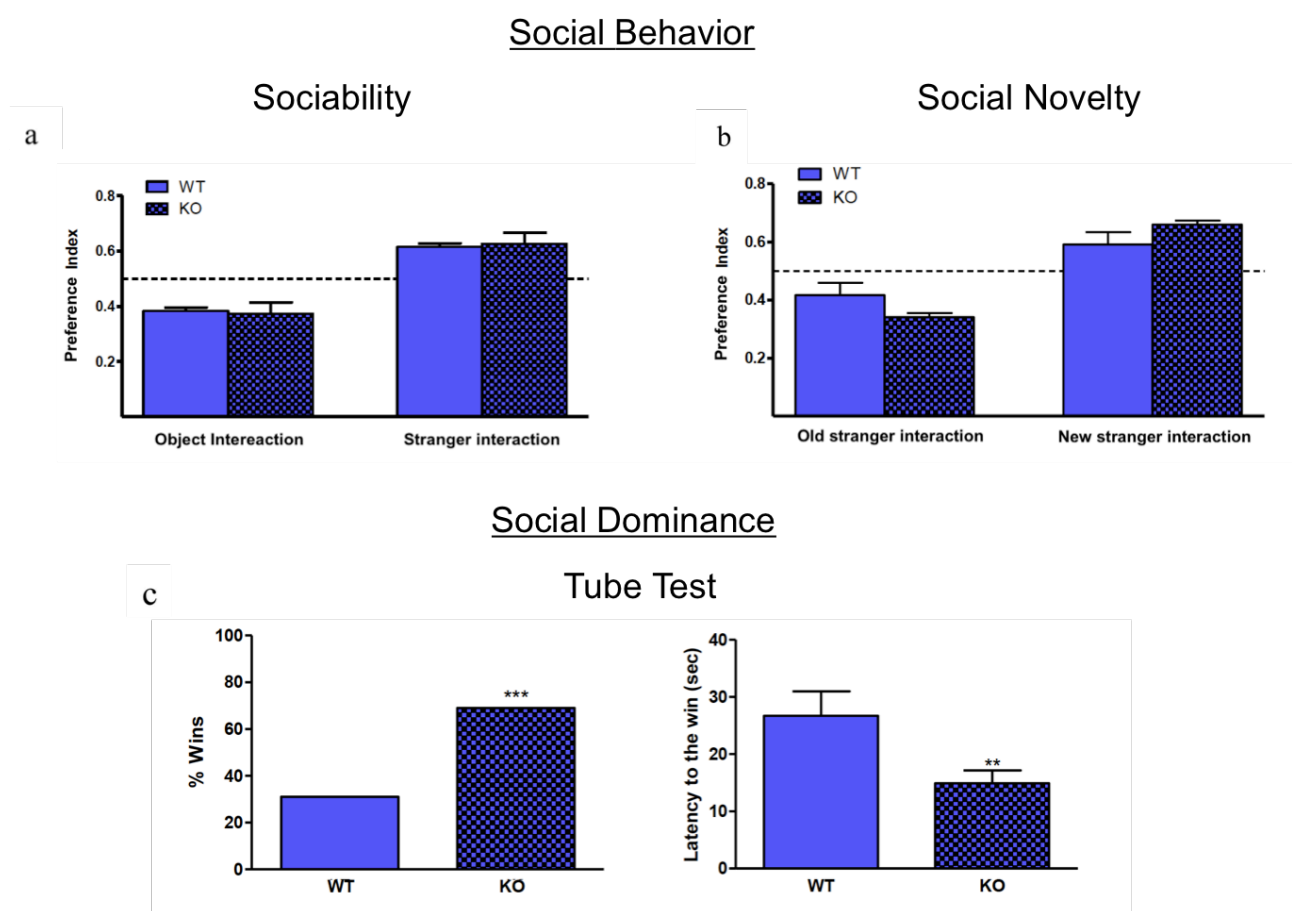


Fig. 13 RNF10^{-/-} mice have normal social interactions but display a marked social dominance.

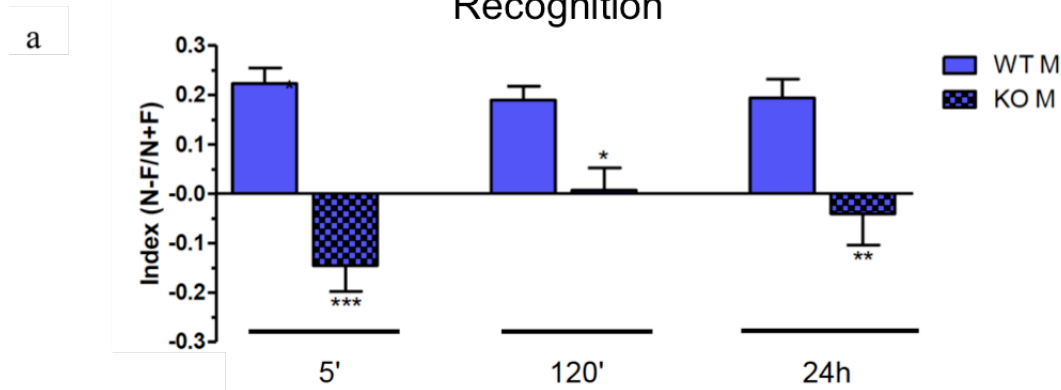
a Quantification of the preference index of RNF10^{-/-} and WT mice to an inanimate object or a stranger conspecific in the sociability test (n=10). **b** Quantification of the preference index of RNF10^{-/-} and WT mice to an old stranger conspecific or a new stranger conspecific in the Social Novelty test (n=10). **c** Quantification of the percentage of winning sessions (left panel) and the latency to the first win (right panel) performed in the Tube Test by RNF10^{-/-} and WT animals (n=10). Statistical analysis: Student T-test; **p < 0.01, ***p < 0.001.

Finally we performed cognitive tests to assess memory and learning capabilities, high cognitive functions that are strictly dependent on some areas, like the hippocampus (Ho, Lee, & Martin, 2011; Citri & Malenka, 2008). We focused on hippocampal-dependent cognitive tests, since bilateral hippocampal area of RNF10^{-/-} mice was significantly altered in the morphological evaluation (see Fig. 9). First we performed Spatial Object Recognition Test to assess working memory. We decided to test the animals in different time points after the familiarization phase, in order to evaluate all kind of memory (very-short, short and long term memory). RNF10^{-/-} mice failed to recognize the object displacement at all the time points analyzed (5 minutes, 120 minutes, 24 hours after the familiarization) (Fig 14a) and showed memory deficits. We also performed Morris Water Maze Test to assess reference memory. During the acquisition phase, RNF10^{-/-} animals showed mild memory deficit trend (significant only on the third day of test), expressed as more time required to find the platform compared to WT animals (Fig 14b). On the contrary, on the reversal phase RNF10^{-/-} animals showed a marked memory deficit, spending significantly more time than controls in finding the platform in all the days of test and requiring more time to locate and arrive on the area of the hidden platform (Fig. 14c).

Taken together these results suggest that RNF10 deficiency *in vivo* induces various behavioral abnormalities like stereotypical behavior and higher aggressiveness. Moreover spatial memory performances, in particular spatial working memory and cognitive flexibility, resulted clearly impaired by RNF10 knockout, implying that RNF10 presence is necessary for the correct execution of hippocampal dependent tasks.

FIGURE 14

Working Memory
Spatial Object Recognition



Reference Memory
Morris Water Maze

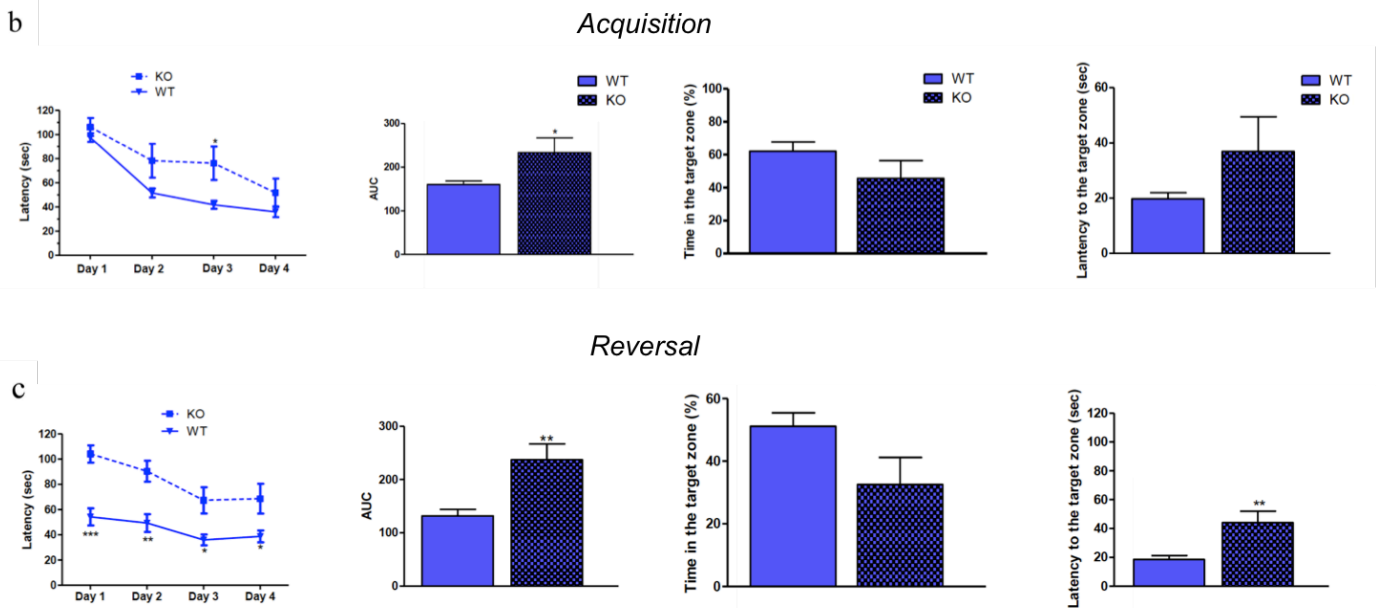


Fig. 14 RNF10^{-/-} mice have impaired spatial memory.

a Mean discrimination index evaluated in the Spatial Object Recognition test, 5 min, 120 min and 24 h after familiarization phase (n=10) relative to RNF10^{-/-} and WT mice. **b** Time course plot (left panel) and relative area under the curve (left-central panel) of the latency to get to the platform evaluated in the Acquisition phase of the Morris Water Maze Test relative to RNF10^{-/-} and WT mice. Time spent in (right-central panel) and latency to get to the target zone (right panel) were also evaluated (n=10). **c** Time course plot (left panel) and relative area under the curve (left-central panel) of the latency to get to the platform evaluated in the Reversal phase of the Morris Water Maze Test relative to RNF10^{-/-} and WT mice. Time spent in (right-central panel) and latency to get to the target zone (right panel) were also evaluated (n=10). Statistical analysis: Student T-test; * p<0.05, **p < 0.01, ***p < 0.001.

7. RNF10 is necessary for the correct formation of the glutamatergic synapse in vivo

The results described above on RNF10^{-/-} mice evidenced the importance of RNF10 for the correct development of some brain structure, among which the hippocampus and, consequently, for the cognitive functions in which the hippocampus is essential, like memory and learning. These alterations seem to underlie a prominent RNF10 role in neurodevelopment, as also suggested by the *in vitro* involvement in the modulation of neuronal morphometry. Thence we decided to extend our analysis on the RNF10 deficient mouse, focusing our attention on the critical period for synaptogenesis that in mice spans through the first three weeks of postnatal life. Since receptors' activity is an early and essential feature for synaptic maturation and development of neuronal circuits, we investigated the molecular composition of the glutamatergic synapse in RNF10 deficient mouse. We performed a Western Blot analysis of the principal components of the postsynaptic excitatory synapse in total homogenates and Triton Insoluble Fractions (TIFs), a cellular fraction enriched in postsynaptic proteins, from RNF10^{-/-} and WT half brains. At Post Natal Day (PND) 14, RNF10^{-/-} mice did not show any significant difference in the expression of ionotropic glutamate receptors and associated scaffolding proteins from WT animals, both in total homogenates (Fig. 15a) and TIFs (Fig. 15 b).

FIGURE 15

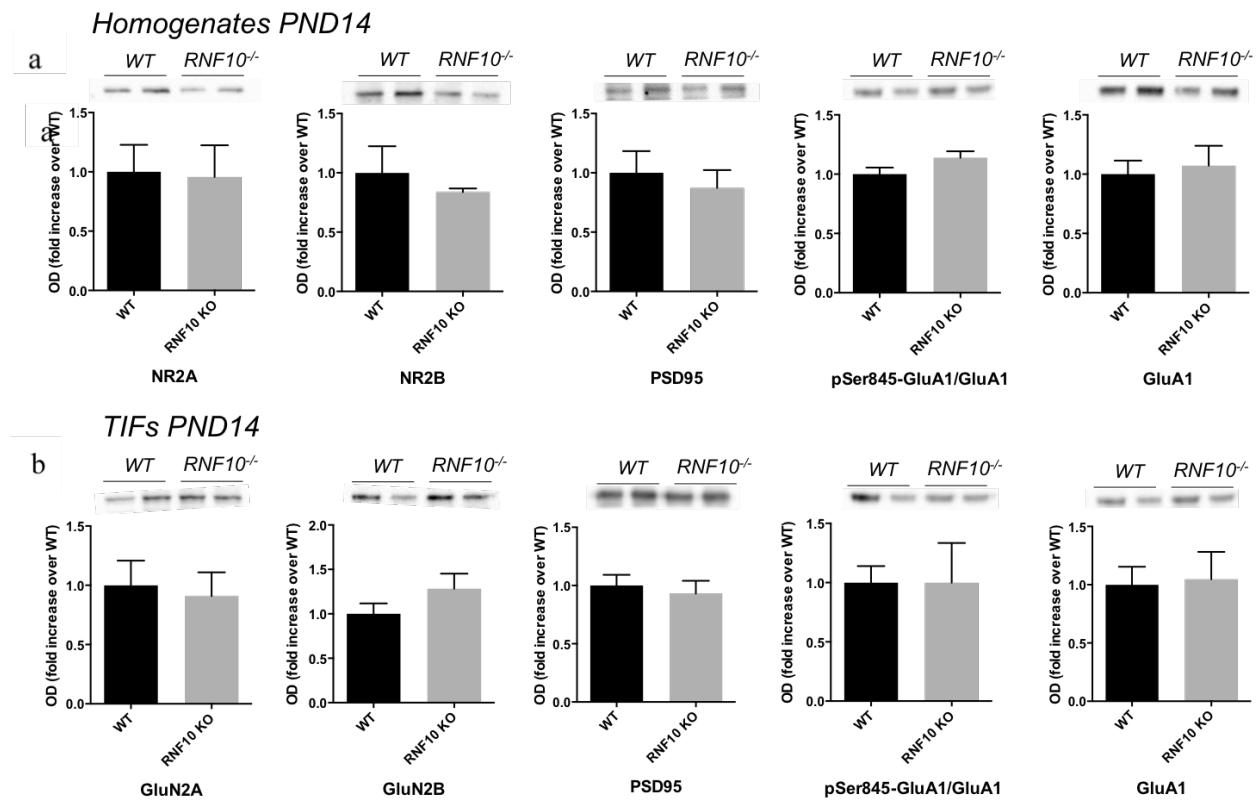


Fig.15 RNF10^{-/-} mice at PND14 don't have alterations in glutamatergic synaptic markers-

a Representative images and quantification of glutamatergic synaptic markers (GluN2A, GluN2B, PSer845-GluA1, GluA1, PSD95) half-brain homogenates of PND14 RNF10^{-/-} and wt mice (n=5). **b** Representative images and quantification of glutamatergic synaptic markers (GluN2A, GluN2B, PSer845-GluA1, GluA1, PSD95) from half-brain Triton Insoluble Fractions of PND14 RNF10^{-/-} and wt mice (n=5). Statistical analysis: Student T-Test.

Interestingly, at PND21 *RNF10*^{-/-} mice showed an alteration of the synaptic levels of GluN2A, a subunit of the glutamate NMDARs that has a major role in synaptic plasticity, and in the GluA1 phosphorylated in Serine845, a post-translational modification of the GluA1 subunit of AMPAR that represents marker of long term potentiation (Fig. 16b). No differences were found in the total levels of these proteins (Fig 16a). This evidence suggests that *RNF10* absence has a significant impact in the glutamatergic synaptic formation, in particular in glutamate receptors localization.

FIGURE 16

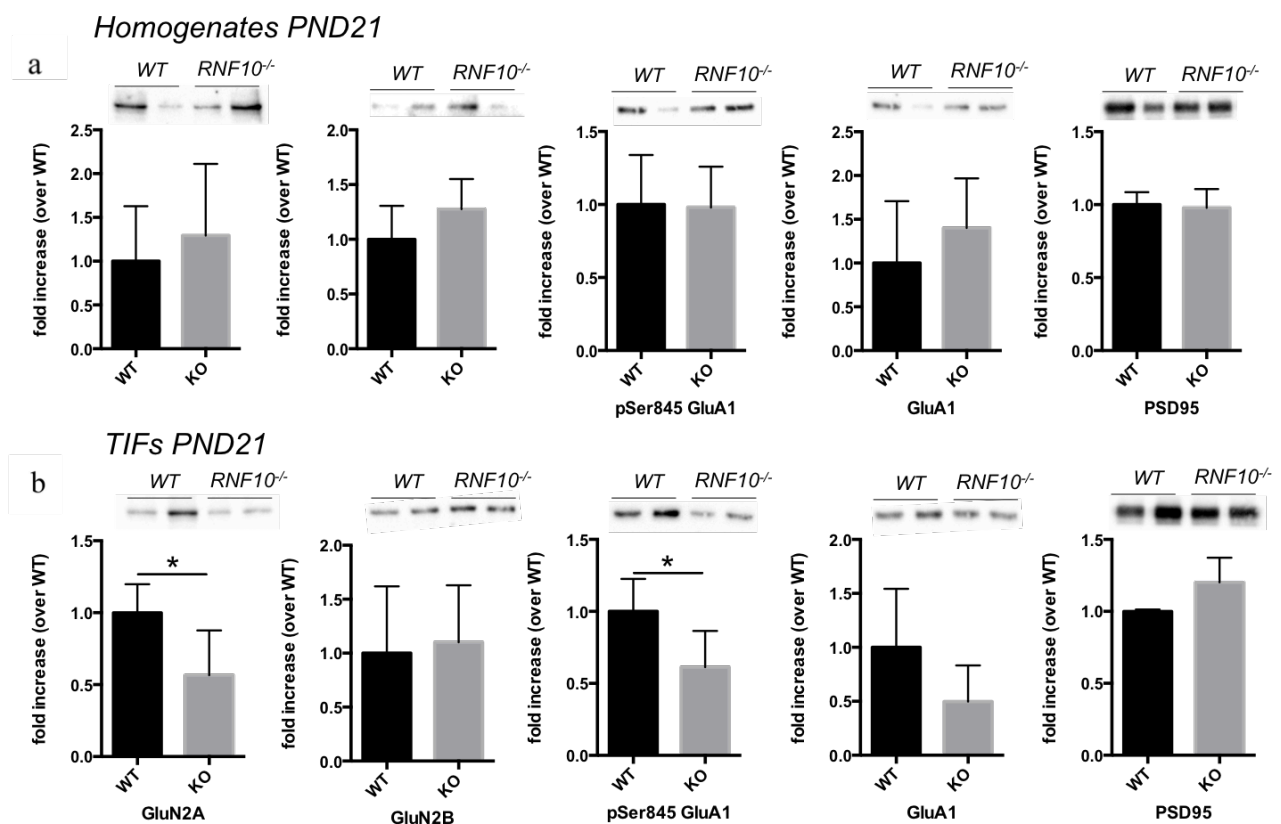


Fig. 16 *RNF10*^{-/-} mice at PND21 show a mislocalization of glutamate receptors

a Representative images and quantification of glutamatergic synaptic markers (GluN2A, GluN2B, PSer845-GluA1, GluA1, PSD95) half-brain homogenates of PND14 *RNF10*^{-/-} and wt mice (n=5). **b** Representative images and quantification of glutamatergic synaptic markers (GluN2A, GluN2B, PSer845-GluA1, GluA1, PSD95) from half-brain Triton Insoluble Fractions of PND14 *RNF10*^{-/-} and wt mice (n=5). Statistical analysis: Student T-Test; *p < 0.05.

This alteration of the excitatory postsynaptic composition in RNF10^{-/-} led us to investigate a possible correlated to defects in dendritic spines. Thence we performed a spine density and morphology analysis on Dil-stained hippocampal slices of RNF10^{-/-} and control mice at PND14 and PND21. As for the molecular analysis, we analyzed animals from PND14 and 21. In according with the WB analysis results, RNF10^{-/-} mice showed aberrant spine morphology just at PND21 (Fig 17b) and not at PND14 (Fig 17a). Interestingly, no differences in spine density were detected at both ages investigated (Fig 17a and b). In particular RNF10^{-/-} hippocampal neurons showed an increase in mushroom-shaped spines, the pool of stable and mature spines, and a concomitant reduction of thin spines, very plastic, unstable and immature compared to WT neurons (17b). Taken together these results enforce the hypothesis that RNF10 plays a crucial role in neuronal development, in particular in glutamatergic synaptic development, acting on a particular time window.

FIGURE 17

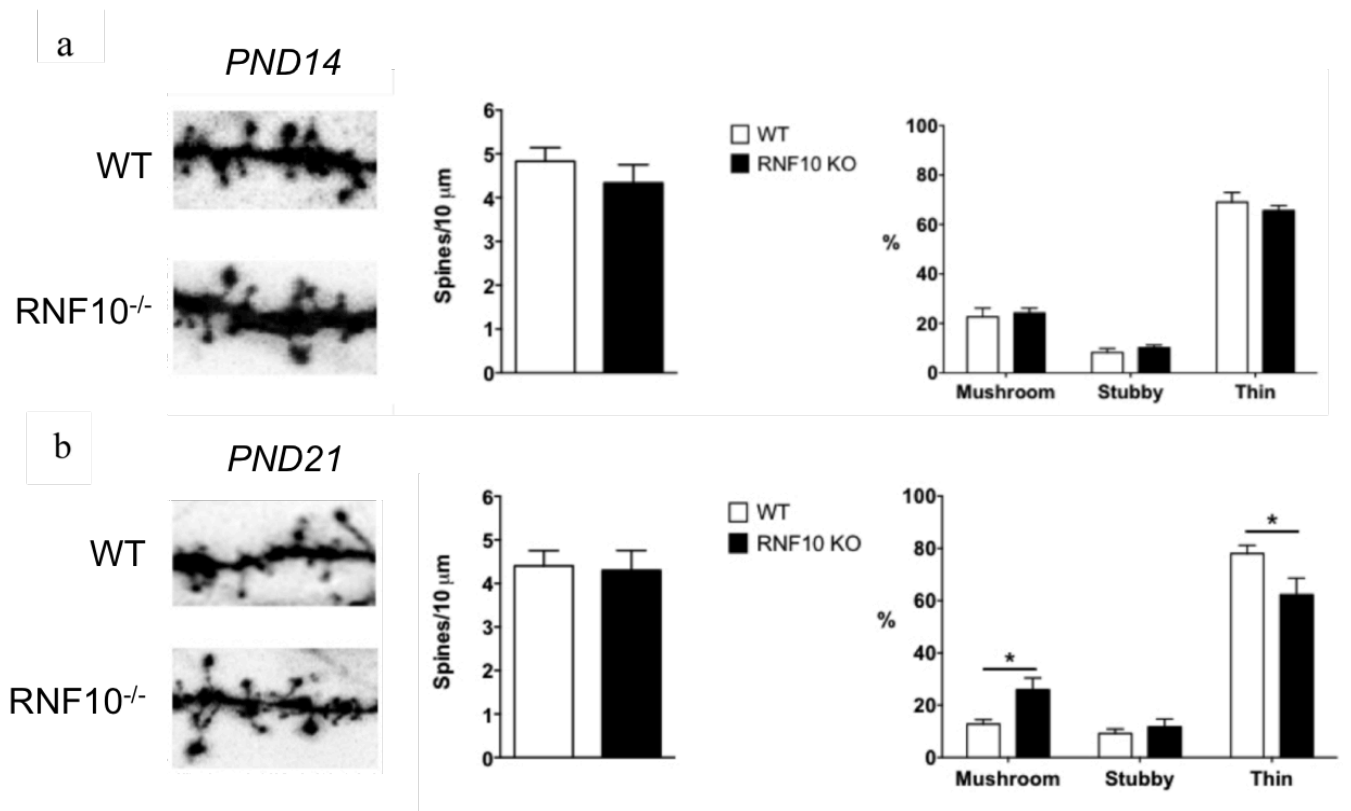


Fig.17 RNF10^{-/-} mice have an alteration in spine morphology but not in spine density

a Representative confocal images and quantification of spine density and morphology of PND14 hippocampal slices dyed with Dil. **b** Representative confocal images and quantification of spine density and morphology of PND21 hippocampal slices dyed with Dil. Statistical analysis: Student T-Test; *p < 0.05

8. RNF10 absence alters neuronal geometry in specific hippocampal regions

Given the tight interconnection between synaptic maturation and dendrite stabilization and maturation (Cline, 2001) and considering the above mentioned results on the in vitro role of RNF10 in dendritic branching, we wondered if synaptic alterations observed in RNF10^{-/-} mice hippocampi could be paralleled by also an alteration of the dendritic arborization of hippocampal neurons. We performed Golgi Staining on hippocampal slices of 2 months old RNF10^{-/-} and WT mice and we performed Sholl Analysis and spine density analysis in different Hippocampal areas (CA1 vs Dentate Gyrus). Interestingly RNF10^{-/-} mice showed a critical simplification of neuronal geometry in CA1 neurons compared to WT animals (Fig. 18a). Surprisingly no difference was observed in dendritic arborization of dentate gyrus neurons, suggesting a region-specific effect of RNF10 deficiency in mice hippocampi (Fig. 18b). Finally, no alteration of spine density was observed in both areas in RNF10^{-/-} mice (Fig. 18a and b) in agreement with results shown in Fig. 17. Altogether these data show that RNF10 absence severely affects dendritic maturation specifically in CA1 region of Hippocampus, but not in dentate gyrus, in absence of compensatory effect on the spine density.

FIGURE 18

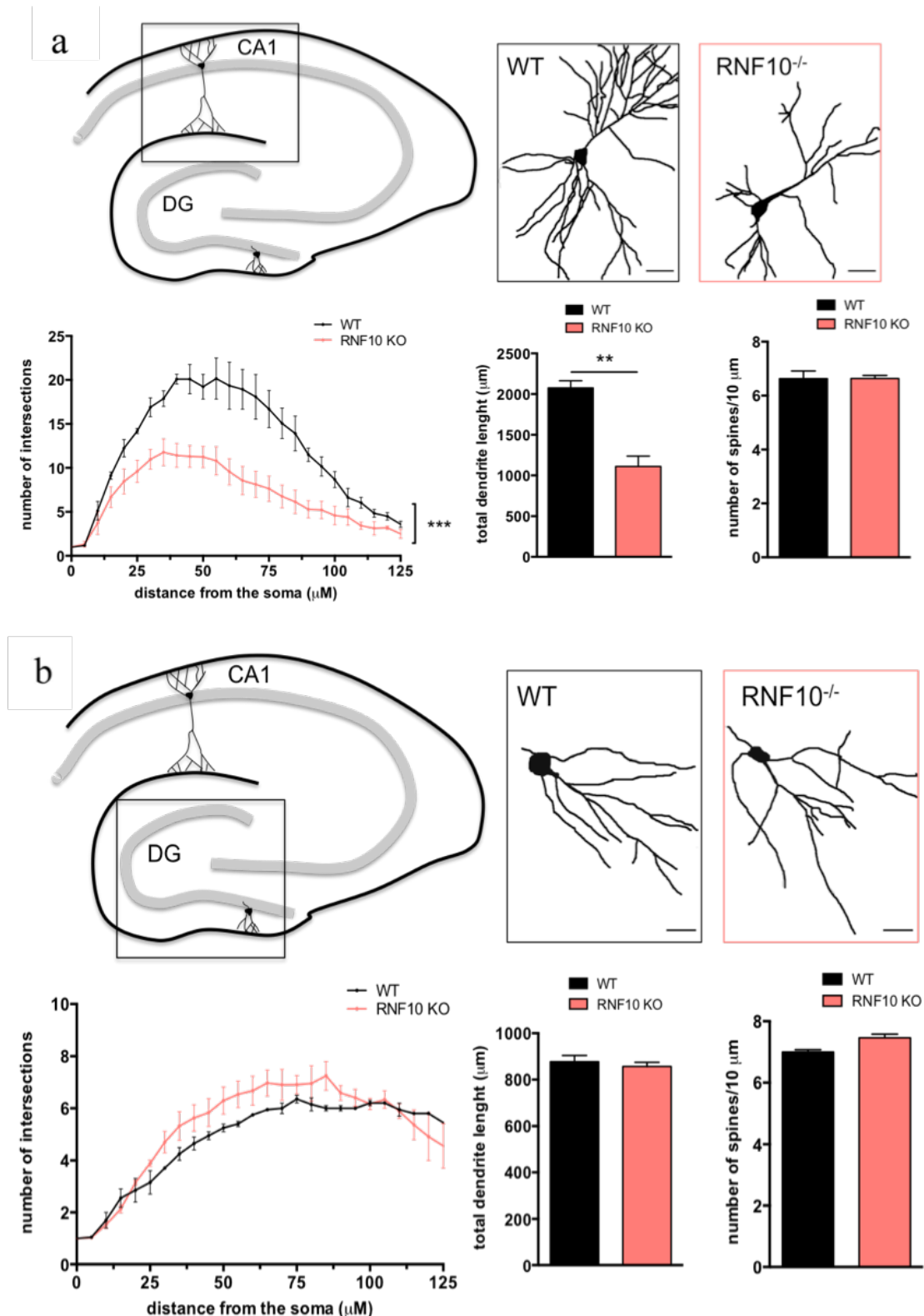


Fig.18 RNF10 depletion in vivo alters neuronal geometry in CA1 region of hippocampus

a Representative sketched neuron and quantification of Sholl analysis, total dendritic length and spine density of CA1 hippocampal neurons from 2 m.o. brain slices of RNF10^{-/-} and WT mice processed with Golgi staining.

b Representative sketched neuron and quantification of Sholl analysis, total dendritic length and spine density of Dentate Gyrus hippocampal neurons from 2 m.o. brain slices RNF10^{-/-} and WT mice processed with Golgi staining.

Statistical analysis: Student T-Test; **p < 0.01; *** p < 0.001.

9. RNF10 absence prevents LTP induction *in vivo*

To further investigate the functional consequences of RNF10 loss *in vivo*, in particular in the hippocampal function, we decided to evaluate field LTP recording in the CA1 region of the hippocampus, stimulating the Schaffer collateral projections from the CA3 area and recording in the CA1 dendrites, using the theta burst stimulation (TBS) protocol (see Methods) in order to resemble the burst discharges of hippocampal pyramidal neurons and induce LTP. All electrophysiological recordings were performed by the group of Christophe Mulle (University of Bordeaux) and by Ana Riberio, a previous PhD student in our lab. In accordance to our morphological and behavioral data, LTP induction was completely abolished in RNF10^{-/-} mice CA1 region of the hippocampus (Fig 19a), confirming the essential role of the synaptonuclear messenger in synaptic plasticity also *in vivo*.

FIGURE 19

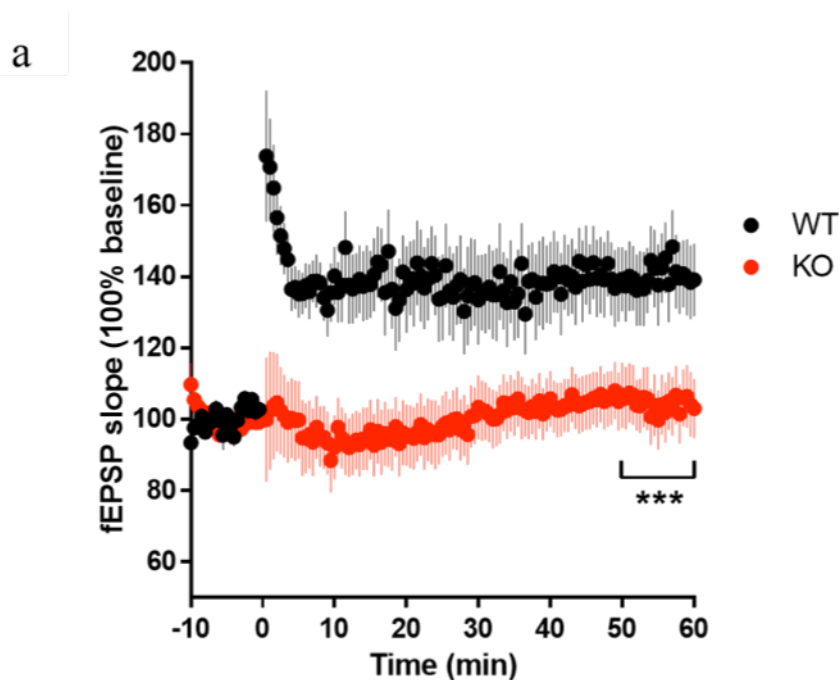


Fig. 19 RNF10^{-/-} animals display a complete abolition of the LTP in CA1 region of hippocampus

a Field Excitatory PostSynaptic Potential recordings of LTP induction by theta stimulation at CA1 region of hippocampus. Statistical analysis: Student T-test; p ***<0.001

DISCUSSION

In neurons multiple signaling mechanisms operate to relay the effect of synaptic stimulation to the nucleus and regulate the expression of genes associated with long-term structural changes of synaptodendritic input, allowing the synapse and the nucleus to communicate with one another (Jordan & Kreutz, 2009) (Cohen & Greenberg, 2008). Moreover, recent papers indicate that the correct functioning of synaptonuclear messengers gives also a fundamental contribution to the regulation of structural synaptic plasticity and, in particular, an altered function or expression of these proteins can lead to a highly significant alteration of dendritic spine density, thus putting forward the idea of a possible role in synaptopathies (Marcello, Di Luca, & Gardoni, 2018)(Dinamarca et al., 2016)(Proepper et al., 2007)(Spilker et al., 2016). Our lab has recently identified RNF10 as a novel synaptonuclear messenger that specifically links activation of synaptic GluN2A-containing NMDARs to nuclear transcription of RNF10 target genes involved in synaptic plasticity. In this PhD project we wanted to describe more in detail the mechanism of RNF10 activation and trafficking, in order to better investigate its function. We focused on the role of post-translational modifications of RNF10 in its trafficking to the nucleus, and we demonstrated that the activation of the synaptic pool of NMDARs and subsequent calcium influx lead to RNF10 phosphorylation by protein kinase C (PKC), triggering synaptic NMDAR/RNF10 complex disruption and RNF10 importin-mediated nuclear translocation. Using a point mutation strategy, we identified a specific PKC-dependent phosphorylation site at Ser31 within RNF10 N-terminal domain as the key driver needed for its dissociation from synaptic NMDARs and consequent trafficking to the nucleus. Moreover, we demonstrated that RNF10 Ser31 phosphorylation drives the transcription of RNF10 target gene $p21^{Waf/Cip1}$. Notably, RNF10 plays an important role in implementing LTP-mediated cellular effects and LTP maintenance, through its role in promoting gene transcription; in addition RNF10 silencing in primary hippocampal neurons completely prevents the induction of LTP and induces a significant reduction of the levels of AMPA and NMDA receptor subunits such as GluA1 and GluN2A, respectively (Dinamarca et al., 2016). In this work we demonstrated that Ser31 phosphorylation is necessary for the capability of RNF10 to convey LTP signaling pathways; in particular we evaluated the phosphorylation in Ser133 of the transcriptional factor CREB as it is considered a marker of synaptic plasticity (Sakamoto, Karelina, & Obrietan, 2011). Synapse-to-nucleus bidirectional communication represents an important process for the regulation of neuronal activity and morphology, in both physiological and pathological conditions, and an altered activity-dependent protein transport from synapse-to-nucleus is likely to be an important factor contributing to synaptic dysfunction in both neurodevelopmental and neurodegenerative disorders (Marcello et al., 2018). In recent years, many potential synaptonuclear protein messengers have been identified such as CREB2, Jacob, Abi-1,

CRTC1 and RNF10, which play key roles in the regulation of neuronal activity and architecture (Marcello et al., 2018). In hippocampal neurons, RNF10 downregulation, silencing and inhibition of its nuclear trafficking have already been associated to a decreased number of dendritic spines (Dinamarca et al., 2016) and now we also found that they determine a significant simplification of dendrites arborization. This evidence reveal the importance of RNF10 as a new regulator of neuronal architecture. Shutting down synaptic plasticity via RNF10 silencing in hippocampal neurons has a long-term impact not only on synaptic formation but also on dendritic development. Experience-dependent dendritic arbor development is best understood as the coordinated bidirectional regulation of synaptogenesis, synaptic strength, and dendritic arbor structure. The presence of iGluRs at synapses renders the synapse functional at resting potential but was also postulated to stabilize the newly added dendritic branches (Cline, 2001). In fact, during developmental periods of synaptogenesis, synaptic activity increases the emergence of fine dendritic branches. Newly extended branches on dendrites form synapses with only NMDARs. As these synapses mature, AMPARs are recruited to the synaptic sites. Mature AMPAR-containing synapses stabilize the branches on which the synapses are located. Stabilized branches then add new branches that, in turn, establish new NMDAR-only synapses, which are either stabilized through the addition of AMPARs or retracted (Cline, 2001). Given the importance of RNF10 in delivering NMDAR signaling and its influence in synaptogenesis and dendritic spine formation, in the light of the relationship between branch and synapse dynamics, we hypothesize that RNF10 silencing could affect also dendritic development. Indeed we found out that RNF10 silencing in hippocampal neurons results in a severe reduction in neuronal arborization. Therefore we also investigated the role of RNF10 Ser31 phosphorylation state in the regulation of spine density and dendritic geometry in hippocampal neurons. We observed that neurons transfected with RNF10S31D, the phosphomimetic construct, show a significant increase in spines number, while RNF10S31A expression lead to the opposite effect, acting as a dominant negative. Notably, no effect on spine density was observed following overexpression of RNF10WT. This result highlights the importance of the PKC dependent phosphorylation to prime RNF10 activation, since the upregulation of the synaptonuclear protein level alone is not sufficient to exert a morphological effect, in an unstimulated condition. Preventing Ser31 phosphorylation had also a significant impact on dendritic arborization, confirming the importance of the PKC-dependent phosphorylation for RNF10 activity. RNF10S31D or RNF10WT transfected neurons instead did not alter significantly dendritic branching. Notably RNF10 downregulation/downactivation had a stronger impact then its overexpression/upregulation in cultured neurons, suggesting that interfering with RNF10 activity, even for the limited time of a transient transfection,

irreversibly impairs neuronal morphology. Therefore RNF10 trafficking to the nucleus emerges as an essential element for the induction of NMDAR-dependent modulation of dendritic arborization and spine density in hippocampal neurons. On the contrary, boosting RNF10 activity for a short period of time it's not sufficient to stably affect neuronal geometry, as dendrite maturation it's a complex process regulated by a great number of proteins acting with a specific timing and order (Bystron et al., 2008). These findings opened a new perspective on the physiological relevance of RNF10 and at the same time raised the question if RNF10/GluN2A complex assembly/disassembly dynamics may represents a general mechanism throughout the central nervous system or if it is specifically related to the hippocampus. To address this issue, the investigation of the role of the synaptonuclear messenger in neurons *in vivo* was required and thence we started to perform a deep phenotypic characterization of RNF10^{-/-} mice, a rodent model generated by KOMP repository Project (see Methods) and about whom no studies are currently reported. Interestingly, RNF10^{-/-} mice are characterized by gross morphological brain alterations that involve in particular the hippocampus as well as of other brain regions, thus suggesting a role of this protein not confined to the hippocampus. Driven by our results on the involvement of the synaptonuclear messenger in spinogenesis and dendritic branching, we decided to investigate the possible role of RNF10 in regulating *in vivo* neurodevelopment during a critical period for synaptogenesis and dendritic development in early postnatal life (between postnatal day 14 and 21) (Rice & Barone, 2000). When analyzing the composition of the glutamatergic synapse in Western Blot, we found that RNF10 knock out *in vivo* induces a reduction of the synaptic levels of some important subunits of iGluRs, in particular of GluN2A and pSer845-GluA1. Moreover these alterations were not present at PND14 but emerged just from PND21. Interestingly during the same time window between PND14 and 21 the synaptic NMDARs subunit composition changes, switching from predominance of GluN2B-containing to GluN2A-containing receptors (Bellone and Nicoll, 2007). This neurodevelopmental subunits switch at neonatal synapses can be bidirectional, depending on the NMDAR activation pattern: LTP promotes GluN2A enrichment in synapses, while LTD reverses the effect (Bellone and Nicoll, 2007). Therefore it's possible that the complete absence of RNF10, an essential protein of the signaling machinery linked to NMDAR activation (Dinamarca et al., 2016), results in an altered developmental GluN2A enrichment, acting in the time window that is critical for synaptic maturation.

In addition, the upregulation of the synaptic localization of GluN2A-containing NMDAR and of the pSer845-GluA1 subunit of AMPAR are key features of the early and late phases of LTP (Barria & Malinow, 2002) (Grosshans, Clayton, Coultrap, & Browning, 2002) (Bellone & Nicoll, 2007) (Esteban et al., 2003). Therefore, since RNF10 silencing *in*

in vitro impairs LTP maintenance in hippocampal neurons (Dinamarca et al., 2016), it's not surprising that RNF10 knock out *in vivo* affects the capability of neurons to regulate the synaptic levels of key proteins in synaptic plasticity. Besides, in accordance to the molecular changes in the glutamatergic synapse, RNF10^{-/-} mice have an age dependent alteration of spine morphology in the hippocampus, that is present at P21 but not 14. In particular we found an increase in the number of mushroom-shaped spines with a concomitant reduction of thin spines levels, but no difference in spine density. Even if these findings apparently contrast with the results obtained from the biochemical analysis, the apparent increase in mushroom-shaped spines, that represent the mature and stable synaptic pool, has probably to be interpreted as an aberrant spine profile, in which spine are bigger, non-plastic and dysfunctional. To support this hypothesis, electrophysiological recordings on RNF10^{-/-} brain slices show that CA1 neurons are completely insensitive to LTP induction, underlying glutamatergic synaptic defects. Moreover hippocampal CA1 neurons from RNF10^{-/-} mice display a dramatic reduction of the dendritic arbor complexity compared to WT neurons, confirming the important role of the synaptonuclear messenger in the correct shaping of neuronal architecture. Surprisingly the absence of RNF10 seems to exert a dendritic branching alteration effect that is confined to CA1 and not the dentate gyrus (DG) region of the hippocampus. From a functional point of view, this region-specific alteration translates into the animal behavior: indeed RNF10^{-/-} mouse has a clear spatial memory impairment that seems to be dependent more on a defect in contextual learning, that relies on CA1 functionality (Sakimoto et al., 2019), rather than a defect in memorization. In fact in the Morris Water Maze Test, RNF10^{-/-} didn't show a remarkable impairment in the acquisition phase, but just in the reversal phase. The evidence collected in this PhD thesis describe a new interesting role of RNF10 as a regulator of neurodevelopment but the mechanisms through which it acts *in vivo* are still unclear. Indeed the effect of RNF10 knockout *in vivo* diverged from RNF10 knockdown *in vitro* because of the increasing complexity of the system and the possibility of compensatory mechanisms that are common in knockout animals. As a consequence the next step in the study of this synaptonuclear messenger will be to clarify RNF10 action in the nucleus, in particular what are its target genes *in vivo* and which pathways are controlled by its activity. Understanding the link between NMDAR activation and gene transcription may be represent a novel therapeutic frontier, as it may open up new strategies of intervention in neuropsychiatric diseases characterized by synaptic defects and neurodevelopmental alteration.

REFERENCES

- Abraham, W. C., & Williams, J. M. (2003). Properties and Mechanisms of LTP Maintenance. *The Neuroscientist*, 9(6), 463-474.
<https://doi.org/10.1177/1073858403259119>.
- Alberini, C. M. (2009). Transcription Factors in Long-Term Memory and Synaptic Plasticity. *Physiol Rev*. <https://doi.org/10.1152/physrev.00017.2008>.
- Alberini, C. M., & Kandel, E. R. (2015). The Regulation of Transcription in Memory Consolidation. *Cold Spring Harb Perspect Biol*.
<https://doi.org/10.1101/cshperspect.a021741>.
- Alfred Sloan, the P., Beckman Foundations, M., Sheng, M., & Jong Kim, M. (2001). *Postsynaptic Signaling and Plasticity Mechanisms. Brain. Res. Mol. Brain. Res* (Vol. 4).
- Arons, M. H., Thynne, C. J., Grabrucker, A. M., Li, D., Schoen, M., Cheyne, J. E., ... Garner, C. C. (2012). Autism-Associated Mutations in ProSAP2/Shank3 Impair Synaptic Transmission and Neurexin-Neuroigin-Mediated Transsynaptic Signaling. *The Journal of Neuroscience*, 32(43), 14966 LP-14978.
<https://doi.org/10.1523/JNEUROSCI.2215-12.2012>.
- Bading, H. (2013). Nuclear calcium signalling in the regulation of brain function. *Nature Reviews Neuroscience*, 14(9), 593-608. <https://doi.org/10.1038/nrn3531>.
- Bagni, C., Tassone, F., Neri, G., & Hagerman, R. (2012). Science in medicine Fragile X syndrome: causes, diagnosis, mechanisms, and therapeutics. *Science in Medicine*, 122(12), 4314-4322. <https://doi.org/10.1172/JCI63141.4314>.
- Bajaj, G., Hau, A. M., Hsu, P., Gafken, P. R., Schimerlik, M. I., & Ishmael, J. E. (2014). Identification of an atypical calcium-dependent calmodulin binding site on the C-terminal domain of GluN2A. *Biochemical and Biophysical Research Communications*, 444(4), 588-594.
<https://doi.org/https://doi.org/10.1016/j.bbrc.2014.01.111>.
- Baleriola, J., Walker, C. A., Jean, Y. Y., Crary, J. F., Troy, C. M., Nagy, P. L., & Hengst, U. (2014). Axonally Synthesized ATF4 Transmits a Neurodegenerative Signal across Brain Regions. *Cell*, 158(5), 1159-1172.
<https://doi.org/https://doi.org/10.1016/j.cell.2014.07.001>.
- Barria, A., Muller, D., Derkach, V., Griffith, L. C., & Soderling, T. R. (1997). Regulatory phosphorylation of AMPA-type glutamate receptors by CaM-KII during long-term potentiation. *Science (New York, N.Y.)*, 276(5321), 2042-2045. Retrieved from

<http://www.ncbi.nlm.nih.gov/pubmed/9197267>.

Beattie, E. C., Carroll, R. C., Yu, X., Morishita, W., Yasuda, H., von Zastrow, M., & Malenka, R. C. (2000). Regulation of AMPA receptor endocytosis by a signaling mechanism shared with LTD. *Nature Neuroscience*, 3(12), 1291-1300. <https://doi.org/10.1038/81823>.

Berry, K. P., & Nedivi, E. (2017). Review Spine Dynamics : Are They All the Same ? *Neuron*, 96(1), 43-55. <https://doi.org/10.1016/j.neuron.2017.08.008>.

Bilousova, T. V, Dansie, L., Ngo, M., Aye, J., Charles, J. R., Ethell, D. W., & Ethell, I. M. (2009). Minocycline promotes dendritic spine maturation and improves behavioural performance in the fragile X mouse model. *Journal of Medical Genetics*, 46(2), 94 LP-102. <https://doi.org/10.1136/jmg.2008.061796>.

Bliss, T.V., and Collingridge, G.L. (1993). A synaptic model of memory: long term potentiation in the hippocampus. *Nature* 361, 31-39. <https://doi.org/10.1038/361031a0>.

Bredt, D. S., & Nicoll, R. A. (2003). AMPA Receptor Trafficking at Excitatory Synapses. *Neuron*, 40(2), 361-379. [https://doi.org/10.1016/S0896-6273\(03\)00640-8](https://doi.org/10.1016/S0896-6273(03)00640-8).

Bowie, D. (2008). Ionotropic glutamate receptors & CNS disorders. *CNS Neurol. Disord. Drug Targets* 7, 129-143. <https://doi.org/10.2174/187152708784083821>.

Ch'ng, T. H., DeSalvo, M., Lin, P., Vashisht, A., Wohlschlegel, J. A., & Martin, K. C. (2015). Cell biological mechanisms of activity-dependent synapse to nucleus translocation of CRTC1 in neurons. *Frontiers in Molecular Neuroscience*, 8(september), 1-19. <https://doi.org/10.3389/fnmol.2015.00048>.

Ch'ng, T. H., & Martin, K. C. (2011). Synapse to Nucleus Signaling. <https://doi.org/10.1016/j.conb.2011.01.011>.

Ch'ng, T. H., Uzgil, B., Lin, P., Avliyakov, N. K., O'Dell, T. J., & Martin, K. C. (2012a). Activity-dependent transport of the transcriptional coactivator CRTC1 from synapse to nucleus. *Cell*, 150(1), 207-221. <https://doi.org/10.1016/j.cell.2012.05.027>.

Ch'ng, T. H., Uzgil, B., Lin, P., Avliyakov, N. K., O'Dell, T. J., & Martin, K. C. (2012b). Activity-Dependent Transport of the Transcriptional Coactivator CRTC1 from Synapse to Nucleus. *Cell*, 150(1), 207-221. <https://doi.org/https://doi.org/10.1016/j.cell.2012.05.027>.

Chen, A., Muzzio, I. A., Malleret, G., Bartsch, D., Verbitsky, M., Pavlidis, P., ... Kandel, E.

R. (2003). Inducible Enhancement of Memory Storage and Synaptic Plasticity in Transgenic Mice Expressing an Inhibitor of ATF4 (CREB-2) and C/EBP Proteins. *Neuron*, 39(4), 655-669. [https://doi.org/https://doi.org/10.1016/S0896-6273\(03\)00501-4](https://doi.org/https://doi.org/10.1016/S0896-6273(03)00501-4).

Citri, A., & Malenka, R. C. (2008a). Synaptic plasticity: Multiple forms, functions, and mechanisms. *Neuropsychopharmacology*, 33(1), 18-41. <https://doi.org/10.1038/sj.npp.1301559>.

Citri, A., & Malenka, R. C. (2008b). Synaptic Plasticity: Multiple Forms, Functions and Mechanisms. *Neuropsychopharmacology*, 33(1), 18-41. <https://doi.org/10.1038/sj.npp.1301559>.

Clements, J. D., & Westbrook, G. L. (1994). Kinetics of AP5 dissociation from NMDA receptors: evidence for two identical cooperative binding sites. *Journal of Neurophysiology*, 71(6), 2566-2569. <https://doi.org/10.1152/jn.1994.71.6.2566>.

Comery, T. A., Harris, J. B., Willems, P. J., Oostra, B. A., Irwin, S. A., Weiler, I. J., & Greenough, W. T. (1997). Abnormal dendritic spines in fragile X knockout mice: maturation and pruning deficits. *Proceedings of the National Academy of Sciences of the United States of America*, 94(10), 5401-5404. <https://www.ncbi.nlm.nih.gov/pubmed/9144249>.

Cull-Candy, S., Kelly, L., and Farrant, M. (2006). Regulation of Ca²⁺-permeable AMPA receptors: synaptic plasticity and beyond. *Curr. Opin. Neurobiol.* 16, 288-297. <https://doi.org/10.1016/j.conb.2006.05.012>.

DeFelipe, J. (2015). The dendritic spine story: an intriguing process of discovery. *Frontiers in Neuroanatomy*, 9, 14. <https://doi.org/10.3389/fnana.2015.00014>.

Derkach, V. A., Oh, M. C., Guire, E. S., & Soderling, T. R. (2007). Regulatory mechanisms of AMPA receptors in synaptic plasticity. *Nature Reviews Neuroscience*, 8, 101. Retrieved from <https://doi.org/10.1038/nrn2055>.

Di Luca, M., Caldarelli, A., Lim, D., Mitro, N., Fagni, L., Mellone, M., ... Karpova, A. (2016). Ring finger protein 10 is a novel synaptonuclear messenger encoding activation of NMDA receptors in hippocampus. *ELife*, 5, 1-29. <https://doi.org/10.7554/elife.12430>.

Dieterich, D. C., Karpova, A., Mikhaylova, M., Zdobnova, I., König, I., Landwehr, M., ... Kreutz, M. R. (2008). Caldendrin-Jacob: A Protein Liaison That Couples NMDA Receptor Signalling to the Nucleus. *PLOS Biology*, 6(2), e34. Retrieved from <https://doi.org/10.1371/journal.pbio.0060034>.

- Divito, C. B., & Underhill, S. M. (2014). Excitatory amino acid transporters: Roles in glutamatergic neurotransmission. *Neurochemistry International*, *73*, 172-180. <https://doi.org/https://doi.org/10.1016/j.neuint.2013.12.008>.
- Durand, C. M., Betancur, C., Boeckers, T. M., Bockmann, J., Chaste, P., Fauchereau, F., ... Bourgeron, T. (2006). Mutations in the gene encoding the synaptic scaffolding protein SHANK3 are associated with autism spectrum disorders. *Nature Genetics*, *39*, 25. Retrieved from <https://doi.org/10.1038/ng1933>.
- Escobar M.L. and Derrick B. (2007). *Neural Plasticity and Memory: From Genes to Brain Imaging*.
- Fiala, J. C., Feinberg, M., Popov, V., & Harris, K. M. (1998). Synaptogenesis Via Dendritic Filopodia in Developing Hippocampal Area CA1. *The Journal of Neuroscience*, *18*(21), 8900 LP-8911. <https://doi.org/10.1523/JNEUROSCI.18-21-08900.1998>.
- Fu, Y.-H., Kuhl, D. P. A., Pizzuti, A., Pieretti, M., Sutcliffe, J. S., Richards, S., ... Caskey, C. T. (1991). Variation of the CGG repeat at the fragile X site results in genetic instability: Resolution of the Sherman paradox. *Cell*, *67*(6), 1047-1058. [https://doi.org/https://doi.org/10.1016/0092-8674\(91\)90283-5](https://doi.org/https://doi.org/10.1016/0092-8674(91)90283-5).
- Geiger, J. R. P., Lübke, J., Roth, A., Frotscher, M., & Jonas, P. (1997). Submillisecond AMPA Receptor-Mediated Signaling at a Principal Neuron–Interneuron Synapse. *Neuron*, *18*(6), 1009-1023. [https://doi.org/10.1016/S0896-6273\(00\)80339-6](https://doi.org/10.1016/S0896-6273(00)80339-6).
- Gherzi, E., Vito, P., Lopez, P., Abdallah, M., & D'Adamio, L. (2004). The intracellular localization of amyloid beta protein precursor (AbetaPP) intracellular domain associated protein-1 (AIDA-1) is regulated by AbetaPP and alternative splicing. *Journal of Alzheimer's Disease : JAD*, *6*(1), 67-78. Retrieved from <http://www.ncbi.nlm.nih.gov/pubmed/15004329>.
- Gipson, C. D., & Olive, M. F. (2017). Structural and functional plasticity of dendritic spines - root or result of behavior? *Genes, Brain, and Behavior*, *16*(1), 101-117. <https://doi.org/10.1111/gbb.12324>.
- Grabrucker, S., Proepper, C., Mangus, K., Eckert, M., Chhabra, R., Schmeisser, M. J., ... Grabrucker, A. M. (2014). The PSD protein ProSAP2/Shank3 displays synpto-nuclear shuttling which is deregulated in a schizophrenia-associated mutation. *Experimental Neurology*, *253*, 126-137. <https://doi.org/https://doi.org/10.1016/j.expneurol.2013.12.015>.

- Greger I.H., Watson J.F., Cull-Candy S.G. (2017). Structural and Functional Architecture of AMPA-Type Glutamate Receptors and Their Auxiliary Proteins. *Neuron* 94, 713-730. <http://dx.doi.org/10.1016/j.neuron.2017.04.009>.
- Hagerman, R. J., Leehey, M., Heinrichs, W., Tassone, F., Wilson, R., Hills, J., ... Hagerman, P. J. (2001). Intention tremor, parkinsonism, and generalized brain atrophy in male carriers of fragile X. *Neurology*, 57(1), 127 LP-130. <https://doi.org/10.1212/WNL.57.1.127>.
- Hansen, K. B., Yi, F., Perszyk, R. E., Furukawa, H., Wollmuth, L. P., Gibb, A. J., & Traynelis, S. F. (2018). Structure, function, and allosteric modulation of NMDA receptors. *J. Gen. Physiol*, 150(8), 1081–1105. <https://doi.org/10.1085/jgp.201812032>.
- Hardingham, G. E., & Bading, H. (n.d.). Synaptic versus extrasynaptic NMDA receptor signalling: implications for neurodegenerative disorders. <https://doi.org/10.1038/nrn2911>.
- Harris, K. M. (1999). Structure, development, and plasticity of dendritic spines. *Current Opinion in Neurobiology*, 9(3), 343–348. [https://doi.org/https://doi.org/10.1016/S0959-4388\(99\)80050-6](https://doi.org/https://doi.org/10.1016/S0959-4388(99)80050-6).
- Herbst, W. A., & Martin, K. C. (2017a). Regulated transport of signaling proteins from synapse to nucleus. *Current Opinion in Neurobiology*, 45, 78–84. <https://doi.org/10.1016/j.conb.2017.04.006>.
- Herbst, W. A., & Martin, K. C. (2017b). ScienceDirect Regulated transport of signaling proteins from synapse to nucleus. *Current Opinion in Neurobiology*, 45, 78–84. <https://doi.org/10.1016/j.conb.2017.04.006>.
- Hering, H., & Sheng, M. (2001). *DENDRITIC SPINES: STRUCTURE, DYNAMICS AND REGULATION*. Retrieved from www.nature.com/reviews/neuro.
- Ho, V. M., Lee, J.-A., & Martin, K. C. (2011). The Cell Biology of Synaptic Plasticity. *Curr. Opin. Neurobiol*, 471, 653. <https://doi.org/10.1126/science.1209168>.
- Holtmaat, A., & Svoboda, K. (2009). Experience-dependent structural synaptic plasticity in the mammalian brain. *Nature Reviews Neuroscience*, 10, 647. Retrieved from <https://doi.org/10.1038/nrn2699>.
- Hoshikawa, S., Ogata, T., Fujiwara, S., Nakamura, K., & Tanaka, S. (2008). A Novel Function of RING Finger Protein 10 in Transcriptional Regulation of the Myelin-Associated Glycoprotein Gene and Myelin Formation in Schwann Cells. *PLOS ONE*, 3(10), e3464. Retrieved from <https://doi.org/10.1371/journal.pone.0003464>.

- Huganir, R.L., and Nicoll, R.A. (2013). AMPARs and synaptic plasticity: the last 25 years. *Neuron* 80, 704-717. <https://doi.org/10.1016/j.neuron.2013.10.025>.
- Inoue, M., Horigane, S., Suzuki, K., Takemoto-Kimura, S., Kamijo, S., Bito, H., ... Fujii, H. (2017). Calmodulin kinases: essential regulators in health and disease. *Journal of Neurochemistry*, 141(6), 808-818. <https://doi.org/10.1111/jnc.14020>.
- Jeffrey, R. A., Ch'ng, T. H., O'Dell, T. J., & Martin, K. C. (2009). Activity-Dependent Anchoring of Importin α at the Synapse Involves Regulated Binding to the Cytoplasmic Tail of the NR1-1a Subunit of the NMDA Receptor. *The Journal of Neuroscience*, 29(50), 15613 LP-15620. <https://doi.org/10.1523/JNEUROSCI.3314-09.2009>.
- Jiang, Y., & Ehlers, M. D. (2013). Modeling Autism by SHANK Gene Mutations in Mice. *Neuron*, 78(1), 8-27. <https://doi.org/https://doi.org/10.1016/j.neuron.2013.03.016>.
- Jordan, B. A., Fernholz, B. D., Boussac, M., Xu, C., Grigorean, G., Ziff, E. B., & Neubert, T. A. (2004). Identification and Verification of Novel Rodent Postsynaptic Density Proteins. *Molecular & Cellular Proteomics*, 3(9), 857 LP-871. <https://doi.org/10.1074/mcp.M400045-MCP200>.
- Jordan, B. A., Fernholz, B. D., Khatri, L., & Ziff, E. B. (2007). Activity-dependent AIDA-1 nuclear signaling regulates nucleolar numbers and protein synthesis in neurons. *Nature Neuroscience*, 10, 427. Retrieved from <https://doi.org/10.1038/nn1867>.
- Karpova, A., Mikhaylova, M., Bera, S., Bär, J., Reddy, P. P., Behnisch, T., ... Kreutz, M. R. (2013). Encoding and Transducing the Synaptic or Extrasynaptic Origin of NMDA Receptor Signals to the Nucleus. *Cell*, 152(5), 1119-1133. <https://doi.org/https://doi.org/10.1016/j.cell.2013.02.002>.
- Kessels, H.W., and Malinow, R. (2009). Synaptic AMPA receptor plasticity and behavior. *Neuron* 61, 340-350. <https://doi.org/10.1016/j.neuron.2009.01.015>.
- Lai, K.-O., Zhao, Y., Ch'ng, T. H., & Martin, K. C. (2008). Importin-mediated retrograde transport of CREB2 from distal processes to the nucleus in neurons. *Proceedings of the National Academy of Sciences*, 105(44), 17175 LP-17180. <https://doi.org/10.1073/pnas.0803906105>.
- Lee, H.-K., Barbarosie, M., Kameyama, K., Bear, M. F., & Huganir, R. L. (2000). Regulation of distinct AMPA receptor phosphorylation sites during bidirectional synaptic plasticity. *Nature*, 405(6789), 955-959. <https://doi.org/10.1038/35016089>.

- Lester, R. A. J., Clements, J. D., Westbrook, G. L., & Jahr, C. E. (1990). Channel kinetics determine the time course of NMDA receptor-mediated synaptic currents. *Nature*, *346*(6284), 565–567. <https://doi.org/10.1038/346565a0>.
- Lim, A. F. Y., Lim, W. L., & Ch'ng, T. H. (2017). Activity-dependent synapse to nucleus signaling. *Neurobiology of Learning and Memory*, *138*, 78–84. <https://doi.org/10.1016/j.nlm.2016.07.024>.
- Lin, J., Friesen, M. T., Bocangel, P., Cheung, D., Rawszer, K., & Wigle, J. T. (2005). Characterization of Mesenchyme Homeobox 2 (MEOX2) transcription factor binding to RING finger protein 10. *Molecular and Cellular Biochemistry*, *275*(1–2), 75–84. <https://doi.org/10.1007/s11010-005-0823-3>.
- Liu, S.J., and Zukin, R.S. (2007). Ca²⁺-permeable AMPA receptors in synaptic plasticity and neuronal death. *Trends Neurosci.* *30*, 126–134. <https://doi.org/10.1016/j.tins.2007.01.006>.
- Lüscher, C., Nicoll, R. A., Malenka, R. C., & Muller, D. (2000). Synaptic plasticity and dynamic modulation of the postsynaptic membrane. *Nature Neuroscience*, *3*(6), 545–550. <https://doi.org/10.1038/75714>.
- Malenka, R. C. (1991). Postsynaptic factors control the duration of synaptic enhancement in area CA1 of the hippocampus. *Neuron*, *6*(1), 53–60. [https://doi.org/10.1016/0896-6273\(91\)90121-F](https://doi.org/10.1016/0896-6273(91)90121-F).
- Malenka RC, Nicoll RA: NMDA-receptor-dependent synaptic plasticity: multiple forms and mechanisms. *Trends Neurosci* 1993, *16*:521-527.
- Marcello, E., Di Luca, M., & Gardoni, F. (2018). Synapse-to-nucleus communication: from developmental disorders to Alzheimer's disease. *Current Opinion in Neurobiology*, *48*, 160–166. <https://doi.org/10.1016/j.conb.2017.12.017>.
- Martel, M.-A., Ryan, T. J., Bell, K. F. S., Fowler, J. H., McMahon, A., Al-Mubarak, B., ... Hardingham, G. E. (2012). The Subtype of GluN2 C-terminal Domain Determines the Response to Excitotoxic Insults. *Neuron*, *74*(3), 543–556. <https://doi.org/10.1016/j.neuron.2012.03.021>.
- Mateu-Huertas, E., Rodriguez-Revenga, L., Alvarez-Mora, M. I., Madrigal, I., Willemsen, R., Milà, M., ... Estivill, X. (2014). Blood expression profiles of fragile X premutation carriers identify candidate genes involved in neurodegenerative and infertility phenotypes. *Neurobiology of Disease*, *65*, 43–54. <https://doi.org/10.1016/j.nbd.2013.12.020>.

- Michaluk, P., Wawrzyniak, M., Alot, P., Szczot, M., Wyrembek, P., Mercik, K., ... Wlodarczyk, J. (2011). Influence of matrix metalloproteinase MMP-9 on dendritic spine morphology. *Journal of Cell Science*, 124(19), 3369 LP-3380. <https://doi.org/10.1242/jcs.090852>.
- Monyer, H., Sprengel, R., Schoepfer, R., Herb, A., Higuchi, M., Lomeli, H., ... Seeburg, P. H. (1992). Heteromeric NMDA Receptors: Molecular and Functional Distinction of Subtypes. *Science*, 256(5060), 1217 LP-1221. <https://doi.org/10.1126/science.256.5060.1217>.
- Nägerl, U. V., Eberhorn, N., Cambridge, S. B., & Bonhoeffer, T. (2004). Bidirectional Activity-Dependent Morphological Plasticity in Hippocampal Neurons. *Neuron*, 44(5), 759–767. <https://doi.org/10.1016/j.neuron.2004.11.016>.
- Newpher, T.M., and Ehlers, M.D. (2008). Glutamate receptor dynamics in dendritic microdomains. *Neuron* 58, 472–497. <https://doi.org/10.1016/j.neuron.2008.04.030>.
- Nicoll, R. A., Kauer, J. A., & Malenka, R. C. (1988). The current excitement in long term potentiation. *Neuron*, 1(2), 97–103. [https://doi.org/10.1016/0896-6273\(88\)90193-6](https://doi.org/10.1016/0896-6273(88)90193-6).
- Opazo, P., and Choquet, D. (2011). A three-step model for the synaptic recruitment of AMPA receptors. *Mol. Cell. Neurosci.* 46, 1–8. <https://doi.org/10.1016/j.mcn.2010.08.014>.
- Panayotis, N., Karpova, A., Kreutz, M. R., & Fainzilber, M. (2015). Macromolecular transport in synapse to nucleus communication. *Trends in Neurosciences*, 38(2), 108–116. <https://doi.org/10.1016/j.tins.2014.12.001>.
- Paoletti, P., Bellone, C., & Zhou, Q. (2013). NMDA receptor subunit diversity: Impact on receptor properties, synaptic plasticity and disease. *Nature Reviews Neuroscience*, 14(6), 383–400. <https://doi.org/10.1038/nrn3504>.
- Parra-Damas, A., & Saura, C. A. (2019). Review Synapse-to-Nucleus Signaling in Neurodegenerative and Neuropsychiatric Disorders. *Biological Psychiatry*. <https://doi.org/10.1016/j.biopsych.2019.01.006>.
- Parra-Damas, A., Valero, J., Chen, M., España, J., Martín, E., Ferrer, I., ... Saura, C. A. (2014). Crtc1 activates a transcriptional program deregulated at early Alzheimer's disease-related stages. *The Journal of Neuroscience : The Official Journal of the Society for Neuroscience*, 34(17), 5776–5787. <https://doi.org/10.1523/JNEUROSCI.5288-13.2014>.
- Pasini, S., Corona, C., Liu, J., Greene, L. A., & Shelanski, M. L. (2015). Specific

Downregulation of Hippocampal ATF4 Reveals a Necessary Role in Synaptic Plasticity and Memory. *Cell Reports*, 11(2), 183-191.
<https://doi.org/https://doi.org/10.1016/j.celrep.2015.03.025>.

Peprah, E. (2012). Fragile X Syndrome: The FMR1 CGG Repeat Distribution Among World Populations. *Annals of Human Genetics*, 76(2), 178-191.
<https://doi.org/10.1111/j.1469-1809.2011.00694.x>.

Proepper, C., Johannsen, S., Liebau, S., Dahl, J., Vaida, B., Bockmann, J., ... Boeckers, T. M. (2007). Abelson interacting protein 1 (Abi-1) is essential for dendrite morphogenesis and synapse formation. *The EMBO Journal*, 26(5), 1397 LP-1409.
<https://doi.org/10.1038/sj.emboj.7601569>.

Ramm, E., Nakagawa, T., Schlager, M. A., Sheng, M., Duong, D. M., Cheng, D., ... Hoogenraad, C. C. (2006). Relative and Absolute Quantification of Postsynaptic Density Proteome Isolated from Rat Forebrain and Cerebellum. *Molecular & Cellular Proteomics*, 5(6), 1158-1170. <https://doi.org/10.1074/mcp.d500009-mcp200>.

Renner, M., & Triller, A. (2013). Synaptic Plasticity and the Mechanism of Alzheimer's Disease. *Research and Perspectives in Alzheimer's Disease*, 53(9), 1689-1699.
<https://doi.org/10.1017/CBO9781107415324.004>.

Reymann, K. G., & Frey, J. U. (n.d.). The late maintenance of hippocampal LTP: Requirements, phases, "synaptic tagging", "late-associativity" and implications.
<https://doi.org/10.1016/j.neuropharm.2006.07.026>.

Sala, C., & Segal, M. (2014). DENDRITIC SPINES: THE LOCUS OF STRUCTURAL AND FUNCTIONAL PLASTICITY. *Physiol Rev*, 94, 141-188.
<https://doi.org/10.1152/physrev.00012.2013>.

Saurin, A. J., Borden, K. L. B., Boddy, M. N., & Freemont, P. S. (1996). Does this have a familiar RING? *Trends in Biochemical Sciences*, 21(6), 208-214.
[https://doi.org/https://doi.org/10.1016/S0968-0004\(96\)80017-X](https://doi.org/https://doi.org/10.1016/S0968-0004(96)80017-X).

Seeburg, P.H., and Hartner, J. (2003). Regulation of ion channel/neurotransmitter receptor function by RNA editing. *Curr. Opin. Neurobiol.* 13, 279-283.
[https://doi.org/10.1016/S0959-4388\(03\)00062-X](https://doi.org/10.1016/S0959-4388(03)00062-X).

Seki, N., Hattori, A., Sugano, S., Muramatsu, M., & Saito, T. (2000). cDNA cloning, expression profile, and genomic structure of human and mouse RNF10/Rnf 10 genes, encoding a novel RING finger protein. *Journal Of Human Genetics*, 45, 38.
Retrieved from <https://doi.org/10.1007/s100380050007>

- Serrano, P., Yao, Y., & Sacktor, T. C. (2005). Brief Communication Persistent Phosphorylation by Protein Kinase M Maintains Late-Phase Long-Term Potentiation. <https://doi.org/10.1523/JNEUROSCI.5132-04.2005>.
- Shepherd, J.D., and Huganir, R.L. (2007). The cell biology of synaptic plasticity: AMPA receptor trafficking. *Annu. Rev. Cell Dev. Biol.* 23, 613–643. <https://doi.org/10.1146/annurev.cellbio.23.090506.123516>.
- Sorra, K. E., & Harris, K. M. (2000). Overview on the structure, composition, function, development, and plasticity of hippocampal dendritic spines. *Hippocampus*, 10(5), 501–511. [https://doi.org/10.1002/1098-1063\(2000\)10:5<501::AID-HIPO1>3.0.CO;2-T](https://doi.org/10.1002/1098-1063(2000)10:5<501::AID-HIPO1>3.0.CO;2-T).
- Spilker, C., Nullmeier, S., Grochowska, K. M., Schumacher, A., Butnaru, I., Macharadze, T., ... Kreutz, M. R. (2016). A Jacob/Nsmf Gene Knockout Results in Hippocampal Dysplasia and Impaired BDNF Signaling in Dendritogenesis. *PLOS Genetics*, 12(3), e1005907. Retrieved from <https://doi.org/10.1371/journal.pgen.1005907>.
- Sutton, M. A., & Schuman, E. M. (2006). Dendritic Protein Synthesis, Synaptic Plasticity, and Memory. *Cell*, 127(1), 49–58. <https://doi.org/https://doi.org/10.1016/j.cell.2006.09.014>.
- Tassone, F., Hagerman, R. J., Iklé, D. N., Dyer, P. N., Lampe, M., Willemsen, R., ... Taylor, A. K. (1999). FMRP expression as a potential prognostic indicator in fragile X syndrome. *American Journal of Medical Genetics*, 84(3), 250–261. [https://doi.org/10.1002/\(SICI\)1096-8628\(19990528\)84:3<250::AID-AJMG17>3.0.CO;2-4](https://doi.org/10.1002/(SICI)1096-8628(19990528)84:3<250::AID-AJMG17>3.0.CO;2-4)
- Thomas, G. M., & Huganir, R. L. (2004). MAPK cascade signalling and synaptic plasticity. *Nature Reviews Neuroscience*, 5, 173. Retrieved from <https://doi.org/10.1038/nrn1346>.
- Thompson, K. R., Otis, K. O., Chen, D. Y., Zhao, Y., O'dell, T. J., & Martin, K. C. (2004). *Synapse to Nucleus Signaling during Long-Term Synaptic Plasticity: a Role for the Classical Active Nuclear Import Pathway*. *Neuron* (Vol. 44). <https://doi.org/10.1016/j.neuron.2004.11.025>.
- Tindi, J. O., Chávez, A. E., Cvejic, S., Calvo-Ochoa, E., Castillo, P. E., & Jordan, B. A. (2015). ANKS1B Gene Product AIDA-1 Controls Hippocampal Synaptic Transmission by Regulating GluN2B Subunit Localization. *The Journal of Neuroscience*, 35(24), 8986 LP-8996. <https://doi.org/10.1523/JNEUROSCI.4029-14.2015>.

- Traynelis, S. F., Wollmuth, L. P., Mcbain, C. J., Menniti, F. S., Vance, K. M., Ogden, K. K., ... Dingledine, R. (2010). Glutamate Receptor Ion Channels: Structure, Regulation, and Function. <https://doi.org/10.1124/pr.109.002451>.
- Van Der Sluijs, P., & Hoogenraad, C. C. (2011). New insights in endosomal dynamics and AMPA receptor trafficking. *Seminars in Cell and Developmental Biology*, 22, 499-505. <https://doi.org/10.1016/j.semcdb.2011.06.008>.
- van Galen, E., Ramakers, G. J. A., Krugers, H. J., Lipp, H.-P., Masneuf, S., Wolfer, D., ... Bösl, M. R. (2011). Dysregulation of Rho GTPases in the α Pix/Arhgef6 mouse model of X-linked intellectual disability is paralleled by impaired structural and synaptic plasticity and cognitive deficits. *Human Molecular Genetics*, 21(2), 268-286. <https://doi.org/10.1093/hmg/ddr457>.
- Verpelli, C., Dvoretzkova, E., Vicidomini, C., Rossi, F., Chiappalone, M., Schoen, M., ... Sala, C. (2011). Importance of Shank3 Protein in Regulating Metabotropic Glutamate Receptor 5 (mGluR5) Expression and Signaling at Synapses. *Journal of Biological Chemistry*, 286(40), 34839-34850. <https://doi.org/10.1074/JBC.M111.258384>.
- Vogt, D. L., Gray, C. D., Young, W. S., Orellana, S. A., & Malouf, A. T. (2007). ARHGAP4 is a novel RhoGAP that mediates inhibition of cell motility and axon outgrowth. *Molecular and Cellular Neuroscience*, 36(3), 332-342. <https://doi.org/https://doi.org/10.1016/j.mcn.2007.07.004>.
- Weis, K. (2002). Nucleocytoplasmic transport: cargo trafficking across the border. *Current Opinion in Cell Biology*, 14(3), 328-335. [https://doi.org/https://doi.org/10.1016/S0955-0674\(02\)00337-X](https://doi.org/https://doi.org/10.1016/S0955-0674(02)00337-X).
- Yi P.L., Chang F.C., Tsai J.J., Hung C.R., Gean P.W. (1995): The involvement of metabotropic glutamate receptors in long-term depression of N-methyl-D-aspartate receptor-mediated synaptic potential in the rat hippocampus. *Neurosci Lett*, 185:207-210. [https://doi.org/10.1016/0304-3940\(95\)11264-W](https://doi.org/10.1016/0304-3940(95)11264-W).
- Yoshihara, Y., De Roo, M., & Muller, D. (2009). Dendritic spine formation and stabilization. *Current Opinion in Neurobiology*, 19(2), 146-153. <https://doi.org/https://doi.org/10.1016/j.conb.2009.05.013>.
- Xiao M.Y., Karpefors M., Niu Y.P., Wigstrom H. (1995). The complementary nature of long-term depression and potentiation revealed by dual component excitatory postsynaptic potentials in hippocampal slices from young rats. *Neuroscience*. 68:625-635. [https://doi.org/10.1016/0306-4522\(95\)00173-g](https://doi.org/10.1016/0306-4522(95)00173-g).

Zhou, Y., Wu, H., Li, S., Chen, Q., Cheng, X.-W., Zheng, J., ... Xiong, Z.-Q. (2006). Requirement of TORC1 for Late-Phase Long-Term Potentiation in the Hippocampus. *PLOS ONE*, 1(1), e16. Retrieved from <https://doi.org/10.1371/journal.pone.0000016>.

Zukin, R. S., Richter, J., & Bagni, C. (2009). Signals, synapses, and synthesis: how new proteins control plasticity . *Frontiers in Neural Circuits* . Retrieved from <https://www.frontiersin.org/article/10.3389/neuro.04.014.2009>.

PhD activity

Congress participation

Date	Title	Location
15/04/2014	"ENGRAMS AND MEMORY TRACES", European Brain Research Institute	Accademia Nazionale dei Lincei, Rome
04-06/12/2017	European Synapse Meeting 2017 (poster presentation: PKC-dependent phosphorylation modulates RNF10 activity in hippocampal neurons; <u>Carrano N</u> , Samaddar T, Marcello E, Di Luca M, Gardoni F.)	Università degli Studi di Milano, Milano
07-11/07/2018	FENS Forum 2018 (poster presentation: PKC-dependent phosphorylation modulates RNF10 synapse-to-nucleus trafficking in hippocampal neurons; <u>Carrano N</u> , Samaddar T, Marcello E, Di Luca M, Gardoni F.)	CityCube Berlin, Berlin
19-22/09/2018	Sif Congress 2018 (poster presentation: PKC-dependent phosphorylation modulates RNF10 activity in hippocampal neurons; <u>Carrano N</u> , Samaddar T, Mauceri D., Marcello E, Di Luca M, Gardoni F)	Zambon Pharma, Bresso
02-04/09/2019	European Synapse Meeting 2019 (poster presentation: Synapse to Nucleus communication: RNF10 role in NMDA receptor-mediated synaptic plasticity; <u>Carrano N</u> , Samaddar T, Mauceri D, Marcello E, Di Luca M, Gardoni F.)	University of Lausanne, Lausanne

Outreach activity

- MEETmeTONIGHT - Faccia a faccia con la scienza, Milan, September 2017
- MEETmeTONIGHT - Faccia a faccia con la scienza, Milan, September 2018

Tutoring

- Tutor of two Master Degree Student thesis
- Tutor in the didactical lab for the course of Experimental Pharmacology (Master Degree in Medicinal Chemistry) Academic years 2017,2018,2019

Secondment

Erasmus+ Traneeship Project, Department of Neurobiology, Heidelberg University (DE) (01/04-01/07/2018); Project Title: "Generation of tools for the study of RNF10 activity"

Publications

Original Papers
The Synaptonuclear Messenger RNF10 Acts as an Architect of Neuronal Morphology, Carrano, N. , Samaddar, T., Brunialti, E. Franchini, L., Marcello, E., Ciana, P., Mauceri, D., Di Luca, M., Gradoni, F., Mol Neurobiol (2019). https://doi.org/10.1007/s12035-019-1631-1
Linking NMDA receptor synaptic retention to synaptic plasticity and cognition, Franchini, L., Stanic, J., Ponzoni, L., Mellone, M., Carrano, N. , Musardo, S., Zianni, E., Olivero, G., Marcello, E., Pittaluga A., Sala, M., Bellone, C., Racca, C., Di Luca, M., Gardoni, F., , iScience (2019). https://doi.org/10.1016/j.isci.2019.08.036 .
Low doses of Perampanel protect striatal and hippocampal neurons against in vitro ischemia by reversing the ischemia-induced alteration of AMPA receptor subunit composition, Mazzocchetti, P., Mancini A., Sciacaluga, M., Megaro A., Bellingacci, L., Di Filippo, M., Nardi Cesarini, E., Romoli, M., Carrano, N. , Gardoni, F., Tozzi, A., Calabresi, P., Costa, C., Neurobiology of Disease (under revision)